PROTON-TRANSFER KINETICS AND EQUILIBRIA IN CONCENTRATED MINERAL ACIDS

By

BRIAN STANLEY VOGT

A DISSERTATION PRESENTED TO THE GRADUATE COUNCIL
OF THE UNIVERSITY OF FLORIDA IN
PARTIAL FULFILLMENT OF THE REQUIREMENTS
FOR THE DEGREE OF DOCTOR OF PHILOSOPHY

UNIVERSITY OF FLORIDA

1983

This dissertation is lovingly dedicated to my dear wife, Carla. Her continual love, patience, and encouragement were instrumental in the completion of this work.

ACKNOWLEDGEMENTS

I would first like to thank Dr. S.G. Schulman, chairman of my supervisory committee, for his patient guidance throughout my graduate career. His perception, experience, and advice were indispensable in the completion of the research which culminated in this dissertation. I would also like to thank the other members of my supervisory committee, Dr. F.A. Vilallonga, Dr. K.B. Sloan, Dr. J.H. Perrin, and Dr. J. D. Winefordner, for their suggestions and support.

I would also like to thank the other members of the research group not only for their friendship, but also for the many thought-provoking discussions and heated arguments which helped all those involved to gain a clearer perspective on the strengths and weaknesses of their scientific understandings. Michael Lovell was particularly helpful in these regards.

Finally, I would like to thank my parents, Stanley and Blanche Vogt, for the understanding and wisdom with which they have encouraged me. They have played an important role in the years of success that I have been privileged to.

TABLE OF CONTENTS

Abstract of Dissertation Presented to the Graduate Council of the University of Florida in Partial Fulfillment of the Requirements for the Degree of Doctor of Philosophy

PROTON-TRANSFER KINETICS AND EQUILIBRIA IN CONCENTRATED MINERAL ACIDS

By

BRIAN STANLEY VOGT

August, 1983

Chairman: Stephen G. Schulman, Ph.D
Major Department: Pharmacy

Ultraviolet-visible absorption and fluorescence spectroscopy were used to study ground- and excited-state proton-transfer reactions. A transition-state reaction scheme was used to propose a model to quantitate the kinetics of excited-state proton transfer in concentrated acid. The Hammett acidity function, H_o, was used as a measure of acidity. The model thus derived included r, the number of water molecules which enter into the excited-state deprotonation reaction of the test compound. Also included was n, the number of water molecules which enter into the ground-state deprotonation reaction of the indicator used to define that range of the H_o scale over which the excited-state ionization of the test compound occurred. The model successfully described

the excited-state ionizations of several aromatic lactams in H_2SO_4 or $HClO_4$. Modification of the model to describe the excited-state ionization of an H_+ type molecule was successful.

It was found that one of the molecules studied demonstrated excited-state prototropic equilibrium. While pK_a^* could be determined, neither the rate constants for the reactions steps nor n and r could be determined. The model predicted that these limitations would apply to all excited-state prototropic equilibria occurring in concentrated acid. The other molecules exhibiting excited-state ionizations in concentrated acid demonstrated nonequilibrium excited-state proton transfer. Values of pK_a^*, the rate constants for the reaction steps, and n and r were determined.

Also devised was a general method of determining the rate constants of the excited-state reaction steps when the ground-state ionization occurs in concentrated acid but the excited-state ionization occurs in dilute solution. This method was successfully applied to several H_o type molecules.

Ground-state ionizations occurring in concentrated acid were successfully described by a modified Henderson-Hasselbach equation. This equation accounted for n and also for r_g, the number of water molecules which enter into the ground-state deprotonation of the test compound.

For all but one of the compounds studied, the Förster successfully related pK_a to pK_a^*.

CHAPTER I
INTRODUCTION

The physical and chemical properties (solubility, pK_a, rates of hydrolysis, etc.) of drugs are usually measured in dilute, aqueous solution. It is frequently assumed that these measurements reflect the correct values of these same properties of the drugs when they are found *in vivo*. However, the experimental solution media are idealized compared to the environments found *in vivo*. For example, plasma is an approximately 8% solution of proteins, electrolytes, lipids, sugars, amino acids, hormones, and metabolic wastes (1), and hence plasma is not a dilute, aqueous solution. Lymphatic fluid and interstitial fluid are similar to plasma (except that they contain less proteins). Cell interiors are another example of media which do not act as dilute solutions, for somewhere between 10% and 60% of the total volume of cells may be water which is "bound up" by cell constituents (2). Indeed, it has been shown that the properties of water in dilute, aqueous solution are dramatically different from the properties of water in cells (2) and around hydrophobic solutes (3). Furthermore, the acidity of aqueous solutions may be enhanced by the addition of neutral electrolytes. For example, a 1 *M* solution of NaCl (approximately 6% NaCl) made up in 0.01 *M*

HCl (pH ≃ 2) has pH ≃ 0.2 (4), and hence the acidity of the solution is changed by almost two orders of magnitude by the addition of the neutral salt. It is conceivable that the presence of high concentrations of solutes in some body fluids could lead to unexpectedly high acidities and low activities of water in those fluids. A study of the physicochemical properties of molecules in concentrated electrolytic media could be useful, for such a study could shed light on whether or not it is legitimate to use properties measured at infinite dilution in water to predict the behavior of the molecules in media which significantly deviate from ideality.

The acid-base properties of functionally substituted aromatic molecules in electronically excited states are frequently thermodynamically and kinetically quite different from these properties in ground electronic states. Because of this, the ground- and excited-state ionizations may occur in media which radically differ from each other insofar as their electrolyte (acidic and/or neutral) compositions are concerned. When the ionizable group is bonded directly to an aromatic ring, UV-visible absorption and fluorescence spectroscopy may be used as tools to study ground- and excited-state proton-transfer reactions. The author has used absorption and fluorescence spectroscopy to study proton-transfer reactions in both dilute, aqueous solutions

and in concentrated electrolytic media. Before discussing the author's research, however, a review of ground- and excited-state acid-base chemistry is in order.

Brønsted-Lowry Acid-Base Chemistry in Ground Electronic States

We shall restrict ourselves to the Brønsted-Lowry definitions (5,6) of acid and base (an acid is a species which can donate a proton and a base is a species which can accept a proton). The acid-base properties of a given organic molecule are a consequence of the presence of one or more electronegative atoms (usually nitrogen, oxygen, or sulfur) in that molecule. In a Brønsted-Lowry acid, at least one of these atoms is present and has covalently bonded to it a hydrogen atom. Sufficiently strong interaction between the solvent and the hydrogen atom results in the loss of the hydrogen atom from the molecule to form a solvated proton and the conjugate base of the organic acid. Brønsted-Lowry bases contain at least one electronegative atom with at least one pair of unshared electrons (lone pair). Protonation (ionization) is the formation of a coordinate-covalent bond between the lone pair on the base and a proton (which may come from the solvent, if it is sufficiently acidic, or from some other source of protons). The conjugate acid of the organic base and the solvent lyate anion (when the solvent is the proton donor) are formed when protonation of the base occurs. The

molecules which we shall consider have conjugate acids and bases which react according to the mechanism

$$BH^+ + SH \underset{k_b}{\overset{k_a}{\rightleftharpoons}} B + SH_2^+ \qquad (1),$$

where B is the conjugate base, BH^+ is the conjugate acid, SH is the solvent, and SH_2^+ is the solvent lyonium ion. The rate constants k_a and k_b are, respectively, the pseudo-first-order rate constant for deprotonation of BH^+ and the second-order rate constant for bimolecular protonation of B. In aqueous solution, SH is water and SH_2^+ is the hydronium ion, and then reaction (1) becomes

$$BH^+ + H_2O \underset{k_b}{\overset{k_a}{\rightleftharpoons}} B + H_3O^+ \qquad (2).$$

It is also possible to have a conjugate acid that is so weakly acidic that solvent lyate anions must be present for the deprotonation reaction to occur, in which case the reaction will be described by

$$BH^+ + S^- \underset{k'_b}{\overset{k'_a}{\rightleftharpoons}} B + SH \qquad (3),$$

where S^- is the solvent lyate anion (in water this is the hydroxide ion) and k'_a and k'_b are, respectively, the second-order rate constant for bimolecular deprotonation of BH^+ and the pseudo-first-order rate constant for protonation of B. The research presented in this dissertation, however,

deals only with molecules which react according to mechanism (2), and hence we shall restrict ourselves to a discussion of that mechanism.

The acid-dissociation equilibrium constant, K_a, for reaction (2) is defined as

$$K_a = \frac{k_a}{k_b} = \frac{a_B a_{H^+}}{a_{BH^+}\, a_w} \qquad (4),$$

where a_B and a_{BH^+} are the activities of the conjugate base and acid, respectively, and a_{H^+} and a_w are the activities of proton and water, respectively. In dilute, aqueous solution $a_w \simeq 1$, and then

$$K_a = \frac{a_B a_{H^+}}{a_{BH^+}} = \frac{[B]\, f_B a_{H^+}}{[BH^+]\, f_{BH^+}} \qquad (5),$$

where [B] and f_B are, respectively, the equilibrium molar concentration and activity coefficient of B, and $[BH^+]$ and f_{BH^+} are, respectively, the equilibrium molar concentration and activity coefficient of BH^+. At infinite dilution, $f_B = 1$ and $f_{BH^+} = 1$, and then equation (5) may be transformed into the familiar Henderson-Hasselbach equation (7,8):

$$pK_a = pH - \log \frac{[B]}{[BH^+]} \qquad (6).$$

In concentrated acidic solutions equation (6) cannot be used. The acidity of the medium (pH < 1) cannot be measured with a pH meter, but it can be measured with the Hammett acidity function (9). This acidity scale is based

upon the spectrophotometrically measured conjugate base/acid ratios of a series of primary nitroaniline indicators which behave according to the reaction

$$HIn^+ + nH_2O \rightleftharpoons In + H^+ \qquad (7),$$

where In and HIn^+ are, respectively, the conjugate base and acid of the indicator, and n is the number of water molecules which react with the hydrated conjugate acid to form the hydrated conjugate base and hydrated proton. The activity of proton is related to the Hammett acidity, H_o (where $H_o = -\log h_o$), by

$$a_{H^+} = h_o a_w^n \frac{f'_+}{f'_o} \qquad (8),$$

where f'_+ and f'_o are the activity coefficients of HIn^+ and In, respectively. In concentrated acid $a_w < 1$, and hence a_w cannot be eliminated from equation (8). The acid-base reaction of the test compound of interest is then

$$BH^+ + r_g H_2O \rightleftharpoons B + H^+ \qquad (9),$$

where r_g is the number of water molecules which react with hydrated, ground-state BH^+ to form hydrated, ground-state B and the hydrated proton. The equilibrium constant for this reaction is defined as

$$K_a = \frac{[B] f_B a_{H^+}}{[BH^+] f_{BH^+} a_w^{r_g}} \qquad (10).$$

Equations (8) and (10) may be combined and put into the logarithmic form

$$pK_a = H_o - \log\frac{[B]}{[BH^+]} - (n-r_g)\log a_w - \log\frac{f_B f'_+}{f_{BH^+} f'_o} \qquad (11).$$

Lovell and Schulman (10-12) have successfully applied equation (11) to the prototropic reactions of a series of unsubstituted and substituted carboxamides and to a series of tertiary anilines, which all ionized in concentrated acid. On the basis of similarity in size and charge of the species involved, they assumed that $f_B f'_+ = f_{BH} + f'_o$, so that equation (11) reduces to

$$pK_a = H_o - \log\frac{[B]}{[BH^+]} - (n-r_g)\log a_w \qquad (12).$$

It remains to be seen whether or not equation (12) is generally applicable.

Prototropic Reactivity in Electronically Excited States

The study of the acid-base chemistry of electronically excited aromatic acids and bases began formally in 1949, when Förster (13) elaborated upon Weber's earlier observation (14) that the fluorescence spectrum of 1-naphthylamine-4-sulfonate exhibits pH dependence different from the pH dependence of its absorption spectrum. Years of subsequent research have shed much light on this subject.

Electronic excitation of an aromatic molecule results in a change in electronic distribution in that molecule. This difference in electronic distribution results in

differences between ground- and excited-state prototropic reactivities. Those functional groups which have lone pairs from which electronic charge is donated to the aromatic system upon molecular excitation become more acidic in the excited state. In the excited state, electronic charge is delocalized from the functional group to the aromatic π system, and hence the electrostatic attraction between the functional group and the proton is lower in the excited state than it is in the ground state. The proton may thus be lost more easily in the excited state, and hence $pK_a^* < pK_a$ (where pK_a^* is the negative logarithm of the acid-dissociation equilibrium constant for the reaction as it occurs in the excited state). Examples of excited-state electronic charge donating groups include -OH, $-O^-$, $-OH_2^+$, -SH, $-S^-$, $-SH_2^+$, $-NH_2$, $-NH^-$, $-NH_3^+$, and pyrrolic nitrogens.

Functional groups that have vacant low-lying π orbitals can accept electronic charge upon molecular excitation. These groups include -COOH, $-COO^-$, $-COOH_2^+$, $-CONH_2$, $-CONH^-$, $-CONH_3^+$, -COSH, $-COS^-$, and $-COSH_2^+$. In the excited state, electronic charge is delocalized from the aromatic π system to the vacant orbital of the functional group, and the resulting increase in electrostatic attraction between the functional group and the proton results in $pK_a^* > pK_a$. Pyridinic nitrogens are excited-state electronic charge acceptors even though they possess a lone pair but not any vacant low-lying π

orbitals. This is a consequence of the electronegativity of the nitrogen being higher than that of the carbons to which it is bonded, and in the excited state charge is localized on the nitrogen. The lone pair projects out in the plane of the ring and is perpendicular to the aromatic π system. This perpendicularity prevents the lone pair from interacting with the aromatic system.

It should be mentioned that excited-state proton transfer can be either intramolecular or intermolecular. Intramolecular excited-state proton transfer has been reviewed (15), and this dissertation is concerned only with intermolecular proton transfer. Furthermore, the excited state of interest can be either an electronically excited singlet or triplet state. The principles of excited-triplet-state proton transfer are the same as those for the singlet state (see references (16-26) for examples), but the research under consideration deals only with proton transfer in ground and excited singlet states.

The Effects of Protonation on Electronic Spectra

Protonation of a functional group which is intimately coupled to an aromatic system may have a profound effect upon the absorption and fluorescence spectra of that molecule. This is a result of the electronic charge stabilization incurred by the presence of the proton at the functional group.

As we have seen, there is a greater degree of charge localization at an excited-state charge accepting group in the excited state than there is at that group in the ground state. Consequently, there will be a greater amount of electrostatic attraction between the proton and the functional group in the excited-state molecule than in the ground-state molecule. Protonation of the excited-state group, therefore, stabilizes the excited state more than protonation of the ground-state group stabilizes the ground state. Since protonation stabilizes the excited state relative to the ground state, the fluorescence and longest wavelength absorption bands shift to longer wavelength (redshift) when the ionizable group is protonated.

Excited-state electronic charge donating groups, however, are possessed of a greater degree of charge localization in the ground state than they are in the excited state. Protonation of these groups, therefore, stabilizes the ground state relative to the excited state, and hence the fluorescence and longest wavelength absorption bands will shift to shorter wavelength (blueshift) when the functional group is protonated.

The Förster Cycle

In 1950, Förster (27) proposed that the energies of the spectral shifts incurred by protonation of an aromatic base could be quantitatively related to the difference

between pK_a and pK_a^*. This relationship has come to be known as the Förster cycle, a schematic diagram of which is shown in Figure 1-1.

Since the energy terms in Figure 1-1 correspond to thermodynamic state functions, it is correct to write

$$E^A + \Delta H_d^* = E^B + \Delta H_d \qquad (13).$$

Förster (27) assumed that the entropies of the ground- and excited-state proton-transfer reactions are identical, in which case equation (13) can be changed to

$$\Delta G - \Delta G^* = E^A - E^B \qquad (14),$$

where ΔG and ΔG^* are the Gibbs free energies of protonation in the ground and excited states, respectively. Furthermore, E^A and E^B can be given by $E^A = Nhc\bar{\nu}_A$ and $E^B = Nhc\bar{\nu}_B$, respectively, where N is Avagadro's number, h is Planck's constant, c is the speed of light, and $\bar{\nu}_A$ and $\bar{\nu}_B$ are, respectively, the frequencies (in wavenumbers) of the $A \rightarrow A^*$ and $B \rightarrow B^*$ transitions. It is also true that $pK_a = \Delta G/2.303RT$ and $pK_a^* = \Delta G^*/2.303\ RT$, where R is the universal gas constant and T is the absolute temperature. Equation (14) can then be transformed into

$$\Delta pK = pK_a - pK_a^* = \frac{Nhc}{2.303RT}(\bar{\nu}_A - \bar{\nu}_B) \qquad (15).$$

In principle, the Förster cycle can be used only when the 0-0 energies ($\bar{\nu}_A$ and $\bar{\nu}_B$) are known. These energies correspond to transitions between ground and excited states which are both vibrationally relaxed and thermally

Figure 1-1

The Förster cycle. A, B, A^*, and B^* refer to the conjugate acid and base molecules in their ground and excited states, respectively. E^A and E^B are the energies of the $A \rightarrow A^*$ and $B \rightarrow B^*$ transitions, respectively. ΔH_d and ΔH_d^* are, respectively, the enthalpies of protolytic dissociation in the ground and excited states.

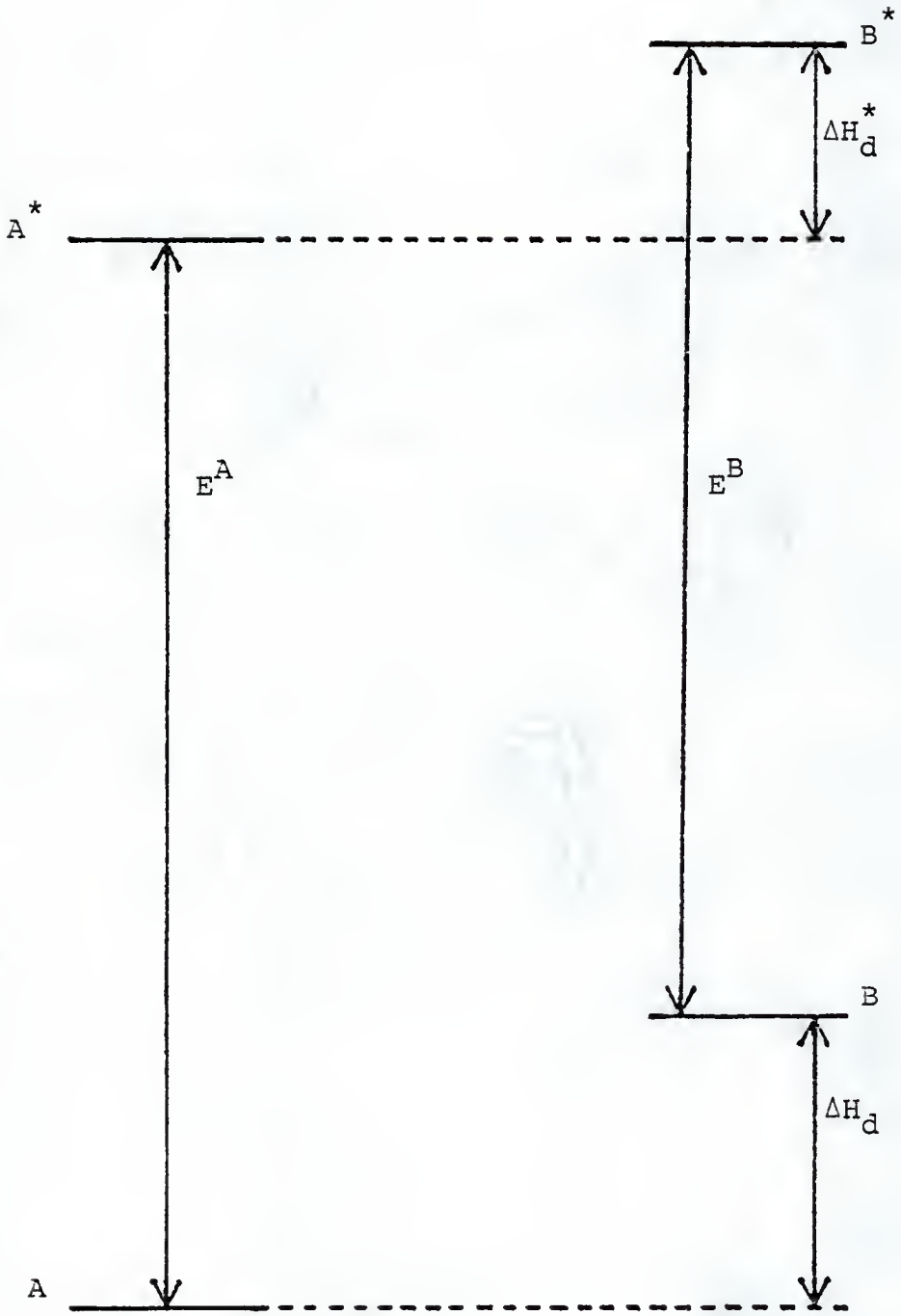
B*
ΔH*d
A*
E^A
E^B
B
ΔHd
A

equilibrated. While both fluorescence and absorption originate from vibrationally relaxed and thermally equilibrated electronic states, they frequently terminate in Franck-Condon electronic states (28). Figure 1-1, therefore, is not an accurate representation of the transitions of interest. Figure 1-2 shows a modified Förster cycle which includes Franck-Condon ground and excited states. It can be seen from Figure 1-2 that absorption may occur at higher energy than the 0-0 energy, and fluorescence may occur at energy lower than the 0-0 energy. Both $\bar{\nu}_A$ and $\bar{\nu}_B$, therefore, may be <u>estimated</u> from the fluorescence and longest wavelength absorption maxima of the conjugate pair, but they will not necessarily reflect the true 0-0 energies.

From Figure 1-2 we see that

$$E^A_{abs} - \Delta H^{A^*}_{te} + \Delta H^*_d = E^B_{abs} + \Delta H_d - \Delta H^{B^*}_{te} \qquad (16)$$

and

$$E^A_{fl} - \Delta H^A_{te} + \Delta H^*_d = E^B_{fl} + \Delta H_d - \Delta H^B_{te} \qquad (17).$$

Still assuming that the entropies of protonation in the ground and excited states are identical, equations (16) and (17) may be transformed into equations (18) and (19), respectively.

$$\Delta pK = \frac{Nhc}{2.303RT}(\bar{\nu}^{abs}_A - \bar{\nu}^{abs}_B) + \Delta H^{B^*}_{te} - \Delta H^{A^*}_{te} \qquad (18)$$

$$\Delta pK = \frac{Nhc}{2.303RT}(\bar{\nu}^{fl}_A - \bar{\nu}^{fl}_B) + \Delta H^A_{te} - \Delta H^B_{te} \qquad (19)$$

Figure 1-2

Modified Förster cycle. A_{te}, B_{te}, A^*_{te}, and B^*_{te} refer to the thermally equilibrated conjugate acid and base molecules in their ground and excited states, respectively. A_{fc}, B_{fc}, A^*_{fc}, and B^*_{fc} refer to the conjugate acid and base in their Franck-Condon ground and excited states, respectively. ΔH^A_{te} and ΔH^B_{te} are the enthalpies of equilibration from the Franck-Condon ground states to the thermally equilibrated ground states of the conjugate acid and base, respectively. $\Delta H^{A^*}_{te}$ and $\Delta H^{B^*}_{te}$ are the enthalpies of equilibrium from the Franck-Condon excited states to the thermally equilibrated excited states of the conjugate acid and base, respectively. E^A_{abs}, E^A_{fl}, E^B_{abs}, and E^B_{fl} refer to the energies of absorption and fluorescence of the conjugate acid and base, respectively. ΔH_d and ΔH^*_d are, respectively, the enthalpies of protolytic dissociation in the ground and excited states.

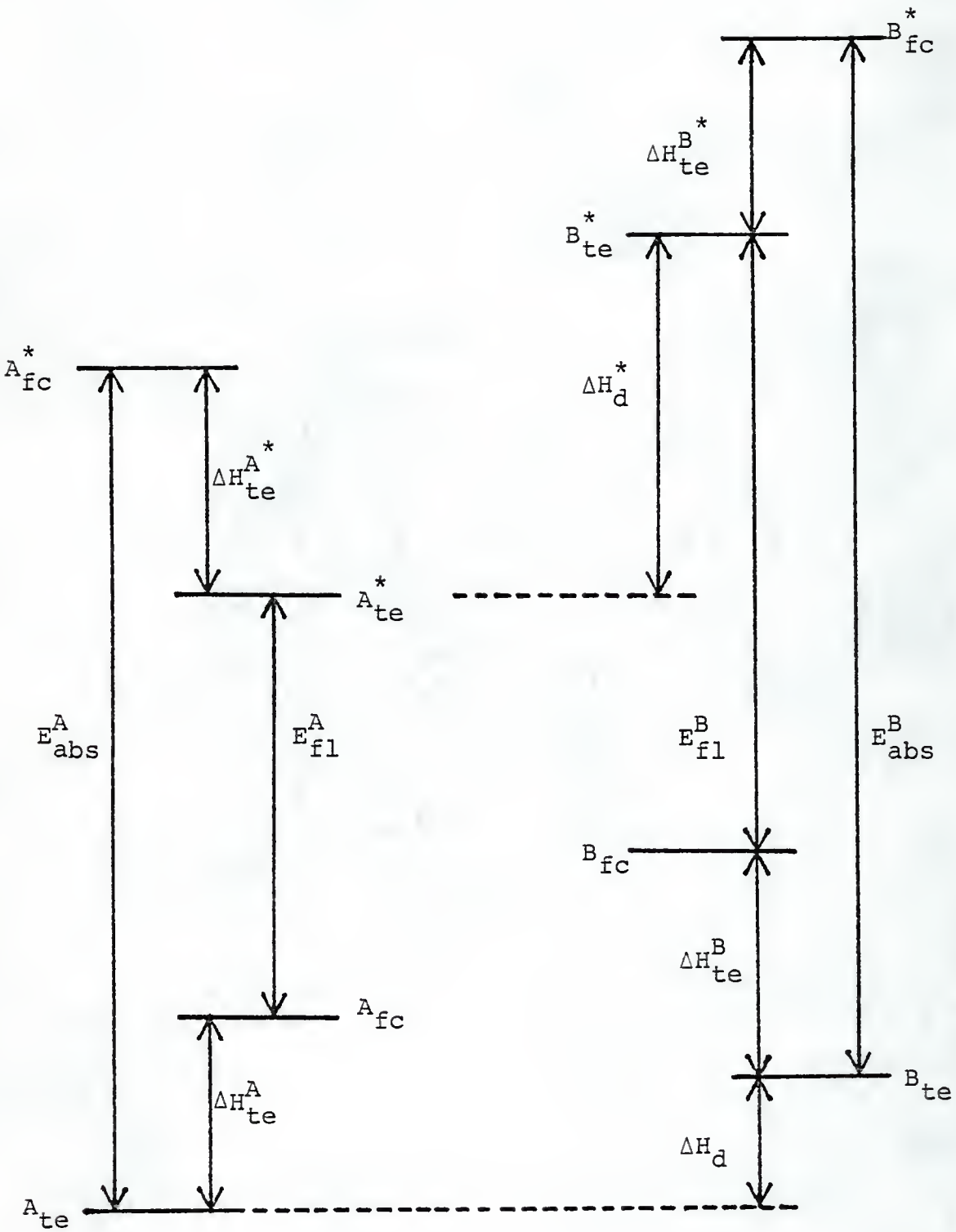
B^*_{fc}
$\Delta H^{B^*}_{te}$
B^*_{te}
ΔH^*_d
A^*_{fc}
$\Delta H^{A^*}_{te}$
A^*_{te}
E^A_{abs}
E^A_{fl}
E^B_{fl}
E^B_{abs}
B_{fc}
ΔH^B_{te}
A_{fc}
B_{te}
ΔH^A_{te}
ΔH_d
A_{te}

Customarily, it is assumed that $\Delta H^{B^*}_{te} = \Delta H^{A^*}_{te}$ and $\Delta H^{B}_{te} = \Delta H^{A}_{te}$, so that equations (18) and (19) reduce to

$$\Delta pK = \frac{Nhc}{2.303RT}(\bar{\nu}^{abs}_{A} - \bar{\nu}^{abs}_{B}) \qquad (20)$$

and

$$\Delta pK = \frac{Nhc}{2.303RT}(\bar{\nu}^{fl}_{A} - \bar{\nu}^{fl}_{B}) \qquad (21),$$

respectively. If pK_a is known, and fluorescence or longest wavelength absorption maxima are also known, and if $\Delta H^{B^*}_{te} = \Delta H^{A^*}_{te}$ and $\Delta H^{A}_{te} = \Delta H^{B}_{te}$, then one can estimate pK^*_a.

When the fluorescence spectrum (as a function of energy) of a molecule is an approximate mirror image of its longest wavelength absorption band, then the vibrational spacings in the ground and excited states are roughly the same (29). In this case the absorption and fluorescence spectra will be equally displaced from the 0-0 energy. It would then be reasonable to estimate $\bar{\nu}_A$ and $\bar{\nu}_B$ by

$$\bar{\nu}_A = \frac{\bar{\nu}^{abs}_{A} + \bar{\nu}^{fl}_{A}}{2} \qquad (22)$$

and

$$\bar{\nu}_B = \frac{\bar{\nu}^{abs}_{B} + \bar{\nu}^{fl}_{B}}{2} \qquad (23),$$

in which case

$$E^A = \frac{E^A_{abs} + E^A_{fl} - \Delta H^{A^*}_{te} + \Delta H^{A}_{te}}{2} \qquad (24)$$

and

$$E^B = \frac{E^B_{abs} + E^B_{fl} - H^{B^*}_{te} + H^B_{te}}{2} \qquad (25).$$

It may then be assumed that $\Delta H^{A^*}_{te} = \Delta H^A_{te}$ and $\Delta H^{B^*}_{te} = \Delta H^B_{te}$. This is at least safer than assuming that $\Delta H^{B^*}_{te} = \Delta H^{A^*}_{te}$ and $\Delta H^B_{te} = \Delta H^A_{te}$, because any difference between $\Delta H^{A^*}_{te}$ and ΔH^A_{te} will be cut in half in the denominator of equation (24) (the same is true of $\Delta H^{B^*}_{te}$ and ΔH^B_{te} in equation (25)). Thus, it is preferable to estimate $\bar{\nu}_A$ and $\bar{\nu}_B$ from equations (22) and (23).

The accuracy of a pK^*_a calculated with the Förster cycle is, of course, dependent upon to what extent the assumptions inherent in the Förster cycle are adhered to and upon how accurately pK_a, $\bar{\nu}_A$, and $\bar{\nu}_B$ are known (some of the inaccuracy in the latter two arises from errors in positioning the monochromators in the spectrophotometer and fluorimeter). Many molecules have excited-state geometries and solvation cages which are similar to their ground-state geometries and solvation cages. Because of this, it is reasonable to assume that the ground- and excited-state entropies of protonation are similar, and then the precision of a pK^*_a calculated with the Förster cycle can be as small as ±0.2 (30). This error and the error in $\bar{\nu}_A$ and $\bar{\nu}_B$ give typical uncertainties of about ±0.3 in Förster cycle pK^*_a's (31). When the assumptions in the Förster cycle are not correct, however, it is not

possible to determine how much uncertainty will be present in a pK_a^* calculated with the Förster cycle. These assumptions have been reviewed in depth (17,26,30,32-39), and any further elaboration upon them here would serve no useful purpose.

The Förster cycle has been used to calculate pK_a^*'s more than any other method (15,17,26,40-44). These calculations have been performed for excited-state ionizations which occur in dilute, aqueous solution and also for some which occur in concentrated acid. Unfortunately, the Förster cycle gives no information concerning the rates of excited-state proton transfer. A method that could give such information could be used to determine not only K_a^*, but also k_a and k_b. The resulting value of pK_a^* could be compared to that calculated with the Förster cycle, and hence the results of each method could be used to confirm or challenge the results of the other. While fluorescence spectroscopy which is time-resolved on the nanosecond and picosecond time scale has been used to determine the rate constants for some excited-state protonation and deprotonation reactions, this technique requires instrumentation that is both very sophisticated and very expensive, and also requires the extensive use of computers for the complicated data reduction that is necessary. We shall restrict ourselves to a discussion of

steady-state kinetics. Representative examples of time-resolved studies of excited-state proton-transfer kinetics may be found in references (45-55).

Steady-State Kinetics of Excited-State Proton-Transfer Reactions

The kinetic equations for excited-state proton-transfer reactions in dilute, aqueous solution were first derived by Weller (56). The excited-state reaction which we are concerned with is

$$BH^{+} \underset{k_d}{\overset{k_f}{\rightleftharpoons}} BH^{+*} \underset{k_b}{\overset{k_a}{\rightleftharpoons}} H^{+} + B^{*} \underset{k'_d}{\overset{k'_f}{\rightleftharpoons}} B \qquad (26),$$

where k_f and k'_f are the rate constants for the fluorescences of BH^{+*} and B^{*}, respectively, and k_d and k'_d are the sums of the rate constants for all nonradiative processes deactivating BH^{+*} and B^{*}, respectively. The fluorescence lifetime of the conjugate acid (present when $pH << pK_a^*$) in the absence of excited-state proton transfer is $\tau_o = 1/(k_f + k_d)$, and that of the conjugate base (present when $pH >> pK_a^*$) in the absence of excited-state proton transfer is $\tau'_o = 1/(k'_f + k'_d)$. Prior to integration, the rate expressions for the disappearance of BH^{+*} and B^{*} from the excited state may be put into the forms

$$-\int_{\alpha_{BH^+}}^{0} d[BH^{+*}] = -\int_0^{\infty} (1/\tau'_o + k_b[H^+])[B^*]\,dt + \int_0^{\infty} k_a[BH^{+*}]dt \qquad (27)$$

and

$$-\int_{\alpha_B}^{0} d[B^*] = \int_0^\infty (1/\tau_o' + k_b[H^+])[B^*]dt - \int_0^\infty k_a[BH^{+*}]dt \qquad (28),$$

where $[B^*]$ and $[BH^{+*}]$ are, respectively, the probabilities of finding a $[B^*]$ or $[BH^{+*}]$ molecule in the excited state at time t. Since the fluorescences of BH^{+*} and B^* are being excited and monitored under steady-state conditions, the right sides of equations (27) and (28) are to be integrated over all time (t = 0 to t = ∞). The lower limits of integration of $[BH^{+*}]$ and $[B^*]$ are α_{BH^+} and α_B, respectively, where α_{BH^+} is the fraction of the ground-state population which is found as the conjugate acid and α_B is the fraction found as the conjugate base. In spectrophotometric terms,

$$\alpha_{BH^+} = \frac{\varepsilon_{BH^+}[BH^+]}{\varepsilon_{BH^+}[BH^+] + \varepsilon_B[B]} \qquad (29)$$

and

$$\alpha_B = \frac{\varepsilon_B[B]}{\varepsilon_{BH^+}[BH^+] + \varepsilon_B[B]} \qquad (30),$$

where ε_B and ε_{BH^+} are the molar absorptivities of the conjugate base and acid, respectively, at the wavelength of excitation. In terms of K_a,

$$\alpha_{BH^+} = \frac{\varepsilon_{BH^+}[H^+]}{\varepsilon_{BH^+}[H^+] + \varepsilon_B K_a} \qquad (31)$$

and

$$\alpha_B = \frac{\varepsilon_B K_a}{\varepsilon_{BH^+}[H^+] + \varepsilon_B K_a} \quad (32).$$

If the rate of attainment of steady-state conditions for the excited-state proton-transfer reaction is much higher than the rates of photophysical deactivation of B^* and BH^{+*}, then $[B^*] = e^{-t/\tau'}$ and $[BH^{+*}] = e^{-t/\tau}$ (57). The fluorescence lifetimes τ and τ' are the lifetimes of the conjugate acid and base, respectively, in the presence of excited-state proton transfer, where $\tau = 1/(k_f + k_d + k_a)$ and $\tau' = 1/(k'_f + k'_d + k_b[H^+])$. The expressions for $[B^*]$ and $[BH^{+*}]$ may be integrated from $t = 0$ to $t = \infty$, and then

$$\int_0^\infty [B^*]dt = \int_0^\infty e^{-t/\tau'}dt = \tau' \quad (33)$$

and

$$\int_0^\infty [BH^{+*}]dt = \int_0^\infty e^{-t/\tau}dt = \tau \quad (34).$$

The quantum yields of fluorescence of the conjugate acid in the absence and presence of excited-state proton transfer are, respectively, $\phi_o = k_f\tau_o$ and $\phi = k_f\tau$. The relative quantum yield of fluorescence of the conjugate acid, ϕ/ϕ_o, is thus related to τ and τ_o by

$$\tau = \tau_o \frac{\phi}{\phi_o} \quad (35).$$

Analogous reasoning for the conjugate base may be used to

show that

$$\tau' = \tau_o' \frac{\phi'}{\phi_o'} \qquad (36),$$

where ϕ_o' and ϕ' are the quantum yields of fluorescence of the conjugate base in the absence and presence of excited-state proton transfer, respectively, and ϕ'/ϕ_o' is the relative quantum yield of fluorescence of the conjugate base. Combination of equation (33) with (35) and of equation (34) with (36) shows that

$$\int_0^\infty [B^*]dt = \tau_o' \frac{\phi'}{\phi_o'} \qquad (37)$$

and

$$\int_0^\infty [BH^{+*}]dt = \tau_o \frac{\phi}{\phi_o} \qquad (38).$$

Therefore, integration of equations (27) and (28) results in

$$\alpha_{BH^+} = \frac{\phi}{\phi_o} + k_a\tau_o \frac{\phi}{\phi_o} - k_b\tau_o'[H^+]\frac{\phi'}{\phi_o'} \qquad (39)$$

and

$$\alpha_B = \frac{\phi}{\phi_o} + k_b\tau_o'[H^+]\frac{\phi'}{\phi_o'} - k_a\tau_o\frac{\phi}{\phi_o} \qquad (40).$$

Equations (39) and (40) can be solved simultaneously for ϕ/ϕ_o and ϕ'/ϕ_o' to yield

$$\frac{\phi}{\phi_o} = \frac{\alpha_{BH^+} + k_b\tau_o'[H^+]}{1 + k_a\tau_o + k_b\tau_o'[H^+]} \qquad (41)$$

and

$$\frac{\phi'}{\phi'_o} = \frac{\alpha_B + k_a\tau_o}{1 + k_a\tau_o + k_b\tau'_o[H^+]} \qquad (42).$$

It is thus seen that $\phi/\phi_o + \phi'/\phi'_o = 1$. Since $\alpha_B + \alpha_{BH^+} = 1$, equations (41) and (42) can be combined to give

$$\frac{\phi/\phi_o}{\phi'/\phi'_o - \alpha_B} = \frac{1}{k_a\tau_o} + \frac{k_b\tau'_o}{k_a\tau_o}[H^+]\frac{\phi'/\phi'_o}{\phi'/\phi'_o - \alpha_B} \qquad (43).$$

A plot of $(\phi/\phi_o)/(\phi'/\phi'_o - \alpha_B)$ versus $([H^+]\phi'/\phi'_o)/(\phi'/\phi'_o - \alpha_B)$ should, therefore, be a straight line with an ordinate intercept of $1/k_a\tau_o$ and a slope of $k_b\tau'_o/k_a\tau_o$. When τ_o and τ'_o can be measured or estimated, then k_a, k_b, and $K_a^* = k_a/k_b$ can be calculated.

Equation (43) was derived assuming that the excited-state proton-transfer reaction attains steady-state conditions before photophysical deactivation of B^* or BH^{+*} can occur. When this is not true, then equation (43) will not rigorously describe the chemistry of interest. A more sophisticated treatment has been derived (58) which accounts for situations where steady-state conditions are not achieved before photophysical deactivation of B^* and BH^{+*} takes place. Use of that treatment will give more accurate values of k_a and k_b when nonsteady-state considerations are significant, but equation (43) will suffice in many situations. It should be noted, however, that the observable rate constants k_a and k_b are subject

to medium effects, and hence equation (43) will not be applicable to an excited-state proton-transfer reaction which occurs in concentrated acid, where the medium is different from one part of the titration inflection region to another. The hypothetical, medium-independent rate constants for the reaction in concentrated acid are $k_a(0)$ and $k_b(0)$, which correspond to the deprotonation and protonation steps, respectively, for the reaction as it would occur in infinitely dilute, aqueous solution. The author's research represents the first attempt to quantitate $k_a(0)$ and $k_b(0)$.

Summary

Proton transfer in both ground and excited states has been thoroughly studied and quantitated for those acid-base reactions which occur at or close to infinite dilution and where $1 < pH < 13$. However, up to the time when the author began his research, no attempts had been made to quantitate the kinetics and equilibria of excited-state proton-transfer reactions in concentrated electrolytic media. It was the goal of the author to develop a successful model for these reactions in concentrated acidic media ($pH < 1$). The author also wished to see if equation (12) has more general application than it has had to date. Finally, the author desired to see if there exists a fundamental relationship between the thermodynamics and kinetics of

proton transfer in dilute, aqueous solution and the thermodynamics and kinetics of proton transfer in concentrated acid.

CHAPTER II
EXPERIMENTAL

Reagents and Chemicals

The water that was used was either deionized, distilled water or doubly deionized water. Sulfuric acid, perchloric acid, chloroform, methanol, ammonium hydroxide, sodium hydroxide, sodium bromide, and potassium hydrogen phthalate were all ACS reagent grade and were purchased from either Fisher Scientific Company (Fair Lawn, NJ) or Scientific Products (McGaw Park, IL). Ethanol was 95% and was purchased locally from hospital stores (J. Hillis Miller Health Center, Gainesville, FL). Thin-layer chromatography plates were fluorescent-indicator impregnated, 250 micron thick silica gel plates and were purchased from Analabs (North Haven, CT). Dry silica gel (100-200 mesh) for atmospheric pressure column chromatography was purchased from Fisher Scientific Company. All acid solutions were standardized against standard NaOH (the NaOH was standardized against potassium acid phthalate). All reagents were checked for spurious absorption and emission prior to their being used for spectroscopic studies.

All weighings were performed on a Mettler Type B6 electronic analytical balance.

Acridone (9-(10H)-acridanone) and 1-isoquinolone (isocarbostyril) were purchased from Aldrich Chemical Company (Milwaukee, WI). Both 2-quinolone and 4-quinolone were purchased from K&K Labs (Plainview, NY). Xanthone (xanthen-9-one) was purchased from Eastman Organic Chemicals (Rochester, NY). The sample of 3-aminoacridine that was used was synthesized and identified by L.S. Rosenberg (59) after the method of Martin and Tong (60).

Acridone was recrystallized three times from EtOH:H_2O (1:1). Xanthone was purified with column chromatography on silica gel using $CHCl_3$ as the mobile phase. Purity was confirmed with TLC on silica gel using $CHCl_3$ as the mobile phase and UV light from a handheld UV lamp as the method of spot visualization (short wavelength UV light excited the fluorescent indicator in the silica, revealing both fluorescent and nonfluorescent spots, while long wavelength UV light visualized only fluorescent spots). Both 2-quinolone and 4-quinolone were recrystallized three times from EtOH:H_2O (1:3). Crystalline 1-isoquinolone was used as received from Aldrich. Purity was confirmed by TLC on silica gel using three different mobile phases ($CHCl_3$, 1:9 MeOH:$CHCl_3$, and 1:4 MeOH:$CHCl_3$). Impure 3-aminoacridine was purified with column chromatography on silica gel. Pure 3-aminoacridine was gradient eluted with MeOH:$CHCl_3$ (the composition of which varied from 1:19 to 2:3) as the mobile phase. Purity was confirmed with TLC

using MeOH:$CHCl_3$ (1:19) as the mobile phase, which was alkalinized by the addition of one drop of NH_4OH. The presence of isosbestic points in the absorption spectra of these compounds further confirmed their purity.

Stock solutions of the compounds were $\approx 10^{-4}$ M to $\approx 10^{-2}$ M and were made up in either H_2O or MeOH. The stock solutions were accurately diluted (by a factor of 100) and the absorbances of the resulting solutions measured at appropriate analytical wavelengths. These absorbances were used in conjunction with published molar absorptivities to calculate the concentrations of the stock solutions. Molar absorptivities of acridone, 2-quinolone, 4-quinolone, and 1-isoquinolone may be found in reference (61). The molar absorptivity of 3-aminoacridine may be found in reference (59). A carefully weighed sample of pure xanthone was used to prepare the stock solution, and hence its concentration was calculated.

Absorption and Fluorescence Studies

Absorption spectra were taken on either a Beckman DB-GT, Beckman Model 25, or Varian Cary 219 spectrophotometer. The Cary 219 was equipped with a cell compartment thermostatted at 25.0±0.2°C. The cell compartment in the DB-GT was thermostatted at 25.0±0.2°C when a constant temperature bath (Brinkmann Lauda K-2/R) was available. The Model 25 had no provision for temperature control. All spectra taken in instruments with

unthermostatted cell compartments were taken at room temperature, which was found to be 24±2°C.

All fluorescence spectra were uncorrected for instrumental response and were taken on a Perkin-Elmer MPF-2A steady-state fluorescence spectrophotometer. This fluorimeter was equipped with a thermostatted cell compartment, which, when a constant temperature bath was available, was kept thermostatted at 25.0±0.2°C. When the ground- and excited-state proton-transfer reactions overlapped, fluorescence was excited at an isosbestic point (at which $\varepsilon_B = \varepsilon_{BH^+}$), and hence equations (31) and (32) reduced to

$$\alpha_{BH^+} = \frac{[H^+]}{[H^+] + K_a} \tag{44}$$

and

$$\alpha_B = \frac{K_a}{[H^+] + K_a} \tag{45},$$

respectively. The quantities ϕ/ϕ_o and ϕ'/ϕ_o' were calculated in terms of fluorescence intensities. The fluorescence intensity, F, at any point on the titration inflection region is, for a given analytical wavelength, given by

$$F=2.3\phi I_o \varepsilon_{BH^+}[BH^+]l + 2.3\phi I_o \varepsilon_B [B]l + 2.3\phi' I_o \varepsilon_B [B]l + 2.3\phi' I_o \varepsilon_{BH^+}[BH^+]l \tag{46},$$

where l is the optical depth of the sample and I_o is the intensity of the exciting light. The first and second terms on the right side of equation (46) correspond to the fluorescence from directly excited conjugate acid and that from the conjugate acid formed by excited-state protonation of the conjugate base, respectively. The third and fourth terms on the right side of equation (46) correspond to the fluorescence from directly excited conjugate base and that from the conjugate base formed by excited-state deprotonation of the conjugate acid, respectively. When $pH >> pK_a$ and $pH >> pK_a^*$, then $F = F_B = 2.3\phi_o' I_o \varepsilon_B C_B l$, from which it is seen that

$$2.3 I_o \varepsilon_B l = \frac{F_B}{\phi_o' C_B} \qquad (47),$$

where $C_B = [B] + [BH^+]$ and F_B is the fluorescence intensity of the isolated conjugate base. When $pH << pK_a$ and $pH << pK_a^*$, then $F = F_{BH^+} = 2.3\phi_o I_o \varepsilon_{BH^+} C_B l$, and then

$$2.3 I_o \varepsilon_{BH^+} l = \frac{F_{BH^+}}{\phi_o C_B} \qquad (48),$$

where F_{BH^+} is the fluorescence intensity of the isolated conjugate acid. Combination of equations (47) and (48) with (46) yields

$$F = F_{BH^+}\frac{\phi [BH^+]}{\phi_o C_B} + F_{BH^+}\frac{\phi [B]}{\phi_o C_B} + F_B\frac{\phi' [B]}{\phi_o' C_B} + F_B\frac{\phi' [BH^+]}{\phi_o' C_B} \qquad (49).$$

When fluorescence is excited at an isosbestic point, then equations (29) and (30) reduce to $\alpha_{BH^+} = [BH^+]/C_B$ and $\alpha_B = [B]/C_B$, respectively. Equation (49) then becomes

$$F = F_{BH^+}\frac{\phi}{\phi}\alpha_{BH^+} + F_{BH^+}\frac{\phi}{\phi}\alpha_B + F_B\frac{\phi'}{\phi_o'}\alpha_B + F_B\frac{\phi'}{\phi_o'}\alpha_{BH^+} \quad (50).$$

Since $\alpha_B + \alpha_{BH^+} = 1$ and $\phi/\phi_o + \phi'/\phi_o' = 1$, equation (50) can be reduced to

$$\frac{\phi}{\phi_o} = \frac{F - F_B}{F_{BH^+} - F_B} \quad (51),$$

and it then follows that

$$\frac{\phi'}{\phi_o'} = \frac{F_{BH^+} - F}{F_{BH^+} - F_B} \quad (52).$$

When the ground- and excited-state proton-transfer reactions do not overlap, then $\alpha_B \to 1$ and $\alpha_{BH^+} \to 0$ or $\alpha_B \to 0$ and $\alpha_{BH^+} \to 1$, and in either case equations (51) and (52) still follow from (50).

Fluorescence lifetimes were measured at room temperature with a TRW model 75A decay-time fluorimeter without excitation or emission filters. This instrument was equipped with a TRW model 31B nanosecond spectral source and was used with an 18 watt deuterium lamp, which was thyratron-pulsed at 5kHz. A TRW model 32A analog decay computer was used to deconvolute the fluorescence decay time of the analyte from the experimentally measured fluorescence decay, which was actually an instrumentally distorted convolution of the lamp pulse and the analyte fluorescence. The TRW instruments were interfaced to a Tektronix model 556

dual-beam oscilloscope, on which the convoluted fluorescence decay from the sample was displayed. Lifetimes >1.7 ns were measurable with this apparatus.

Measurements of Acidity

All pH measurements were made at room temperature with a Markson ElektroMark pH meter equipped with a silver/silver-chloride combination glass electrode. The pH meter was standardized against Fisher Scientific Company pH buffers or Markson Scientific Inc. (Del Mar, CA) pH buffers at room temperature. These buffers were accurate to ±0.02 pH unit and were of pH 1.00, 4.00, 7.00, and 10.00. The precision of the pH meter was estimated to be ±0.01 pH unit, and it was used for the measurement of pH > 1.

The Hammett acidity function was used as a measure of the acidity of solutions in which pH < 1. This acidity scale may be used to quantitate the acidity of media when the species involved have neutral conjugate bases and singly charged conjugate acids. Values of H_o in $HClO_4$ and H_2SO_4 may be found in references (62-64). Values of a_w in the same media may be found in references (65-69).

Titration Methods

Solutions for absorption and fluorescence studies were put into UV-visible quartz cuvettes with pathlengths of 10 mm and volume capacities of ≈4 mls. Absorption spectra were taken against a reference solution of composition

identical to that which the sample was put in (that is, the reference solution was either water or acid).

Aliquots of stock solution (≈200μl) were injected into a series of 10 ml volumetric flasks and the flasks filled to the lines with either water or acid (the stock solution solvent was first evaporated under dry nitrogen when the stock solution was methanolic) and the concentration of acid corrected for any dilution. For titrations where pH > 1, 2 mls of the aqueous solution were placed in the sample cuvette, the spectrum recorded, and the pH measured and recorded immediately after recording the spectrum. An aliquot of an acidic solution of the analyte was then added to the cuvette with a micropipette, the spectrum recorded, and the pH again measured and recorded. Very small changes in pH (≈0.1 unit) were effected by dipping the end of a heat-fused Pasteur pipette into an acidic solution of the analyte and then into the aqueous solution in the cuvette (submicroliter volumes of titrant were added in this way). The formal concentration of the analyte was, therefore, constant throughout the titration. The pH was varied until no further significant changes in the spectrum were observed.

For titrations where pH < 1, 2.000 mls of an acid solution of the analyte were put into a cuvette. The spectrum of the analyte and the molarity of the acid were recorded. An accurately known volume of a solution of

the analyte in a solution of different acid concentration was then added to the 2 mls of solution already in the cuvette. The solution was then stirred with a fine glass rod. The resulting acid concentration was calculated, and then the spectrum of the analyte and the acid molarity were recorded. The acid solutions which were mixed were prepared so as to differ by two or fewer molar units in order to minimize partial molar volume effects and temperature changes due to heat of mixing and heat of dilution. This procedure was repeated with different initial and final concentrations of acid until no further significant changes in the spectrum were observed. Solutions for all titrations were prepared immediately prior to their being used to minimize the possibility of degradation of the test compound.

Analytical wavelengths were chosen to be at or as close to a peak maximum as possible while still yielding the greatest difference between the spectra of the conjugate acid and base. This was done to maximize analytical sensitivity, accuracy, and precision.

Computation

Routine calculations (and sometimes simple linear regression analysis--see Appendix A) were performed on a card-programmable calculator (Texas Instruments TI-59). Complex calculations (simple and multiple linear regression analyses--see Appendices A and B) were performed on either

an International Business Machines IBM 4341 or on a Digital Equipment Corporation DEC VAX 11/780. All computer programs were written in BASIC (beginners all-purpose symbolic instruction code) by the author. The BASIC language on the IBM 4341 was used through MUSIC (McGill University system for interactive computing), while BASIC on the VAX 11/780 was used through DEC VMS (DEC virtual memory system).

CHAPTER III
GROUND- AND EXCITED-STATE PROTON-TRANSFER IN ACRIDONE AND XANTHONE

Introduction

The titration behavior of melecules which become much more basic (or much less acidic) in the excited state than they are in the ground state will be described by a simplified form of equation (43). Since $pK_a^* >> pK_a$, $\alpha_B \rightarrow 1$, and then equation (43) can be reduced and rearranged (70) to

$$\frac{\phi/\phi_o}{\phi'/\phi'_o} = \frac{k_b \tau'_o}{1 + k_a \tau_o} [H^+] \qquad (53).$$

Even if τ_o and τ'_o are known, there is no linear form equation (53) can be put into such that k_a, k_b, and K_a^* can be extracted from the data of a single fluorimetric titration. A method (71-73) of titration involving the use of HCl has been developed which, in favorable circumstances, does permit the used of a linear plot to extract k_a and k_b from a single titration. In this method, the fluorescence of the conjugate acid is quenched by Cl^- while the proton transfer is effected by H^+, where both the Cl^- and H^+ come from the HCl. However, this method is limited in its application to those molecules which ionize at pH such that the rate of proton transfer is approximately the same as the rate of quenching of the

conjugate acid fluorescence. Furthermore, ϕ/ϕ_o and ϕ'/ϕ_o' must be calculated independently of each other, and hence the fluorescence spectra of the conjugate acid and base must be well resolved from each other. These conditions must all be met before the HCl method can be used. It was desirable, therefore, to devise a more generally applicable method of determing k_a and k_b.

It can be seen from equation (53) that the slope, m, of a plot of $(\phi/\phi_o)/(\phi'/\phi_o')$ versus $[H^+]$ will be

$$m = \frac{k_b \tau_o'}{1 + k_a \tau_o} \qquad (54),$$

which can be rearranged to

$$\frac{\tau_o'}{m} = \frac{1}{k_b} + \frac{k_a}{k_b} \tau_o \qquad (55).$$

If a quencher can be added to the titration medium that will quench the fluorescence of the conjugate acid so that $(1 + k_a\tau_o)$ will vary with quencher concentration relative to $k_b\tau_o'$, then m will be a function of quencher concentration. A series of titrations, each with a different constant concentration of quencher in the titration medium, should then yield a different value of m and τ_o for each titration (if the fluorescence of the conjugate base is also quenched, then different values of τ_o' will also be obtained). According to equation (55), a plot of τ_o'/m versus τ_o should

be a straight line with an ordinate intercept of $1/k_b$ and a slope of k_a/k_b. Values of k_a, k_b, and K_a^* could thus be derived from the series of titrations of the molecule of interest.

Acridone (Figure 3-1) is a molecule in which $pK_a^* >> pK_a$ (31,74), and hence its fluorimetric titration behavior should be described by equation (53). Furthermore, since the ground-state ionization occurs in relatively dilute solution ($pK_a = -0.32$) (75), the media in which the ground- and excited-state ionizations occur are not appreciably different. Since the assumptions inherent in the Förster cycle are normally correct for ionizations which occur in dilute, aqueous solution, the pK_a^* of acridone calculated according to equation (55) should agree with the value of its pK_a^* calculated with the Förster cycle. Such a comparison could be used to determine whether or not equation (55) correctly describes the excited-state chemistry of interest. If it does, then equation (55) could be used with confidence to determine the pK_a^* of a molecule in which the ground-state ionization occurs in concentrated acid. The Förster cycle could then be used to see if the excited-state ionization (which occurs in dilute, aqueous solution) can be related to the ground-state ionization (which occurs in concentrated acid).

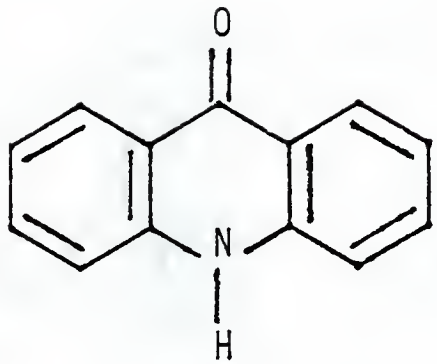

Figure 3-1

Structure of acridone.

Results and Discussion

The fluorescence lifetimes of neutral and protonated acridone are presented as a function of the molarity of Br^- (derived from NaBr) in Table 3-1. Since τ_o varies with $[Br^-]$ but τ_o' is invariant, equation (55) should be applicable to the titration data. Figure 3-2 shows a quenching curve for protonated acridone (this was used in the calculation of τ_o in the presence of quencher--see note b of Table 3-1 for details). Figure 3-3 shows fluorimetric titration curves for acridone in the presence of different concentrations of Br^-. It is of interest to note that the titration curve shifts to higher pH as τ_o decreases. This occurs because the rate of the dissociation reaction decreases when τ_o decreases. This shift to higher pH is predicted by equation (53), which shows that $[H^+]$ at the inflection point (the pH where $\phi/\phi_o = \phi'/\phi_o' = 0.5$) will decrease when m increases (values of m as a function of $[Br^-]$ are also shown in Table 3-1). Figure 3-4 shows a plot of τ_o'/m versus τ_o for acridone. As predicted by equation (55), the plot is linear. Values of k_a, k_b and pK_a^* calculated from the slope and intercept of the line in Figure 3-4 are presented in Table 3-2 along with pK_a^*(F.C.) calculated from the Förster cycle (31). It can be seen from equation (55) that, for any two different pairs of values of m, τ_o', and τ_o,

Table 3-1

Variation with bromide ion concentration of τ_o', τ_o, and m for acridone.

$[Br^-]$, M	τ_o', ns[a]	τ_o, ns[b]	m
0	14.8±0.5	26.0±0.4	13±1[c]
5.0×10^{-3}	14.8±0.5	18.7	33±8
1.0×10^{-2}	14.8±0.5	15.6	40±3
3.0×10^{-2}	14.8±0.5	9.7	59±3
5.0×10^{-2}	14.8±0.5	6.7	71±5
1.0×10^{-1}	14.8±0.5	3.7	104±9
4.0×10^{-1}	14.8±0.5	0.59	169±6
5.0×10^{-1}	14.8±0.5	0.45	175±9

[a]The lifetime of neutral acridone was measured in water at pH = 7.0.

[b]The lifetime of protonated acridone was calculated as $\tau_o = (\phi/\phi_o) \times \tau_o^a$, where ϕ/ϕ_o is the relative quantum yield of fluorescence at the bromide ion concentration of interest (values of ϕ/ϕ_o are shown in Figure 3-2) and τ_o^a is the fluorescence lifetime of protonated acridone in the absence of quencher (measured in 2.3 M $HClO_4$, $H_o = -1.0$).

[c]Taken from reference (31).

Figure 3-2

Variation with bromide ion concentration of the relative quantum yield of fluorescence (ϕ/ϕ_o) of 5 X 10^{-6} M protonated acridone. Analytical wavelength = 456 nm. Excitation wavelength = 350 nm.

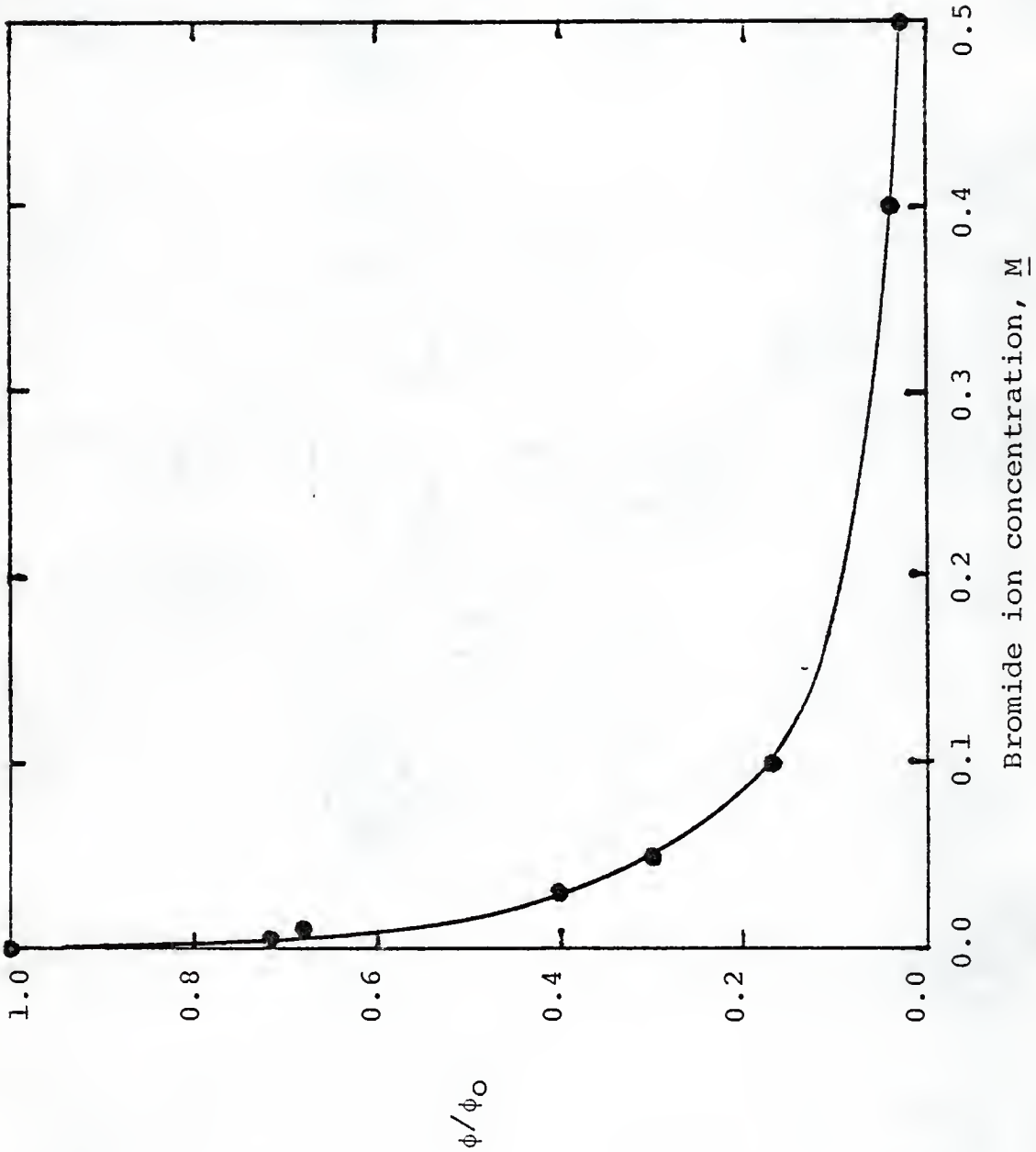
1.0
0.8
0.6
0.4
0.2
0.0
ϕ/ϕ_o
0.0
0.1
0.2
0.3
0.4
0.5
Bromide ion concentration, M

Figure 3-3

Variation of the relative quantum yield of fluorescence (ϕ'/ϕ_o') of 5×10^{-6} M neutral acridone with pH at various bromide ion concentrations. (A) $[Br^-] = 0$, (B) $[Br^-] = 5.0 \times 10^{-3}$ M, (C) $[Br^-] = 5.0 \times 10^{-2}$ M, (D) $[Br^-] = 1.0 \times 10^{-1}$ M, (E) $[Br^-] = 5.0 \times 10^{-1}$ M. Analytical wavelength = 440 nm. Excitation wavelength = 350 nm.

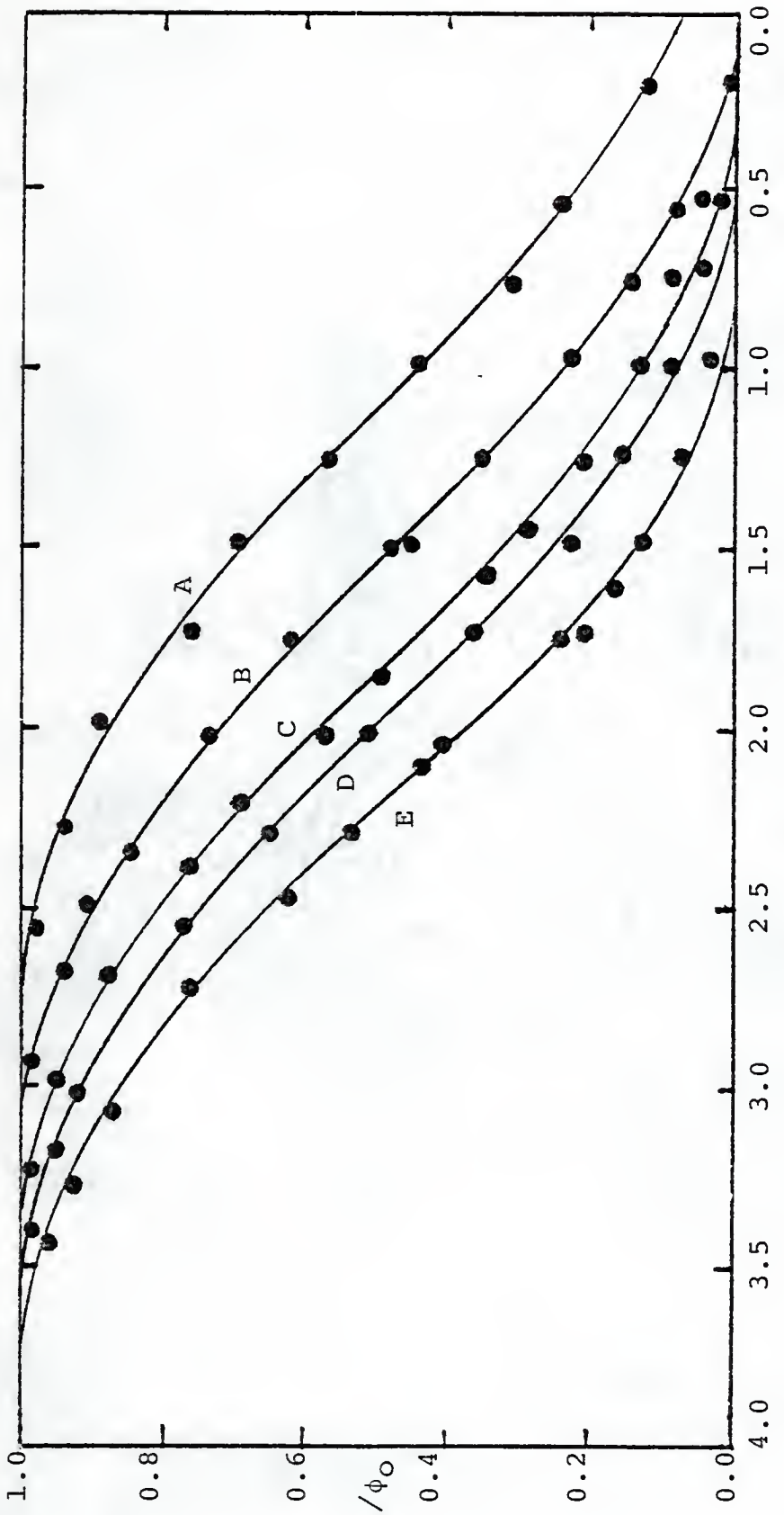
1.0
0.8
0.6
0.4
0.2
0.0
ϕ/ϕ_o
4.0
3.5
3.0
2.5
2.0
1.5
1.0
0.5
0.0
pH
A
B
C
D
E

Figure 3-4

Plot of τ_o'/m versus τ_o for acridone.

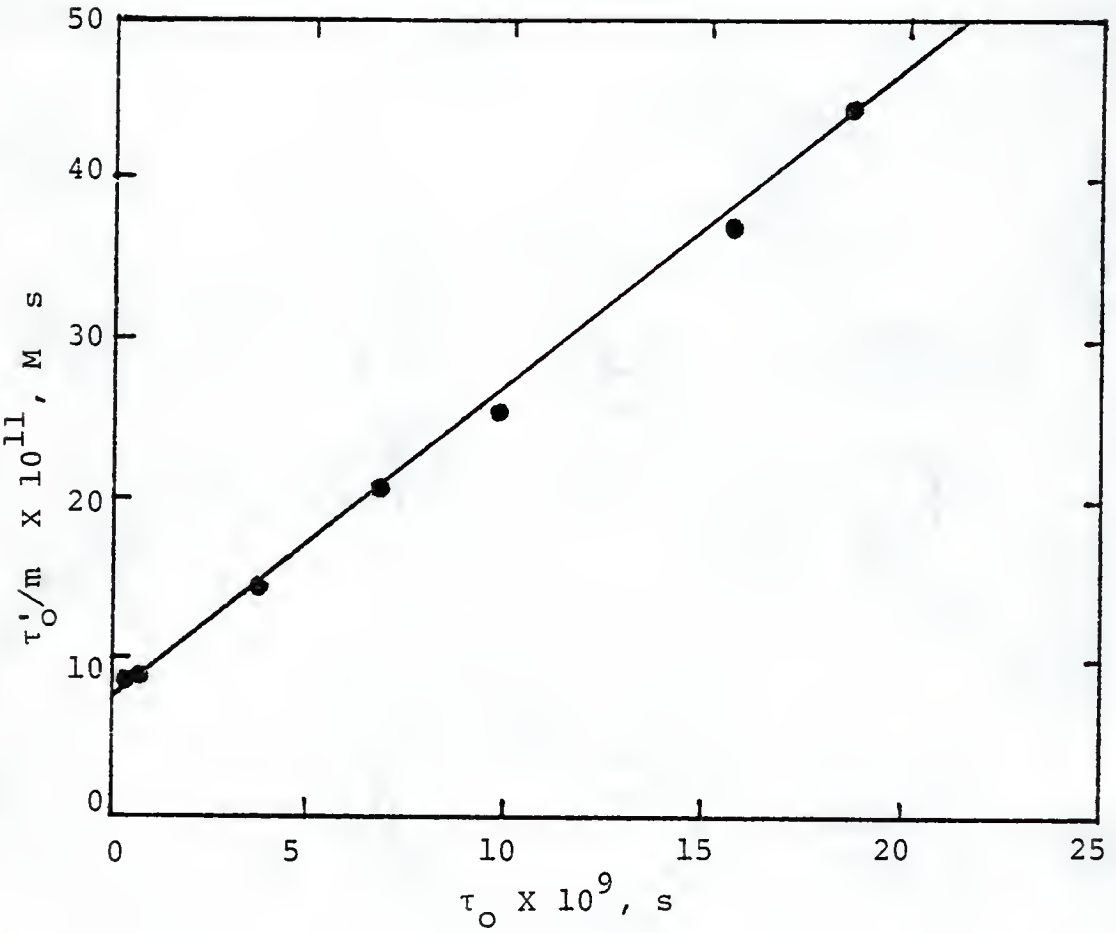
50
40
30
20
10
0
0
5
10
15
20
25
$\tau'_o/m \times 10^{11}$, M s
$\tau_o \times 10^9$, s

Table 3-2

Rate constants and pK_a^* for the excited-state proton transfer between neutral and protonated acridone.

k_a, s^{-1}	k_b, $M^{-1}s^{-1}$	pK_a^*
2.7×10^{8}[a]	1.4×10^{10}[a]	1.71[a]
$2.9 \pm 0.3 \times 10^{8}$[b]	$1.5 \pm 0.1 \times 10^{10}$[b]	1.71 ± 0.04[b]
		1.6 ± 0.3[c]

[a]Determined graphically from Figure 3-3.

[b]Calculated from the data in Table 3-1.

[c]pK_a^*(F.C.), taken from the Förster cycle calculation in reference (31).

$$\frac{1}{k_b} = \frac{\tau'_{o_1}}{m_1} - \frac{k_a}{k_b}\tau_{o_1} \qquad (56)$$

and

$$\frac{1}{k_b} = \frac{\tau'_{o_2}}{m_2} - \frac{k_a}{k_b}\tau_{o_2} \qquad (57).$$

Equations (56) and (57) may be combined to yield

$$k_a/k_b = (\tau'_{o_1}/m_1 - \tau'_{o_2}/m_2)/(\tau_{o_1} - \tau_{o_2}) \qquad (58),$$

so that only two titrations are needed to estimate K_a^*. This value of K_a^* can then be used in conjunction with equation (55) to determine k_b, and then k_a can be calculated. Values of k_a, k_b, and pK_a^* calculated in this way are also presented in Table 3-2. The excellent agreement between pK_a^* and pK_a^*(F.C.) suggests that equations (55-58) may be used with confidence to determine pK_a^* when the excited-state reaction occurs according to mechanism (26) and when $pK_a^* >> pK_a$.

Xanthone (Figure 3-5) has a ground-state ionization in concentrated acid (76,77) and an excited-state ionization in dilute, aqueous solution (76,77). While pK_a has been estimated using the Hammett acidity function without including a_w (76), it has not been seen whether equation (12) is applicable or not. Furthermore, pK_a^* has been

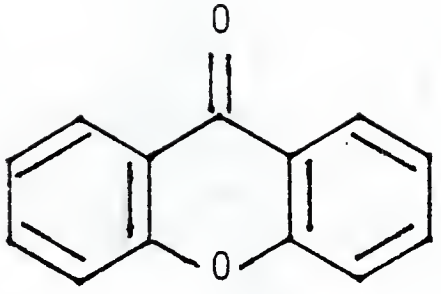

Figure 3-5

Structure of xanthone.

estimated (76), but it was assumed that $pK_a^* = pH$ at the inflection point. Equation (53) shows that this assumption is incorrect.

In terms of absorbances, equation (12) is

$$pK_a = H_o - \log \frac{A - A_{BH^+}}{A_B - A} - (n-r_g)\log a_w \qquad (59),$$

where A is the absorbance anywhere on the inflection region of the titration, and A_{BH^+} and A_B are, respectively, the absorbances of the isolated conjugate acid and base at the analytical wavelength of interest. Equation (59) may be put into antilogarithmic form and rearranged to

$$A = A_{BH^+} + \frac{K_a A_B}{h_o a_w^{n-r_g}} - \frac{K_a A}{h_o a_w^{n-r_g}} \qquad (60),$$

from which it is seen that a multiple linear regression (see Appendix B) may be used to fit for A_{BH^+}, $K_a A_B$, and K_a, and then A_B may also be calculated. A computer program to perform this type of fit was written by the author. The program was constructed to vary integral values of $(n-r_g)$ until a good fit was obtained. The fit was judged to be good when the fitted A_{BH^+} and A_B agreed with the measured A_{BH^+} and A_B and when the coefficient of multiple determination approximated unity. Figure 3-6 shows a spectrophotometric titration curve of xanthone. The titration was fitted using equation (60), and the best fit was obtained with $(n-r_g) = 0$, which yielded $pK_a = -4.17 \pm 0.03$.

Figure 3-6

Plot of absorbance versus H_o for 6.5×10^{-6} M xanthone in H_2SO_4. Analytical wavelength = 329 nm.

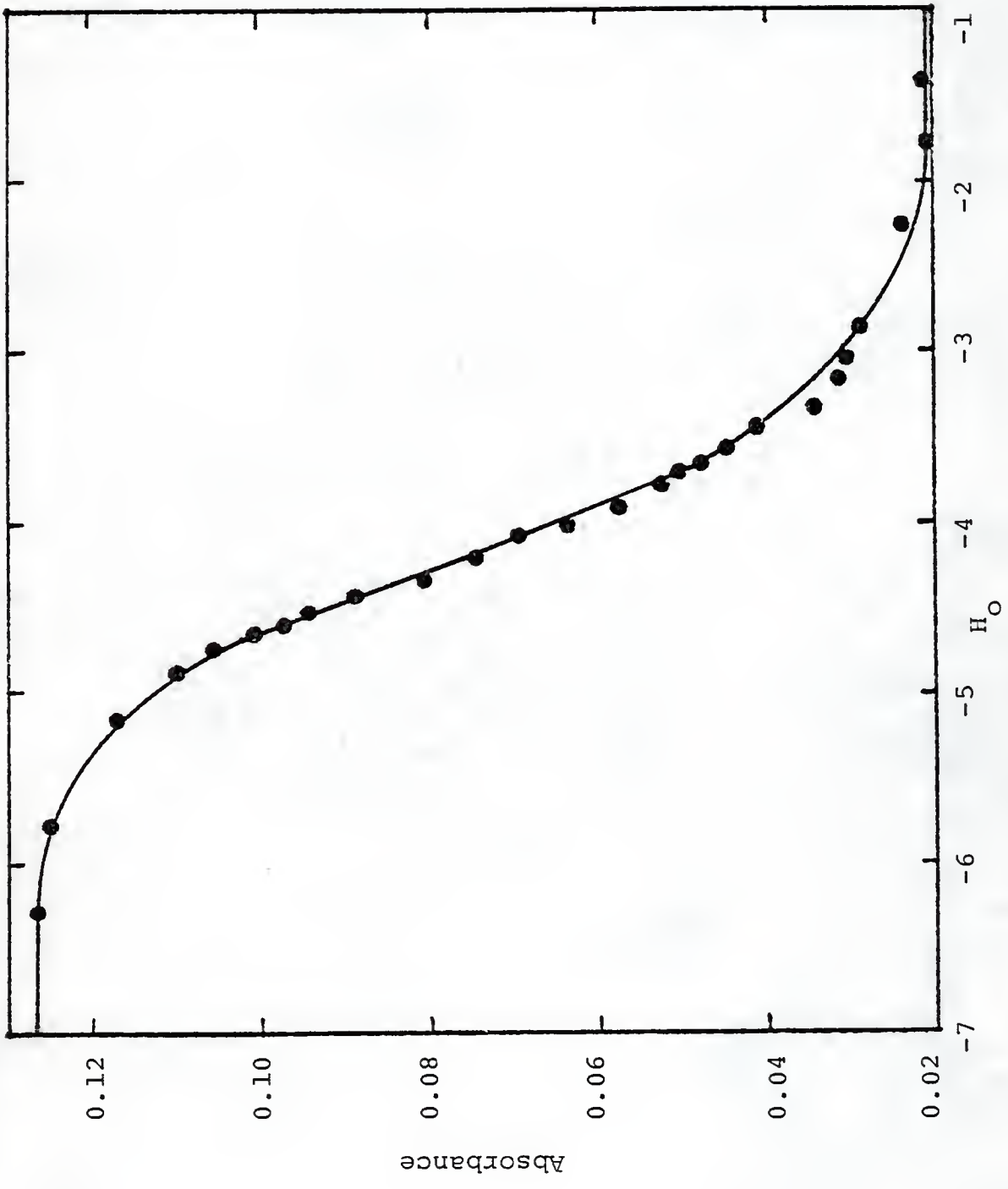
Absorbance
0.12
0.10
0.08
0.06
0.04
0.02
-7
-6
-5
-4
-3
-2
-1
H_o

This value of pK_a agrees with the value of $pK_a = -4.1$ published in reference (76). When $(n-r_g) = 0$, the fit amounts to fitting the data with the Hammett acidity function without including a_w because then $a_w^{n-r_g} = 1$. It is not surprising, therefore, that the pK_a determined in this work agrees with that already published. This does not say that the data should not be fitted with equation (60): it only means that, in this case, $n = r_g$.

Figure 3-7 shows the variation of τ_o and τ_o' with $[Br^-]$. Since τ_o significantly varies while τ_o' remains constant, the titration behavior of xanthone should be similar to that of acridone. Figure 3-8 shows that this is the case, for the titration curve of xanthone shifts to higher pH with increasing Br^- concentration. Table 3-3 presents m (as well as τ_o and τ_o') for xanthone as a function of $[Br^-]$, and Figure 3-9 shows a plot of τ_o'/m versus τ_o for xanthone. Once again, the plot is linear, which indicates that equation (55) is being obeyed. It is possible, therefore, that equation (55) will find general application to molecules of the type under consideration. This method is limited to molecules where τ_o can be varied, but no limitations concerning pH or spectral overlap are apparent at this time.

Table 3-4 presents the absorption and fluorescence maxima of neutral and protonated xanthone. The value of pK_a^*(F.C.) calculated with the value of $pK_a = -4.17$ is

Figure 3-7

Plot of the fluorescence lifetime of 2 X 10^{-6} M xanthone versus bromide ion concentration. (A) τ_o (protonated xanthone), (B) τ_o' (neutral xanthone).

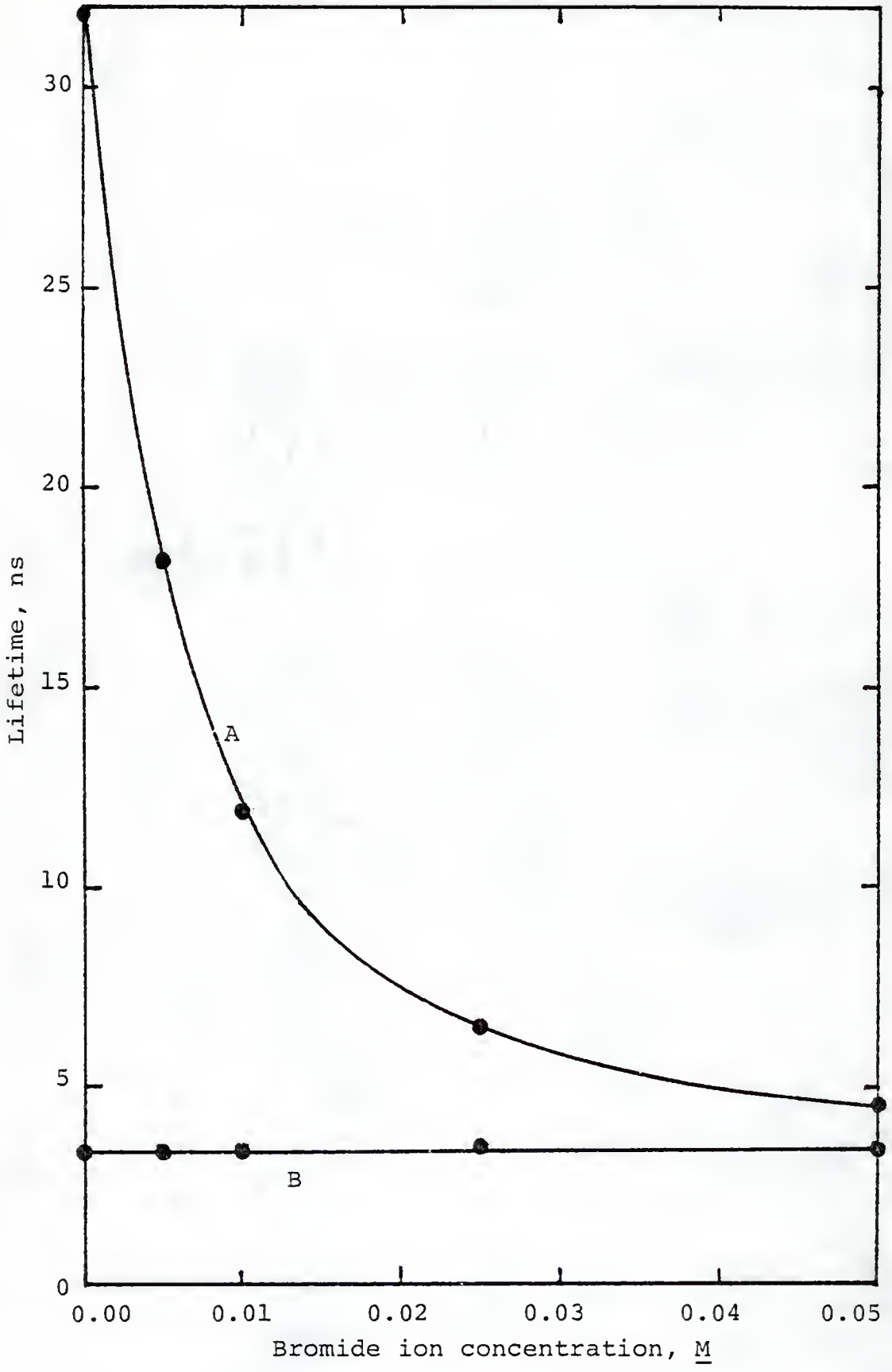
30
25
20
15
10
5
0
Lifetime, ns
A
B
0.00
0.01
0.02
0.03
0.04
0.05
Bromide ion concentration, M

Figure 3-8

Variation of the relative quantum yield of fluorescence (ϕ'/ϕ_o') of 2 X 10^{-6} M neutral xanthone with H_o at various bromide ion concentrations. (A) $[Br^-] = 0$, (B) $[Br^-] = 2.5 \times 10^{-3}$ M, (C) $[Br^-] = 5.0 \times 10^{-3}$ M, (D) $[Br^-] = 1.0 \times 10^{-2}$ M, (E) $[Br^-] = 2.5 \times 10^{-2}$ M. The molecule was titrated with H_2SO_4. Analytical wavelength = 358 nm. Excitation wavelength = 326 nm.

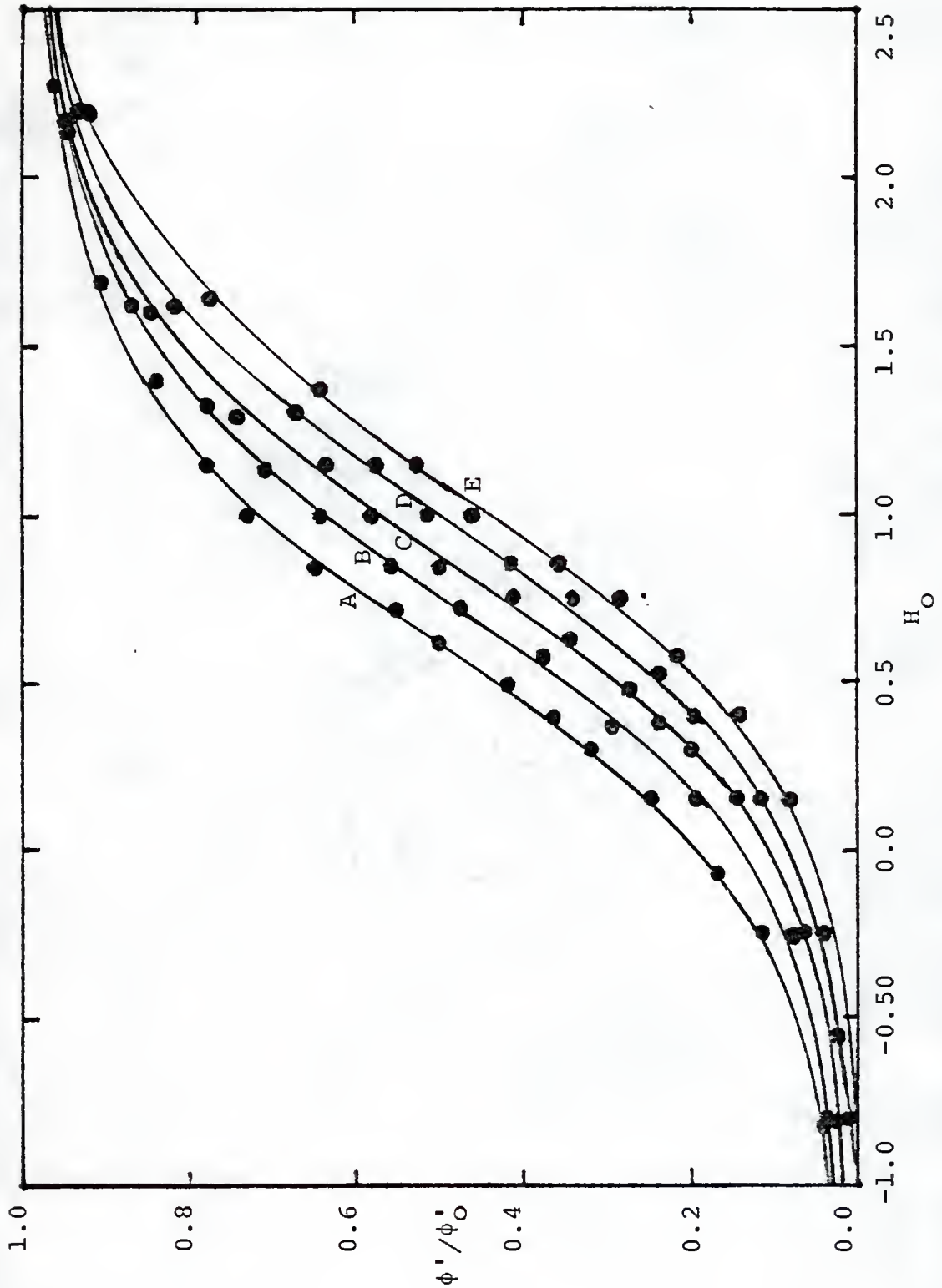
1.0
0.8
0.6
0.4
0.2
0.0
ϕ'/ϕ'_o
-1.0
-0.50
0.0
0.5
1.0
1.5
2.0
2.5
H_o
A
B
C
D
E

Table 3-3

Variation with bromide ion concentration of τ_o', τ_o, and m for xanthone.

$[Br^-]$, M	τ_o', ns[a]	τ_o, ns[b]	m
0	3.4±0.1	31.8±0.8	5.3±0.2
2.5×10^{-3}	3.4[c]	23.3[c]	6.5±0.1
5.0×10^{-3}	3.4±0.1	18.2±0.4	7.4±0.1
1.0×10^{-2}	3.4±0.2	11.8±0.3	9.69±0.08
2.5×10^{-2}	3.5±0.2	6.5±0.4	12.8±0.1

[a]Determined in water, pH = 5.5.

[b]Determined in 4.0 M H_2SO_4, H_o = -1.7.

[c]Estimated from Figure 3-7.

Figure 3-9

Plot of τ_o'/m versus τ_o for xanthone.

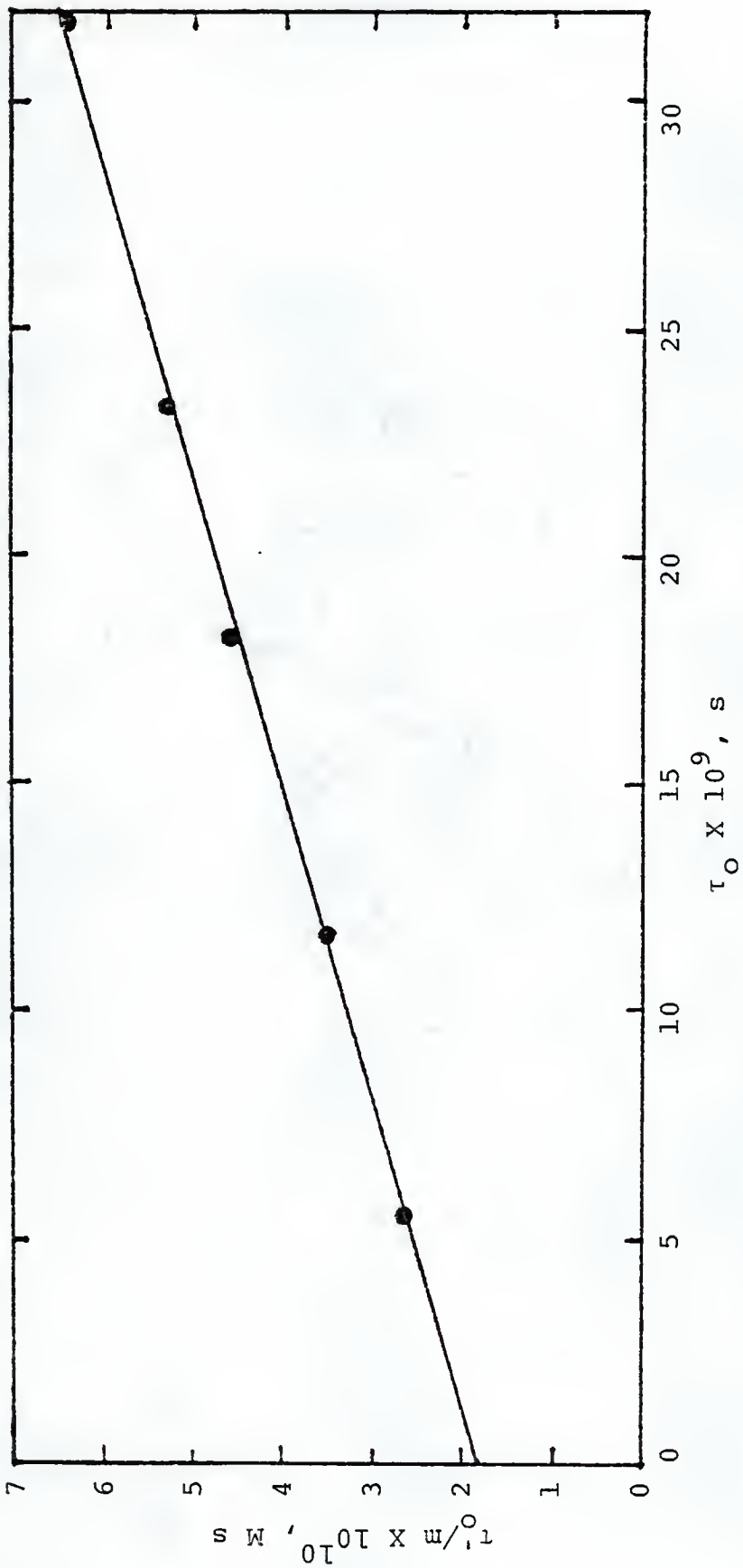
$\tau_o'/m \times 10^{10}$, m s
$\tau_o \times 10^9$, s
0
1
2
3
4
5
6
7
0
5
10
15
20
25
30

Table 3-4

Fluorescence ($\bar{\nu}_f$) and longest wavelength absorption ($\bar{\nu}_a$) maxima of neutral and protonated xanthone.

xanthone species	$\bar{\nu}_a$, cm^{-1}	$\bar{\nu}_f$, cm^{-1}
neutral	2.91×10^4	2.60×10^4
cation	2.57×10^4	2.25×10^4

presented in Table 3-5 along with k_a, k_b, and pK_a^* estimated graphically from Figure 3-9. This value of pK_a^* does not agree with pK_a^*(F.C.). It was observed that the absorption spectrum of isolated neutral xanthone shifts to shorter wavelength (by ≈3 nm) as the medium (H_2SO_4) was changed to more dilute H_2SO_4. This solvent effect on the spectrum of neutral xanthone introduces significant error into the estimation of its 0-0 energy, and hence pK_a^*(F.C.) will also be inaccurate. It thus seems likely that a substantial amount of the discrepancy between pK_a^* and pK_a^*(F.C.) in Table 3-5 is due to the solvent-effect-induced failure of the Förster cycle. The nature of the solvent effect is not known. Since the activity of water in the sulfuric acid in which the solvent effect occurs deviates significantly from unity (65,66), it is possible that the state of hydration of neutral xanthone changes when the medium changes. If a hydration change of this type affects the absorption spectrum, then this explains the solvent effect. If the hydration change is occurring but does not affect the spectrum, then the solvent effect remains unexplained. To date, no experiment has been done which could confirm or disprove the change-in-hydration hypothesis.

It is not possible, therefore, at least in the case of xanthone, to use the Förster cycle to relate the thermodynamics of proton transfer in dilute, aqueous solution

Table 3-5

Ground-state acid-dissociation constant of protonated xanthone and rate constants and pK_a^* for the excited-state proton transfer between neutral and protonated xanthone.

pK_a	k_a, s^{-1}	k_b, $M^{-1}s^{-1}$	pK_a^*
-4.17 ± 0.03[a]	$8.3\pm0.6 \times 10^{7}$[b]	$5.6\pm0.3 \times 10^{9}$[b]	1.83 ± 0.02[b] 3.2 ± 0.3[c]

[a]Determined spectrophotometrically in this work with $(n - r_g) = 0$.

[b]Determined graphically from Figure 3-9.

[c]pK_a^*(F.C.), estimated from the Förster cycle.

to the thermodynamics of proton transfer in concentrated acid. If this is a consequence of changes in hydration of a given reactant, then the standard state of that reactant is different in the ground- and excited-state reactions. If this is the case, then it may not even be thermodynamically correct to predict the value of pK_a^* (or pK_a, if the Förster cycle is used in reverse) in one medium based upon measurements in another. However, it will be seen from other data presented in this dissertation that the Förster cycle is generally quite successful in predicting pK_a^*, even when the ground- and excited-state ionizations occur in media of substantially different acid composition. The behavior of xanthone does, however, suggest that the prediction of the behavior of a molecule in one medium based upon measurements in a different medium should be done only with caution.

CHAPTER IV
EXCITED-STATE PROTON TRANSFER IN 2-QUINOLONE AND 4-QUINOLONE

Introduction

Some molecules become so acidic in their excited states that their excited-state ionizations occur in concentrated acid. As has already been seen in Chapter I, equation (43) will not correctly describe the excited-state proton-transfer reactions of these molecules because k_a and k_b are usually medium-dependent. Therefore, equation (43) must be modified to include the medium-independent rate constants $k_a(0)$ and $k_b(0)$ before the kinetics of excited-state proton transfer in concentrated acid can be quantitated.

The mechanism of the excited-state proton transfer of interest can be written as

$$BH^{+*}(H_2O)_x + rH_2O \rightleftharpoons X^{\pm} \rightleftharpoons B^*(H_2O)_y + H^+(H_2O)_z \quad (61),$$

where x, y, and z are the numbers of water molecules hydrating BH^{+*}, B^*, and H^+, respectively, and $X^{\pm}$ is the transition-state species common to both the protonation and deprotonation reactions. The coefficient r is the number of water molecules which react with hydrated BH^{+*} to form $X^{\pm}$. By mass balance it is seen that $r = y + z - x$, and it is assumed that x, y, z, and r remain constant over the inflection region of a given titration. It is then simpler

to write equation (61) as

$$BH^{+*} + rH_2O \rightleftharpoons X^{\ddagger} \rightleftharpoons B^* + H^+ \qquad (62).$$

If $X_a^{\ddagger}$ is the transition-state subspecies formed by the combination of BH^{+*} with r water molecules and $X_b^{\ddagger}$ is the transition-state subspecies formed by the combination of B^* and H^+, then the equilibrium constants for the formation of $X_a^{\ddagger}$ and $X_b^{\ddagger}$ are, respectively, defined as

$$K_a^{\ddagger} = \frac{[X_a^{\ddagger}] f_x}{[BH^{+*}] f_+ a_w^r} \qquad (63)$$

and

$$K_b^{\ddagger} = \frac{[X_b^{\ddagger}] f_x}{[B^*] f_o a_{H^+}} \qquad (64),$$

where $[X_a^{\ddagger}]$, $[BH^{+*}]$, $[X_b^{\ddagger}]$, and $[B^*]$ are the equilibrium concentrations of $X_a^{\ddagger}$, BH^{+*}, $X_b^{\ddagger}$, and B^*, respectively. The activity coefficients f_+ and f_o correspond to BH^{+*} and B^*, respectively. It is assumed that the activity coefficients of $X_a^{\ddagger}$ and $X_b^{\ddagger}$ are identical. These coefficients are both designated as f_x. The rate of production of BH^{+*}, r_b, and the rate of production of B^*, r_a, are given by

$$r_b = k_b^{\ddagger}[X_b^{\ddagger}] - k_a[BH^{+*}] - \frac{[BH^{+*}]}{\tau_o} \qquad (65)$$

and

$$r_a = k_a^{\ddagger}[X_a^{\ddagger}] - k_b[H^+][B^*] - \frac{[B^*]}{\tau_o'} \qquad (66),$$

where $k_a^{\ddagger}$ is the rate constant for the dissociation of $X_a^{\ddagger}$ in the direction of the conjugate base and $k_b^{\ddagger}$ is the rate constant for the rearrangment of $X_b^{\ddagger}$ in the direction of the conjugate acid. Equation (64) may be combined with (65) to yield

$$r_b = k_b^{\ddagger} K_b^{\ddagger} [B^*] \frac{f_o}{f_x} a_{H^+} - k_a [BH^{+*}] - \frac{[BH^{+*}]}{\tau_o} \quad (67),$$

which becomes

$$r_b = k_b(0) [B^*] \frac{f_o}{f_x} a_{H^+} - k_a [BH^{+*}] - \frac{[BH^{+*}]}{\tau_o} \quad (68).$$

Equations (63) and (66) may be combined to give

$$r_a = k_a^{\ddagger} K_a^{\ddagger} [BH^{+*}] \frac{f_+}{f_x} a_w^r - k_b [H^+] [B^*] - \frac{[B^*]}{\tau_o'} \quad (69),$$

which becomes

$$r_a = k_a(0) [BH^{+*}] \frac{f_+}{f_x} a_w^r - k_b [H^+] [B^*] - \frac{[B^*]}{\tau_o'} \quad (70).$$

It is seen from reaction (26) that r_a and r_b may also be given by

$$r_a = k_a [BH^{+*}] - k_b [H^+] [B^*] - \frac{[B^*]}{\tau_o'} \quad (71)$$

and

$$r_b = k_b [H^+] [B^*] - k_a [BH^{+*}] - \frac{[BH^{+*}]}{\tau_o} \quad (72).$$

Combination of equation (70) with (71) yields

$$k_a = k_a(0) \frac{f_+}{f_x} a_w^r \quad (73),$$

while combination of equations (68) and (72) gives

$$k_b = k_b(0)a_H + \frac{f_o}{f_x} \qquad (74).$$

Equation (8) may be combined with equation (74) to yield

$$k_b = k_b(0)h_o a_w^n \frac{f'_+ f_o}{f_x f'_o} \qquad (75).$$

The medium-dependent rate constants k_a and k_b are thus related to the medium-independent rate constants $k_a(0)$ and $k_b(0)$ by equations (73) and (75), respectively. Substitution of these equations into equation (43) results in

$$\frac{\phi/\phi_o}{\phi'/\phi'_o - \alpha_B} a_w^r = \frac{1}{k_a(0)\tau_o \frac{f_+}{f_x}} + \frac{k_b(0)\tau'_o}{k_a(0)\tau_o} h_o a_w^n \frac{\phi'/\phi'_o}{\phi'/\phi'_o - \alpha_B} \frac{f'_+ f_o}{f_x f'_o} \qquad (76).$$

The activity coefficients f_+, f'_+, and f_x all correspond to singly charged species of similar size while f_o and f'_o correspond to uncharged species of similar size. These similarities in size and identities in charge make it reasonable to assume that $f_+/f_x = f'_+ f_o / f_+ f'_o = 1$, in which case equation (76) becomes

$$\frac{\phi/\phi_o}{\phi'/\phi'_o - \alpha_B} a_w^r = \frac{1}{k_a(0)\tau_o} + \frac{k_b(0)\tau'_o}{k_a(0)\tau_o} h_o a_w^n \frac{\phi'/\phi'_o}{\phi'/\phi'_o - \alpha B} \qquad (77),$$

which should correctly describe the excited-state proton-transfer kinetics of reactions which occur in concentrated acid. A plot of $((\phi/\phi_o)/(\phi_o'/\phi_o'-\alpha_B))a_w^r$ versus $h_o a_w^n(\phi'/\phi_o')/(\phi'/\phi_o'-\alpha_B)$ should be a straight line with an ordinate intercept of $1/k_a(0)\tau_o$ and a slope of $k_b(0)\tau_o'/k_a(0)\tau_o$.

Several molecules (78) which have excited ionizations which occur in acid such that the inflection points are found at pH < 1 are 2-quinolone (Figure 4-1) and 4-quinolone (Figure 4-2). It is of interest to see whether or not these ionizations are described by equation (77).

Results and Discussion

The absorption and fluorescence maxima of neutral and protonated 2-quinolone, as well as their fluorescence lifetimes, are presented in Table 4-1. The spectrophotometric titration of 2-quinolone is shown in Figure 4-3. These titration data were best fitted according to equation (60) with $(n-r_g) = 4$, which yielded $pK_a = -0.30\pm0.03$.

Figure 4-4 shows the fluorimetric titration curve of 2-quinolone. Figures 4-5 and 4-6 show plots of $((\phi/\phi_o)/(\phi'/\phi_o'-\alpha_B))a_w^r$ versus $h_o a_w^n(\phi'/\phi_o')/(\phi'/\phi_o'-\alpha_B)$ for 2-quinolone with various values of r and n = 3 (Figure 4-5) or n = 4 (Figure 4-6). Values of ϕ'/ϕ_o' for both 2-quinolone and 4-quinolone were calculated according to the

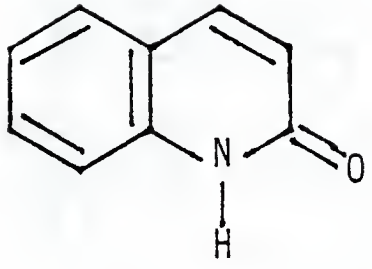

Figure 4-1

Structure of 2-quinolone.

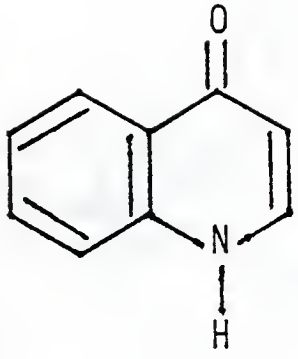

Figure 4-2

Structure of 4-quinolone.

Table 4-1

Fluorescence ($\bar{\nu}_f$) and longest wavelength absorption ($\bar{\nu}_a$) maxima and fluorescence lifetimes of neutral and protonated 2-quinolone.

2-quinolone species	$\bar{\nu}_a$, cm^{-1}	$\bar{\nu}_f$, cm^{-1}	fluorescence lifetime, ns
neutral	3.12×10^4	2.72×10^4	2.1 ± 0.2[a]
cation	3.33×10^4	2.65×10^4	10.4 ± 0.5[b]

[a] τ_o', measured in water, pH = 2.0.

[b] τ_o, measured in 7.5 $\underline{M}$ H_2SO_4, $H_o = -4.0$.

Figure 4-3

Plot of absorbance versus H_o for 1 X 10^{-4} M 2-quinolone in H_2SO_4. Analytical wavelength = 269 nm.

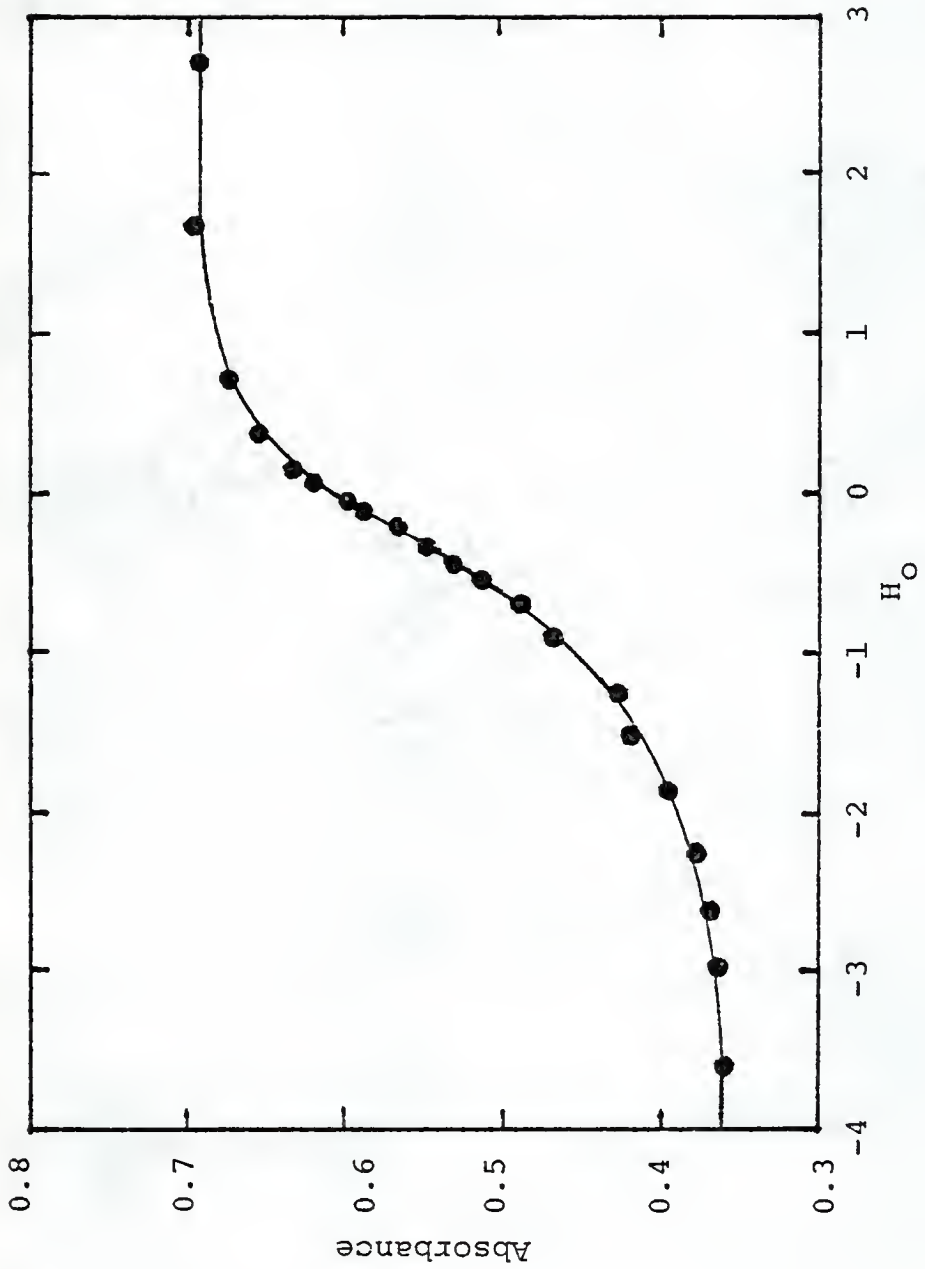
Absorbance
0.8
0.7
0.6
0.5
0.4
0.3
-4
-3
-2
-1
0
1
2
3
H_O

Figure 4-4

Plot of the relative quantum yield of fluorescence (ϕ/ϕ_o) of 3 X 10^{-5} M protonated 2-quinolone in $HClO_4$ versus H_o. Analytical wavelength = 370 nm. Excitation wavelength = 280 nm (isosbestic point).

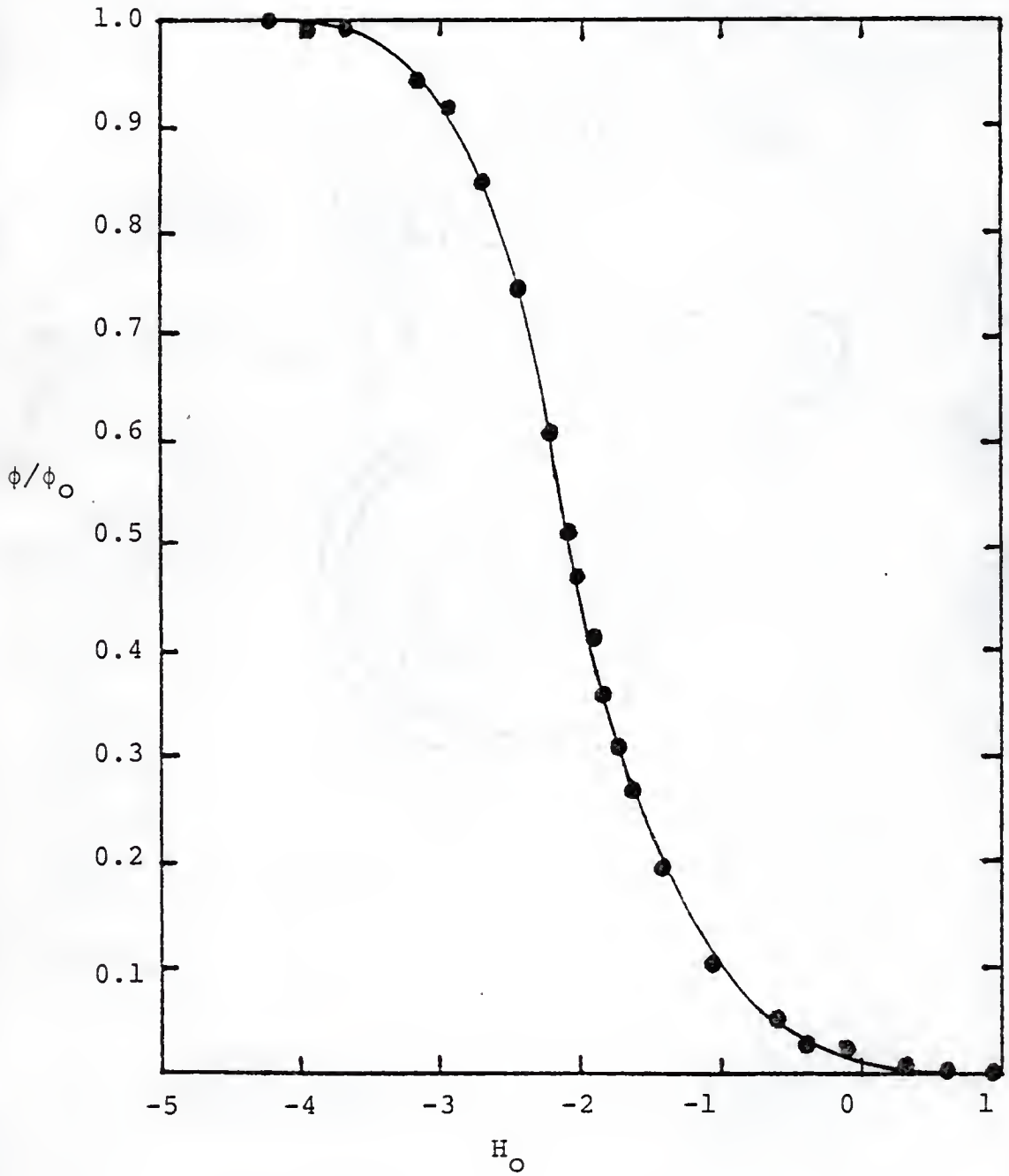
1.0
0.9
0.8
0.7
0.6
ϕ/ϕ_o
0.5
0.4
0.3
0.2
0.1
-5
-4
-3
-2
-1
0
1
H_o

Figure 4-5

Plot of $((\phi/\phi_o)/(\phi'/\phi_o'-\alpha_B))a_w^r$ versus $h_o a_w^n(\phi'/\phi_o')/(\phi'/\phi_o'-\alpha_B)$ for 2-quinolone with n = 3. (A) r = 1, (B) r = 2, (C) r = 3, (D) r = 4, (E) r = 5.

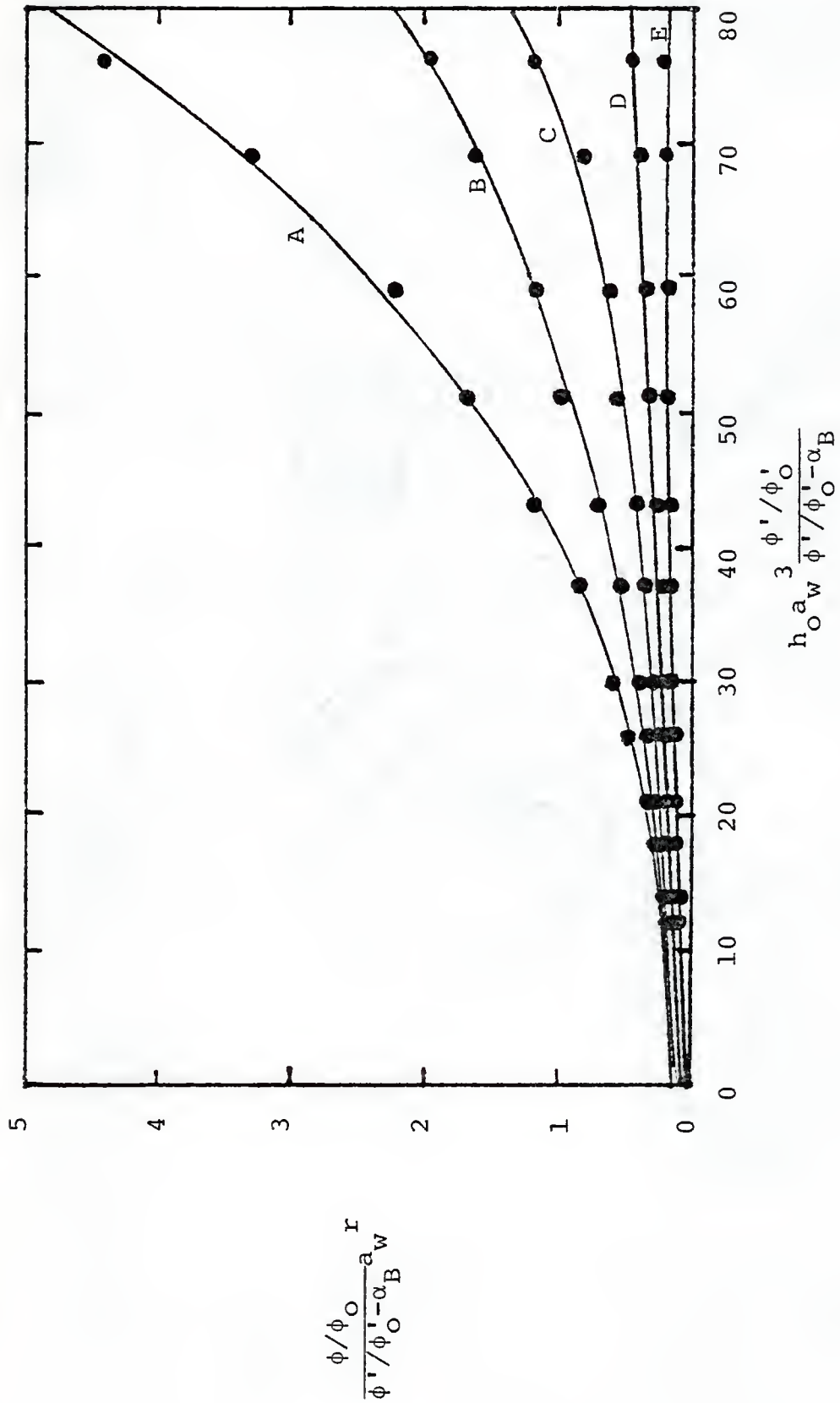
A
B
C
D
E
0
1
2
3
4
5
0
10
20
30
40
50
60
70
80
$\frac{\phi/\phi_o}{\phi'/\phi'_o-\alpha_B} a_w^r$
$h_o a_w^3 \frac{\phi'/\phi'_o}{\phi'/\phi'_o-\alpha_B}$

Figure 4-6

Plot of $((\phi/\phi_o)/(\phi'/\phi_o'-\alpha_B))a_w^r$ versus $h_o a_w^n(\phi'/\phi_o')/(\phi'/\phi_o'-\alpha_B)$ for 2-quinolone with n = 4. (A) r = 1, (B) r = 2, (C) r = 3, (D) r = 4, (E) r = 5, (F) r = 6.

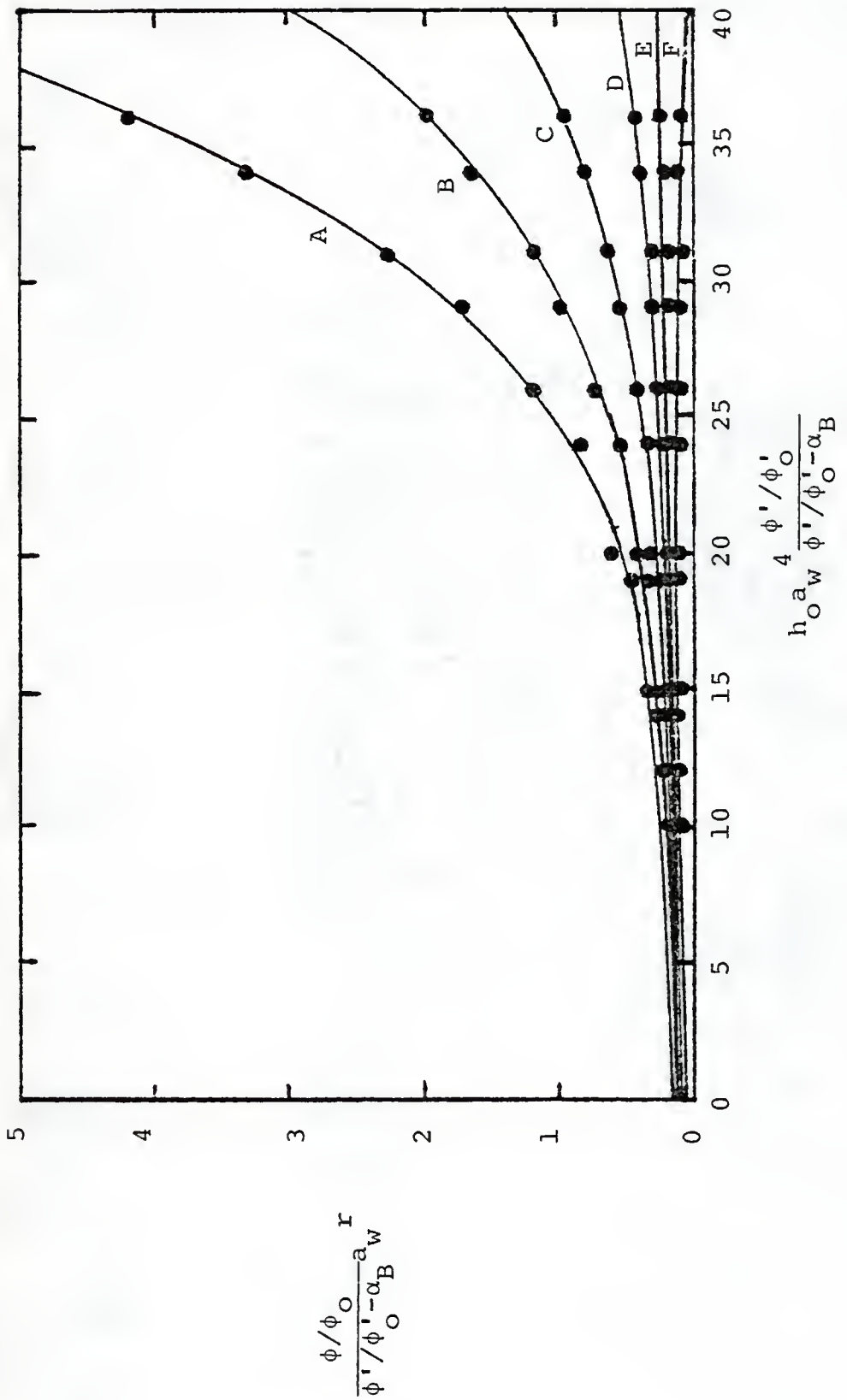
A
B
C
D
E
F
0
1
2
3
4
5
0
5
10
15
20
25
30
35
40
$\frac{\phi/\phi_o}{\phi'/\phi'_o - \alpha_B} a_w^r$
$h_o a_w^4 \frac{\phi'/\phi'_o}{\phi'/\phi'_o - \alpha_B}$

relationship $\phi'/\phi_o' = 1 - \phi/\phi_o$ because the fluorescence spectra of the protonated species overlap and eclipse those of the neutral species. It can be seen that most combinations of n and r result in curved plots. The best fit to a straight line (chosen on the basis of the highest linear least-squares correlation coefficient--see Appendix A) was obtained with n = 3 and r = 4 (plot D in Figure 4-5). The linearity of plot D in Figure 4-5 suggests several things. In the first place, the titration data of 2-quinolone in concentrated acid are fitted well with equation (77), which suggests that the model is valid. Secondly, the assumption that $f_+/f_x = f_+'f_o/f_xf_o' = 1$ is probably a good assumption. Thirdly, the value of n in reaction (7) for this region of acidity is n = 3 and the value of r in reaction (62) is r = 4 for 2-quinolone. These observations are consistent with the values of n = 3 and n = 4 proposed by Teng and Lenzi (79) and by Bascombe and Bell (80) for solutions in which $H_o > -3.5$. Values of $k_a(0)$, $k_b(0)$, and $pK_a^*(0) = -\log(k_a(0)/k_b(0))$ are presented in Table 4-2, along with pK_a^*(F.C.) and pK_a.

The fluorescence lifetimes and spectral maxima of neutral and protonated 4-quinolone are presented in Table 4-3. The fluorescence lifetime, τ_o', of neutral 4-quinolone was estimated with the Strickler-Berg equation (81). The ratio of the radiative lifetimes of protonated and neutral 4-quinolone (estimated with the Strickler-Berg equation),

Table 4-2

Ground-state acid-dissociation constant of protonated 2-quinolone and rate constants and pK_a^* for the excited-state proton transfer between neutral and protonated 2-quinolone.

pK_a	$k_a(0)$, s^{-1}	$k_b(0)$, $M^{-1}s^{-1}$	pK_a^*
-0.30 ± 0.03[a]	$4\pm1 \times 10^{9}$[b]	$1.0\pm0.3 \times 10^{8}$[b]	-1.58 ± 0.06[c]
			-1.8 ± 0.3[d]

[a] Determined spectrophotometrically in this work with $(n - r_g) = 4$.

[b] Determined graphically from Figure 4-5 with $n = 3$ and $r = 4$.

[c] $pK_a^*(0)$, determined graphically from Figure 4-5 with $n \cong 3$ and $r = 4$.

[d] pK_a^*(F.C.), estimated with the Förster cycle.

Table 4-3

Fluorescence ($\bar{\nu}_f$) and longest wavelength absorption ($\bar{\nu}_a$) maxima and fluorescence lifetimes of neutral and protonated 4-quinolone.

4-quinolone species	$\bar{\nu}_a$, cm^{-1}	$\bar{\nu}_f$, cm^{-1}	fluorescence lifetime, ns
neutral	3.04×10^4	2.98×10^4	0.79 ± 0.04[a]
cation	3.32×10^4	2.76×10^4	21 ± 1[b]

[a] τ_o', estimated with the Strickler-Berg equation.

[b] τ_o, measured in 5.9 M $HClO_4$, $H_o = -2.8$.

the ratio of their quantum yields, and the measured value of τ_o were used in this calculation. The absorption and fluorescence spectra of 4-quinolone exhibit a fairly good mirror-image relationship and a small Stokes shift; hence, the value of τ_o' estimated with the Strickler-Berg equation is reasonably accurate (82-84).

Figure 4-7 shows the spectrophotometric titration of 4-quinolone. This ground-state ionization occurs in dilute, aqueous solution, and hence the titration data were fitted using equation (60) with $a_w = 1$, in which equation (60) reduces to an antilogarithmic form of the Henderson-Hasselbach equation. This analysis yielded $pK_a = 2.22 \pm 0.01$.

The fluorimetric titration curve of 4-quinolone is shown in Figure 4-8. The small step in the titration curve at pH $\simeq$ 2 is probably the result of a vanishingly small rate of protonation of the excited neutral molecule at that pH and higher pH (56). The titration data of 4-quinolone plotted according to equation (77) are shown for n = 3 in Figure 4-9 and n = 4 in Figure 4-10, with r taking various values in each figure. The activity of water significantly deviates from unity only in the most acidic portion of the fluorimetric titration of 4-quinolone, and hence it is expected that the inclusion of a_w in the kinetic treatment will not make as dramatic a difference as it did with 2-quinolone. This is the case; indeed, plots B (n = 4, r = 3) and C (n = 4, r = 4) in Figure 4-10 are

Figure 4-7

Plot of absorbance versus pH for 1 X 10^{-4} M 4-quinolone in water. Analytical wavelength = 327 nm.

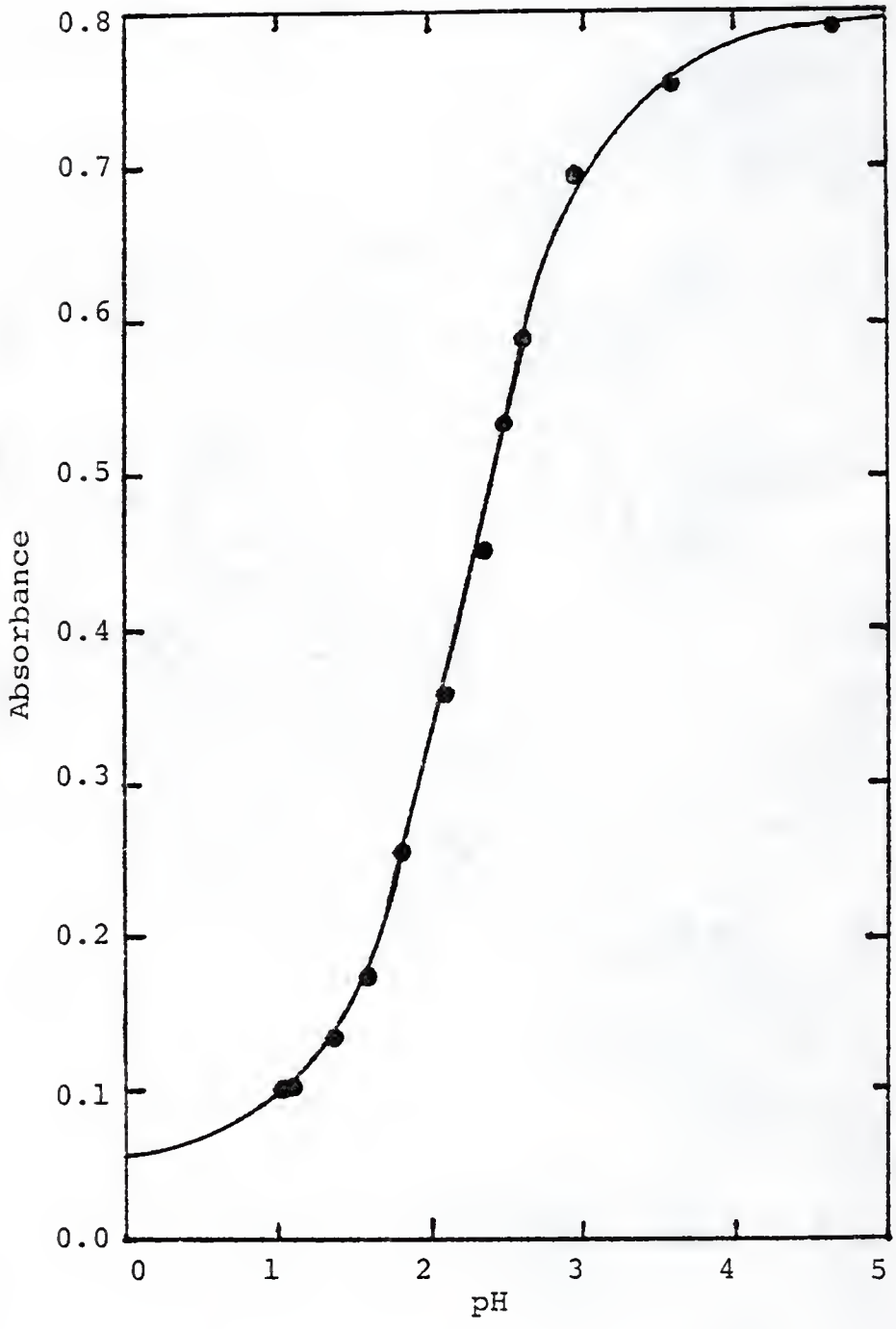
0.8
0.7
0.6
0.5
0.4
0.3
0.2
0.1
0.0
Absorbance
0
1
2
3
4
5
pH

Figure 4-8

Plot of the relative quantum yield of fluorescence (ϕ/ϕ_o) of 3 X 10^{-5} M protonated 4-quinolone versus H_o. The molecule was titrated with $HClO_4$. Analytical wavelength = 360 nm. Excitation wavelength = 302 nm (isosbestic point).

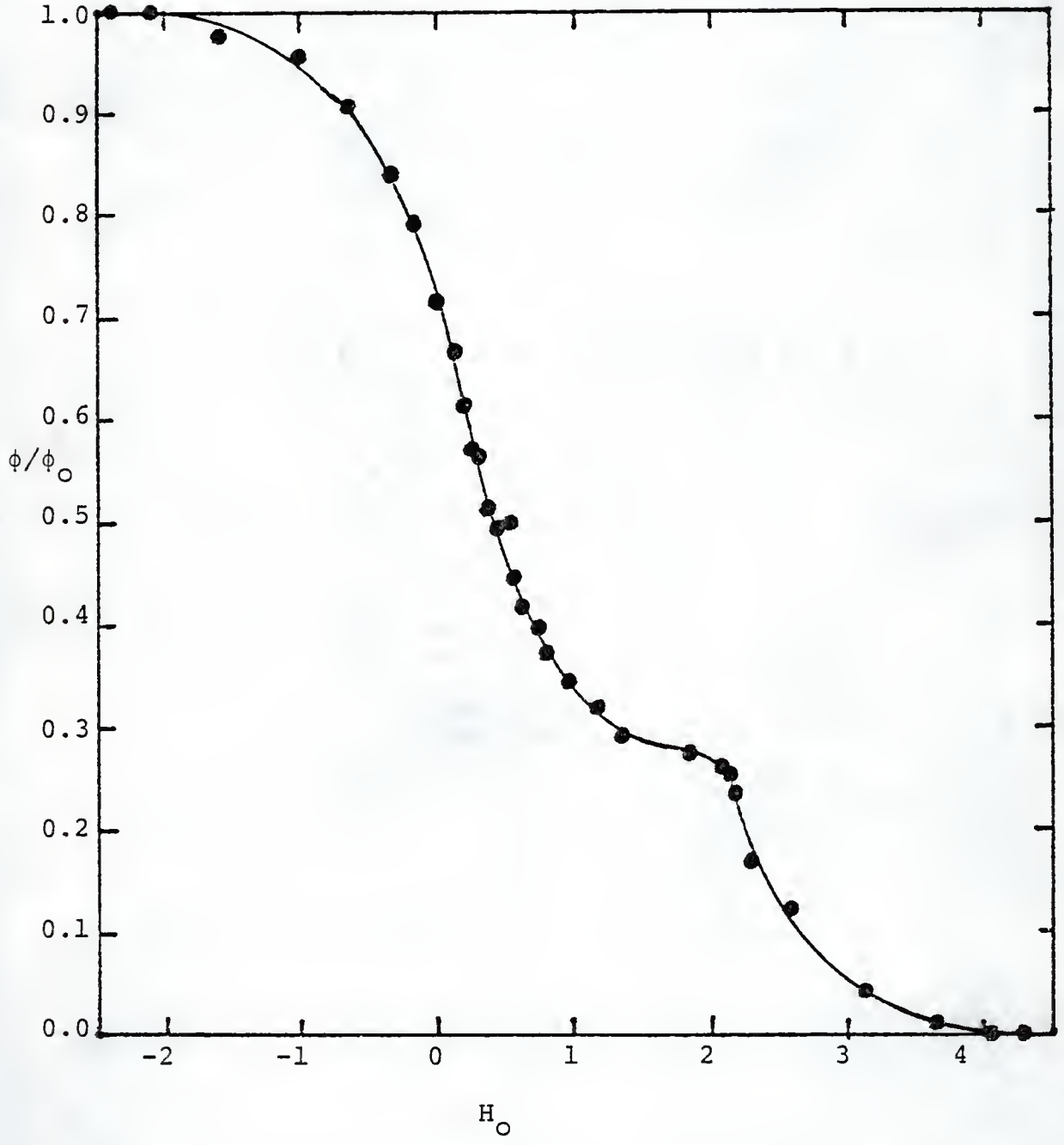
1.0
0.9
0.8
0.7
0.6
ϕ/ϕ_o
0.5
0.4
0.3
0.2
0.1
0.0
-2
-1
0
1
2
3
4
H_o

Figure 4-9

Plot of $((\phi/\phi_o)/(\phi'/\phi_o'-\alpha_B))a_w^{\ r}$ versus $h_o a_w^{\ n}(\phi'/\phi_o')/(\phi'/\phi_o'-\alpha_B)$ for 4-quinolone with n = 3. (A) r = 1, (B) r = 2, (C) r = 3, (D) r = 4, (E) r = 5.

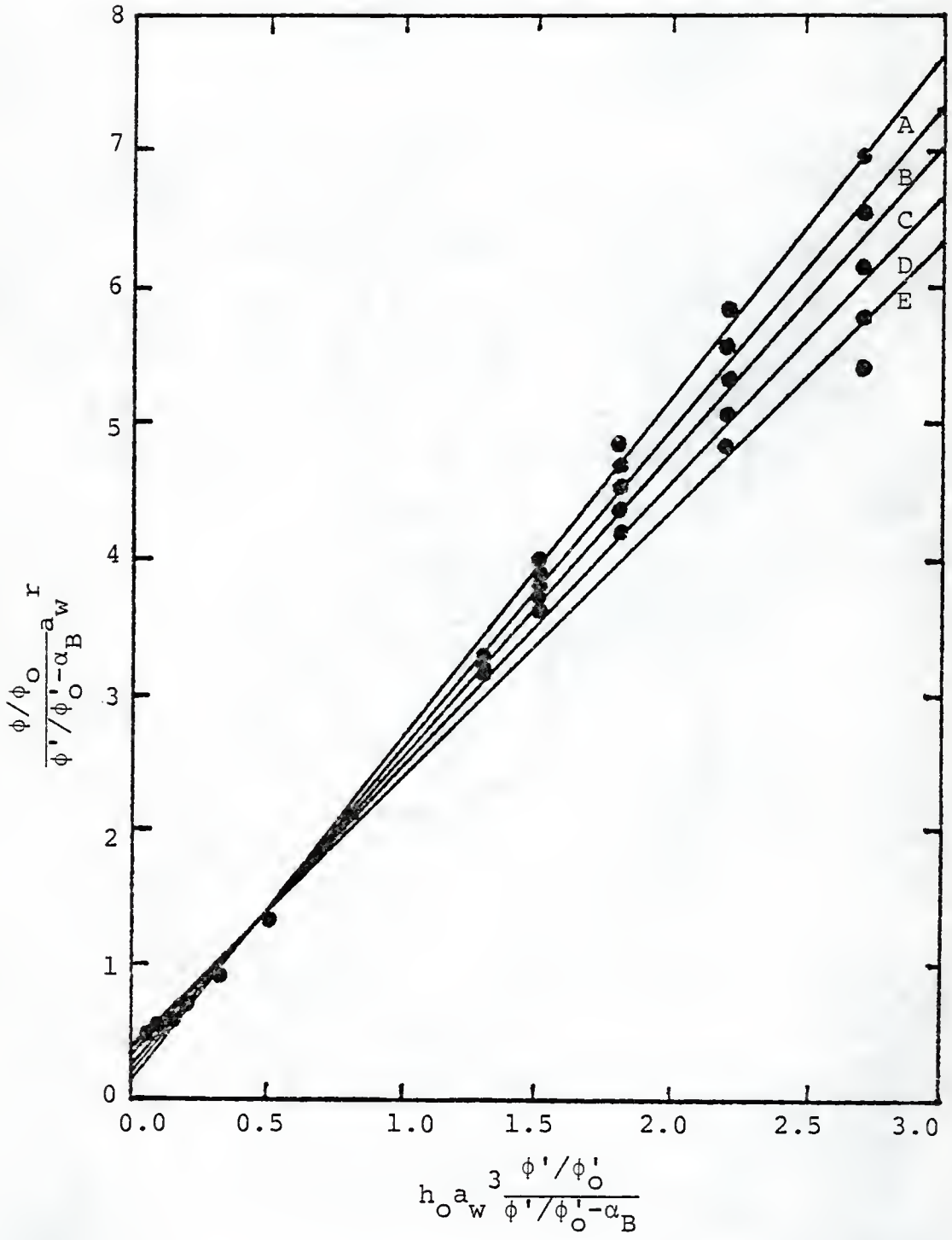
8
7
6
5
4
3
2
1
0
0.0
0.5
1.0
1.5
2.0
2.5
3.0
A
B
C
D
E
$\frac{\phi/\phi_o}{\phi'/\phi'_o-\alpha_B} a_w^r$
$h_o a_w^3 \frac{\phi'/\phi'_o}{\phi'/\phi'_o-\alpha_B}$

Figure 4-10

Plot of $((\phi/\phi_o)/(\phi'/\phi_o'-\alpha_B))a_w^r$ versus $h_o a_w^n(\phi'/\phi_o')/(\phi'/\phi_o'-\alpha_B)$ for 4-quinolone with n = 4. (A) r = 2, (B) r = 3, (C) r = 4, (D) r = 5, (E) r = 6.

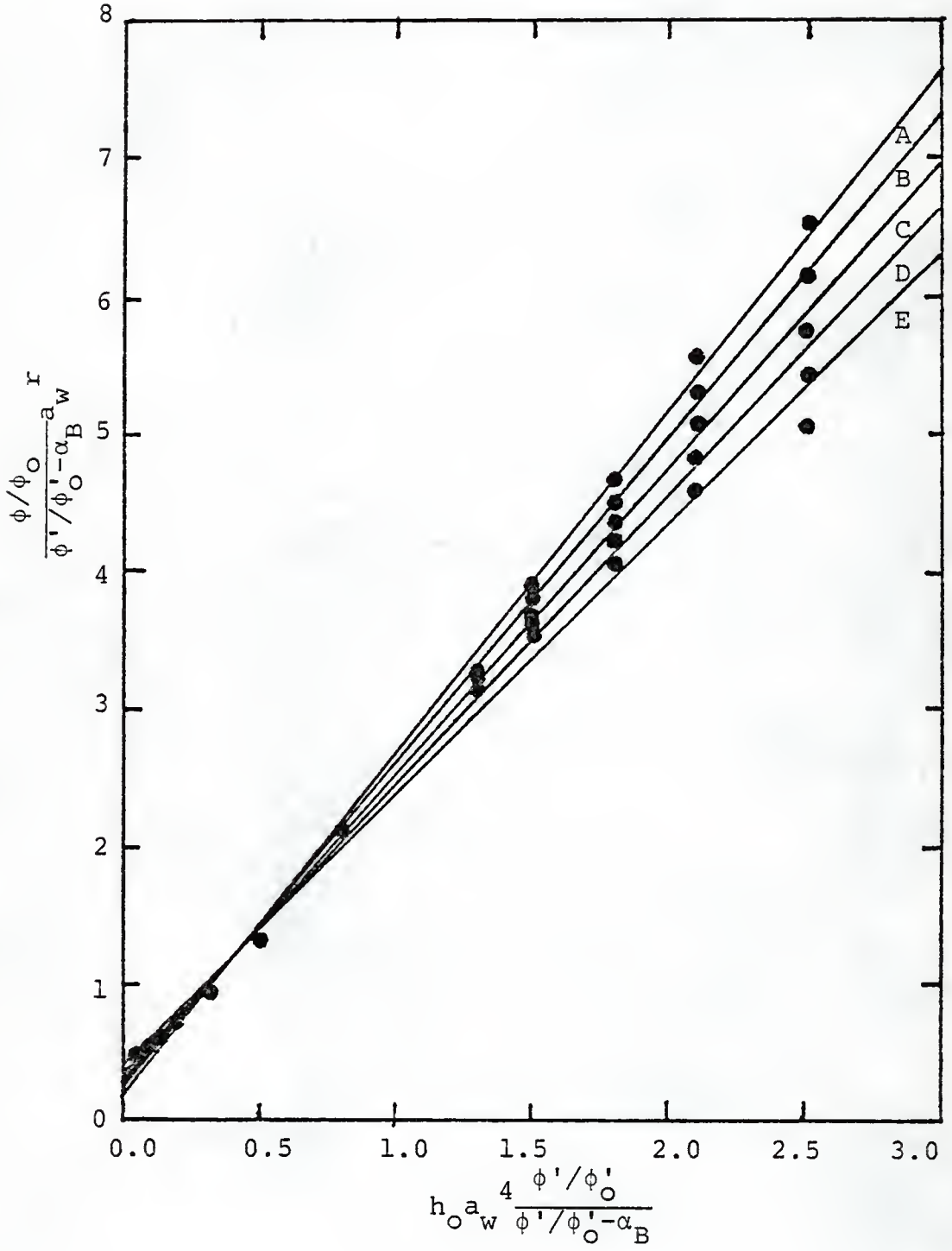
8
7
6
5
4
3
2
1
0
0.0
0.5
1.0
1.5
2.0
2.5
3.0
A
B
C
D
E
$\frac{\phi/\phi_o}{\phi'/\phi_o'-\alpha_B}^{a_w}$
$h_o a_w \frac{4\,\phi'/\phi_o'}{\phi'/\phi_o'-\alpha_B}$

identically straight lines. It is not possible, therefore, to discern whether it is three or four water molecules which react with the hydrated, protonated 4-quinolone in the deprotonation step of the excited-state reaction. The value of n = 4, however, is still in keeping with the values of n previously proposed (79,80) for the region of acidity in which the excited-state proton transfer of 4-quinolone occurs. It is not surprising that n was found to be three in the case of 2-quinolone but four in the case of 4-quinolone because the Hammett indicators (9) which were used to define the Hammett acidity function in these respective regions of acidity are different and their deprotonation reactions may have different hydration requirements. This is reasonable not only because of structural differences between the indicators, but also because the activity of water at the inflection point of the fluorimetric titration of 4-quinolone ($a_w \simeq 0.98$) is quite different from that at the inflection point of the fluorimetric titration of 2-quinolone ($a_w \simeq 0.66$). These differences in the availability of water could result in different numbers of water molecules entering into reactions which occur in solutions of significantly different acid composition.

If the various indicator and quinolone species each have several different hydrates, then it is possible that n and r are not constant, in which case equation (77)

would not correctly describe the excited-state chemistry of interest. Since the plots obtained with equation (77) are linear, it appears that, at least to a first approximation, n and r may be considered to be constant.

Values of $k_a(0)$, $k_b(0)$, and $pK_a^*(0)$ for 4-quinolone with n = 4 and r = 3 and also with n = 4 and r = 4 are presented in Table 4-4 (pK_a and pK_a^*(F.C.) are also shown in Table 4-4). The agreement between $pK_a^*(0)$ and pK_a^*(F.C.) for the excited-state ionizations of 2-quinolone and 4-quinolone further suggests that the model under consideration is valid. Furthermore, it suggests that the Förster cycle can be used with some confidence to relate the acid-base properties of a molecule in one medium to those properties in another. In the cases of 2-quinolone and 4-quinolone, at least two sets of circumstances are consistent with the latter suggestion. Firstly, it is possible that the hydrations of the quinolone species do not change with changing acid concentration (at least not over the concentration ranges studied in this work). Secondly, it is possible that their hydrations do change, but that they change in such a way that the standard free energies of all the species involved in a given reaction change by the same amount when going from one medium to another. These changes would cancel out and would not be apparent in the estimation of pK_a^* with the Förster cycle. Once again,

Table 4-4

Ground-state acid-dissociation constant of protonated 4-quinolone and rate constants and pK_a^* for the excited-state proton transfer between neutral and protonated 4-quinolone.

pK_a	$k_a(0)$, s^{-1}	$k_b(0)$, $M^{-1}s^{-1}$	pK_a^*
2.22±0.01[a]	2.0±0.6 X 10^8[b]	1.3±0.5 X 10^{10}[b]	1.80±0.08[c]
	1.7±0.5 X 10^8[d]	1.0±0.3 X 10^{10}[d]	1.77±0.05[e]
			1.7±0.3[f]

[a]Determined spectrophotometrically in this work. The value of $(n - r_g)$ could not be determined since $a_w = 1$ over the inflection region of the titration.

[b]Determined graphically from Figure 4-10 with n = 4 and r = 3.

[c]$pK_a^*(0)$, determined graphically from Figure 4-10 with n = 4 and r = 3.

[d]Determined graphically from Figure 4-10 with n = 4 and r = 4.

[e]$pK_a^*(0)$, determined graphically from Figure 4-10 with n = 4 and r = 4.

[f]pK_a^*(F.C.), estimated with the Förster cycle.

it has not yet been determined if the actual circumstance is the first, second, or some other yet unconsidered possibility.

Finally, the excited-state proton-transfer reactions of both 2-quinolone and 4-quinolone do not attain equilibrium within the lifetimes of their lowest excited singlet states. This is intuitively obvious from the fact that the rate constants for the protonation and deprotonation steps were measurable. A quantitative explanation of this conclusion is found in the next chapter, where the criteria for and the implications of the establishment of equilibrium within the lifetime of the excited state will be discussed.

CHAPTER V
EQUILIBRIUM EXCITED-STATE PROTON TRANSFER IN 1-ISOQUINOLONE

Introduction

When the rates of the excited-state protonation and deprotonation reactions are equal, the excited-state reaction is at prototropic equilibrium. It has been shown (85) that $1/k_a(0)\tau_o \rightarrow 0$ when this condition is met. Equation (77) then reduces to

$$\frac{\phi/\phi_o}{\phi'/\phi_o' - \alpha_B} a_w^r = \frac{k_b(0)\tau_o'}{k_a(0)\tau_o} h_o a_w^n \frac{\phi'/\phi_o'}{\phi'/\phi_o' - \alpha_B} \qquad (78).$$

A plot of $((\phi/\phi_o)/(\phi'/\phi_o' - \alpha_B))a_w^r$ versus $h_o a_w^n (\phi'/\phi_o')/(\phi'/\phi_o' - \alpha_B)$ will thus pass through the origin (that is, the ordinate intercept will be zero). The value of the intercept, therefore, may be used as a diagnostic to determine whether or not a given excited-state proton-transfer reaction attains equilibrium within the lifetime of the excited state. The closer the reaction is to equilibrium, the closer to zero will be the intercept of data plotted according to equation (77). Since the ordinate intercept of plot D in Figure 4-5 and the intercepts of plots B and C in Figure 4-10 are not zero, it may be concluded that the excited-state proton-transfer reactions of 2-quinolone and 4-quinolone do not

attain equilibrium within the lifetimes of their excited states. A molecule which demonstrates excited-state prototropic equilibrium is 1-isoquinolone (Figure 5-1) (86).

Results and Discussion

The fluorescence lifetimes and absorption and fluorescence maxima of neutral and protonated 1-isoquinolone are presented in Table 5-1. Figure 5-2 shows the absorptiometric titration of 1-isoquinolone. These data were best fitted according to equation (60) with $(n - r_g) = 1$, which gave a value of $pK_a = -1.38 \pm 0.03$.

The fluorimetric titration of 1-isoquinolone is shown in Figure 5-3. The fluorescence spectra of neutral and protonated 1-isoquinolone show considerable overlap, and thus ϕ'/ϕ_o' was calculated according to the relationship $\phi'/\phi_o' = 1 - \phi/\phi_o$. Figure 5-4 shows the fluorimetric titration data of 1-isoquinolone plotted according to equation (77) with n = 2 and r = 2. The plot is a straight line which passes through the origin, and it is concluded that the excited-state proton-transfer reaction of 1-isoquinolone attains equilibrium within the lifetime of the excited state.

Examination of equation (78) shows that, when a given excited-state proton transfer attains equilibrium, then all plots of $((\phi/\phi_o)/(\phi'/\phi_o'-\alpha_B))a_w^r$ versus $h_o a_w^n(\phi'/\phi_o')/(\phi'/\phi_o'-\alpha_B)$ will have the same slope and intercept regardless of the values of n and r as long as

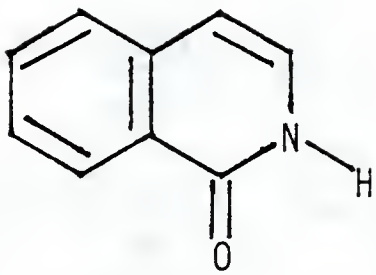

Figure 5-1

Structure of 1-isoquinolone.

Table 5-1

Fluorescence ($\bar{\nu}_f$) and longest wavelength absorption ($\bar{\nu}_a$) maxima and fluorescence lifetimes of neutral and protonated 1-isoquinolone.

1-isoquinolone species	$\bar{\nu}_a$, cm^{-1}	$\bar{\nu}_f$, cm^{-1}	fluorescence lifetime, ns
neutral	3.10×10^4	2.73×10^4	2.0 ± 0.1[a]
cation	3.21×10^4	2.77×10^4	2.6 ± 0.1[b]

[a] τ_o', measured in water, pH = 1.7.

[b] τ_o, measured in 8.4 $\underline{M}$ H_2SO_4, H_o = -4.1.

Figure 5-2

Plot of absorbance versus H_o for 1 X 10^{-4} M 1-isoquinolone in H_2SO_4. Analytical wavelength = 275 nm.

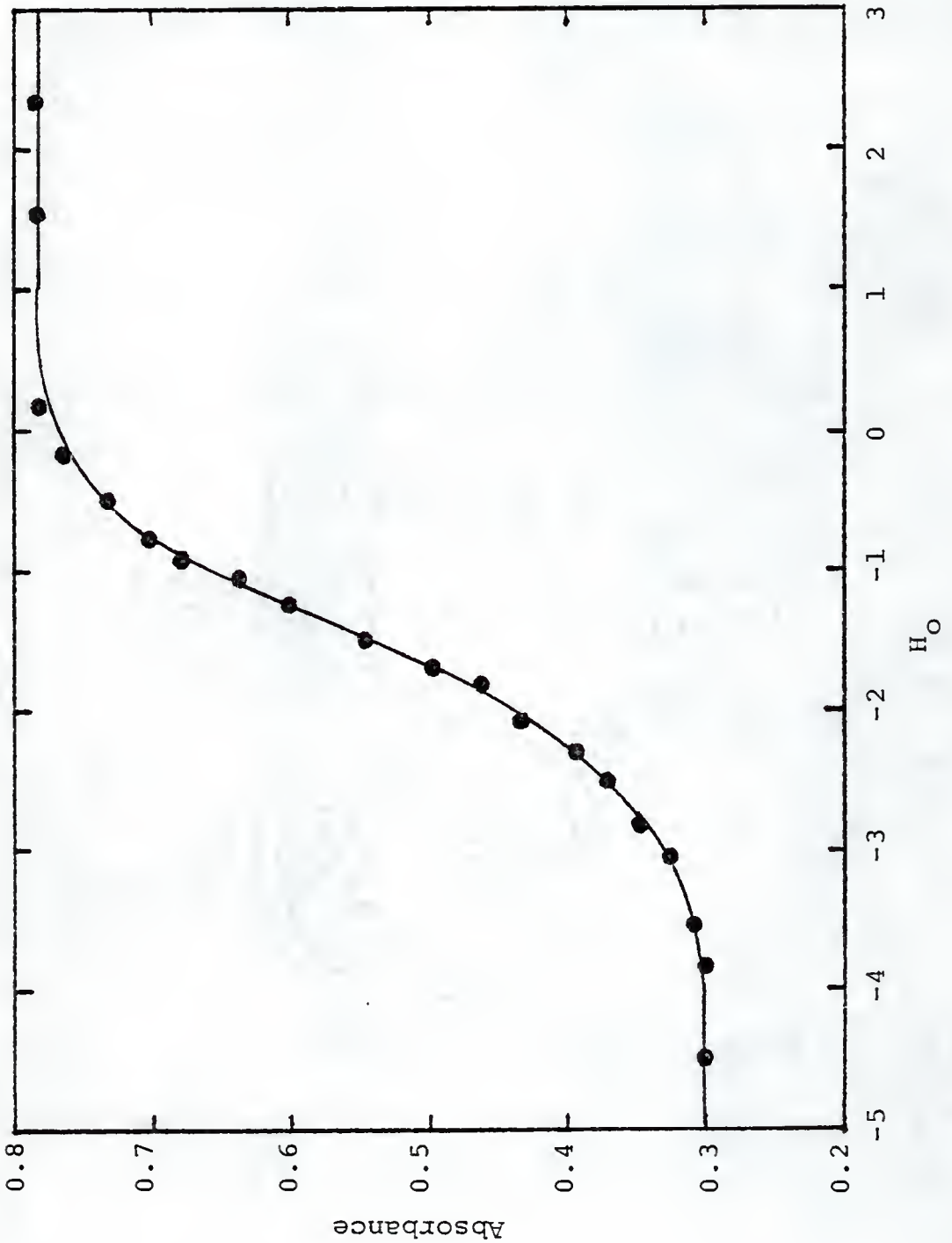
Absorbance
0.8
0.7
0.6
0.5
0.4
0.3
0.2
3
2
1
0
-1
-2
-3
-4
-5
H_o

Figure 5-3

Plot of the relative quantum yield of fluorescence (ϕ/ϕ_o) of 2.5 X 10^{-5} M protonated 1-isoquinolone in H_2SO_4 versus H_o. Analytical wavelength = 360 nm. Excitation wavelength = 252 nm (isosbestic point).

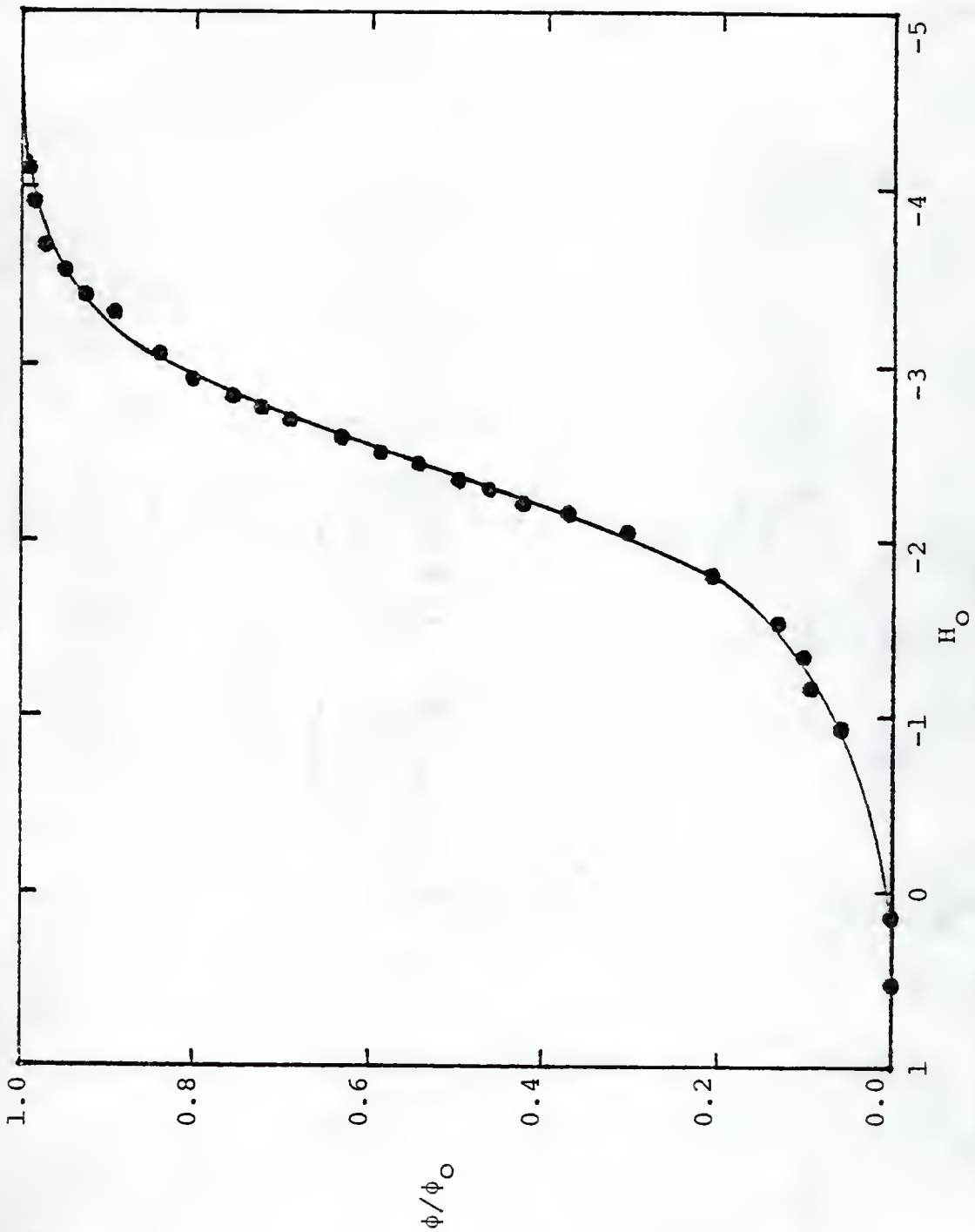
1.0
0.8
0.6
0.4
0.2
0.0
ϕ/ϕ_o
1
0
-1
-2
-3
-4
-5
H_o

Figure 5-4

Plot of $((\phi/\phi_o)/(\phi'/\phi_o'-\alpha_B))a_w^{\ r}$ versus $h_o a_w^{\ n}(\phi'/\phi_o')/(\phi'/\phi_o'-\alpha_B)$ for 1-isoquinolone with n = 2 and r = 2.

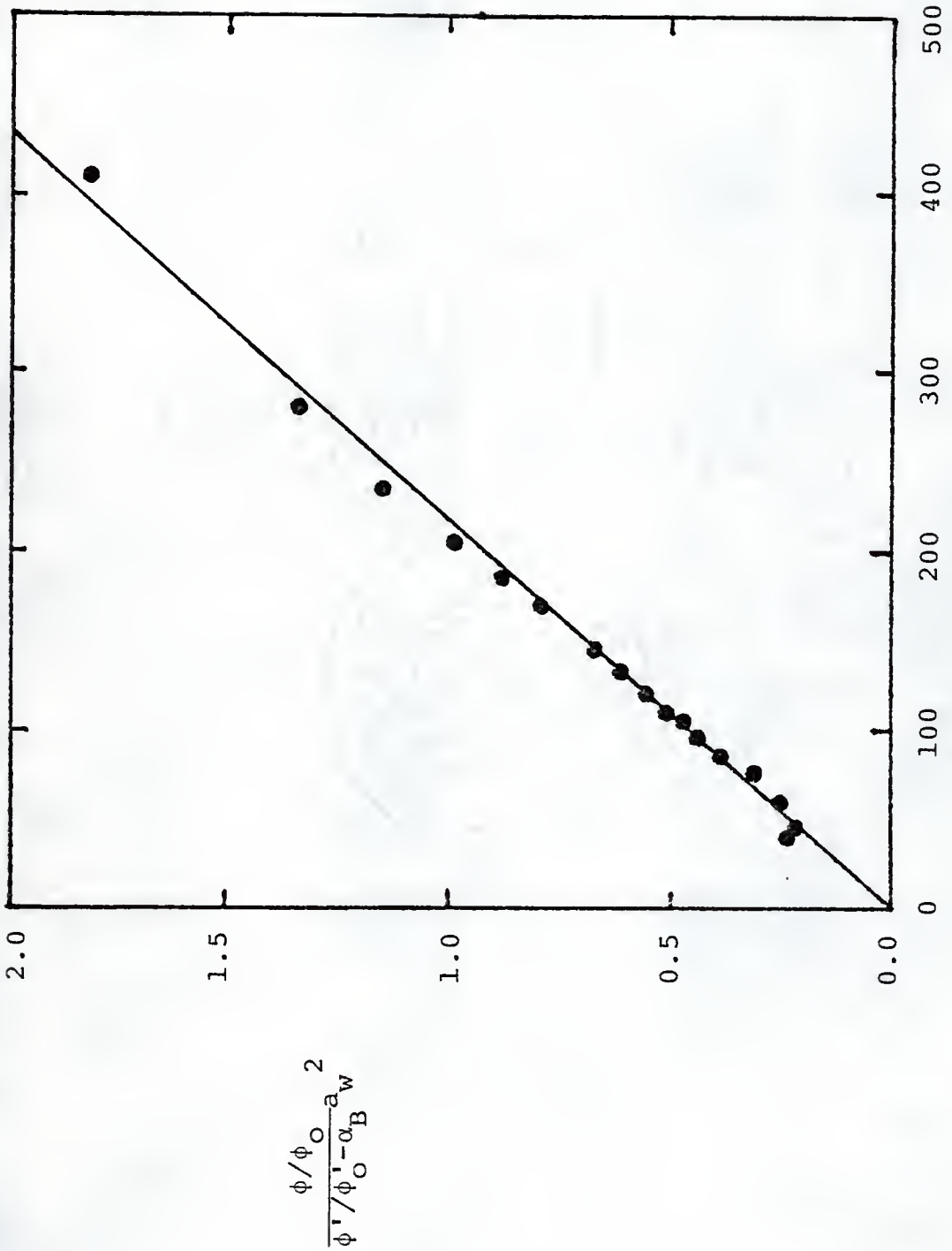
2.0
1.5
1.0
0.5
0.0
0
100
200
300
400
500
$\frac{\phi/\phi_o}{\phi'/\phi_o'-\alpha_B} a_w^2$
$h_o a_w^2 \frac{\phi'/\phi_o'}{\phi'/\phi_o'-\alpha_B}$

(n - r) is constant. These plots will be linear, however, only when the correct (n - r) is used in the analysis. The linearity of the plot shown in Figure 5-4 suggests that the correct value of (n - r) for 1-isoquinolone is (n - r) = 0. It is expected, therefore, that the fluorimetric titration data of 1-isoquinolone plotted according to equation (77) will yield straight lines with identical slopes and null intercepts for all combinations of n and r such that (n - r) = 0. This expectation is confirmed in Table 5-2, which presents values of the slopes and intercepts of these lines with $0 \leq n \leq 4$ and $0 \leq r \leq 4$ such that n = r. In all cases the intercept is zero (within experimental error) and the slopes are identical (within experimental error). Test values of $5 \leq n \leq 8$ and $5 \leq r \leq 8$ with n = r yielded the same results. This further confirms that the excited-state proton transfer of 1-isoquinolone attains equilibrium within the lifetime of the excited state and that (n - r) = 0 for this reaction.

Equation (78) shows that the attainment of excited-state prototropic equilibrium has several consequences concerning our knowledge of the reaction. In the first place, it is not possible to determine the number of water molecules (n) which enter into the Hammett indicator reaction or the number of water molecules (r) which enter into the excited-state deprotonation reaction of interest. Only the (n - r)

Table 5-2

Ground- and excited-state acid-dissociation constants for the proton transfer between neutral and protonated 1-isoquinolone.

pK_a	n	r	intercept[b]	slope[b]	pK_a^*
-1.38±0.03[a]	0	0	$4.9\pm5.5 \times 10^{-2}$	$4.55\pm0.06 \times 10^{-3}$	-2.23±0.03[c]
	1	1	$1.6\pm2.7 \times 10^{-2}$	$4.57\pm0.07 \times 10^{-3}$	-2.23±0.03[c]
	2	2	$0.4\pm1.5 \times 10^{-2}$	$4.59\pm0.09 \times 10^{-3}$	-2.22±0.03[c]
	3	3	$0.1\pm1.1 \times 10^{-2}$	$4.6 \pm 0.1 \times 10^{-3}$	-2.22±0.03[c]
	4	4	$0.5\pm1.5 \times 10^{-2}$	$4.5 \pm 0.4 \times 10^{-3}$	-2.23±0.04[c]
					-2.23±0.04[d]
					-2.2 ± 0.3[e]

[a]Determined spectrophotometrically in this work with $(n - r_g) = 1$.

[b]For 1-isoquinolone data plotted according to equation (77).

[c]$pK_a^*(0)$, determined graphically from the slope of the line obtained with from 1-isoquinolone data plotted according to equation (77) with the appropriate values of n and r.

[d]$pK_a^*(0)$, the average of the values of $pK_a^*(0)$ determined with $n = r$ for $0 \leq n \leq 4$ and $0 \leq r \leq 4$.

[e]pK_a^*(F.C.), estimated from the Förster cycle.

difference can be determined. Secondly, it is not possible to estimate $k_a(0)$ and $k_b(0)$. When τ_o and τ_o' are known, $pK_a^*(0)$ may be calculated because the slopes (in Table 5-2) all represent values of $k_b(0)\tau_o'/k_a(0)\tau_o$. Values of $pK_a^*(0)$ calculated in this manner, as well as the values of pK_a and pK_a^*(F.C.), are also presented in Table 5-2. Even though $k_a(0)$ is not known, we may still conclude that the rate of the dissociation reaction is high (85). It is seen that pK_a^*(F.C.) = -2.2±0.3 is identical to $pK_a^*(0)$ = -2.23±0.04. This agreement not only further confirms the validity of equation (77), but also suggests that equation (60) correctly describes the ground-state ionization of 1-isoquinolone.

CHAPTER VI
NONEQUILIBRIUM EXCITED-STATE PROTON TRANSFER IN 3-AMINOACRIDINE

Introduction

The molecules considered thus far are all of the H_o type (that is, they have neutral conjugate bases and singly charged conjugate acids). The number of fluorescent H_o type molecules which are appropriate for the study of excited-state proton-transfer reactions in concentrated acid is limited by several things. Firstly, the uncharged conjugate base species are sometimes relatively insoluble. This is particularly true with molecules that have three rings. Secondly, those that are soluble may not exhibit excited-state ionizations in concentrated acid. Thirdly, those that do exhibit excited-state ionizations in concentrated acid do not necessarily have conjugate acids and bases which are possessed of measurable fluorescence lifetimes. This consideration is, of course, more of a problem with older fluorescence lifetime equipment than it is with newer, more sophisticated equipment (most of which can measure fluorescence lifetimes shorter than those measurable with the TRW apparatus described in Chapter II). Finally, even when the first three considerations present no problems, the compound of interest may decompose in concentrated acid (the neutral

conjugate bases are sometimes more susceptible to this degradation than are the conjugate acid species). Degradation of an aromatic compound in concentrated acid is usually indicated by a time-dependent change in wavelength and/or intensity in the spectrum of either the conjugate acid or base (or both).

These difficulties are lessened with H_+ type molecules, which have monocationic conjugate bases and dicationic conjugate acids. The use of H_+ type compounds requires the use of the H_+ scale (87) to quantitate the acidity of the medium. Indicators of this type react according to the mechanism

$$H_2In^{++} + nH_2O \rightleftharpoons HIn^+ + H^+ \qquad (79),$$

where H_2In^{++} and HIn^+ are the indicator conjugate acid and base species, respectively. In analogy to equation (8), a_{H^+} is related to h_+ by

$$a_{H^+} = h_+ a_w^n \frac{f'_{++}}{f'_+} \qquad (80),$$

where f'_+ and f'_{++} are the activity coefficients of HIn^+ and H_2In^{++}, respectively, and $h_+ = \text{antilog}(-H_+)$. The excited-state reaction of interest is then

$$BH_2^{++} \underset{k_d}{\overset{k_f}{\rightleftharpoons}} BH_2^{++*} \underset{k_b}{\overset{k_a}{\rightleftharpoons}} H^+ + BH^{+*} \underset{k'_d}{\overset{k'_f}{\rightleftharpoons}} BH^+ \qquad (81).$$

The modification of equation (43) for H_+ type compounds parallels that for H_o type compounds, and, in analogy to

equation (76), culminates in

$$\frac{\phi/\phi_o}{\phi'/\phi_o'-\alpha_B}a_w^r = \frac{1}{k_a(0)\tau_o\frac{f_{++}}{f_x}} + \frac{k_b(0)\tau_o'}{k_a(0)\tau_o}h_+a_w^n\frac{\phi'/\phi_o'}{\phi'/\phi_o'-\alpha_B}\frac{f_{++}'f_+}{f_xf_o'} \qquad (82),$$

where f_+ and f_{++} are the activity coefficients for the H_+ type conjugate base (BH^{+*}) and conjugate acid (BH_2^{++*}), respectively, and f_x is the activity coefficient of the transition-state species in the excited-state reaction

$$BH_2^{++*} + rH_2O \rightleftharpoons X^{\ddagger} \rightleftharpoons BH^{+*} + H^+ \qquad (83).$$

Because of similarities in charge and size, it is now reasonable to assume that $f_{++}/f_x = f_{++}'f_+/f_xf_+' = 1$, in which case equation (82) reduces to

$$\frac{\phi/\phi_o}{\phi'/\phi_o'-\alpha_B}a_w^r = \frac{1}{k_a(0)\tau_o} + \frac{k_b(0)\tau_o'}{k_a(0)\tau_o}h_+a_w^n\frac{\phi'/\phi_o'}{\phi'/\phi_o'-\alpha_B} \qquad (84),$$

and a plot of $((\phi/\phi_o)/(\phi'/\phi_o'-\alpha_B))a_w^r$ versus $h_+a_w^n(\phi'/\phi_o')/(\phi'/\phi_o'-\alpha_B)$ should be linear with a slope of $k_b(0)\tau_o'/k_a(0)\tau_o$ and an ordinate intercept of $1/k_a(0)\tau_o$.

An H_+ type molecule which is amenable to study in concentrated acid is 3-aminoacridine (88), the structure of which is shown in Figure 6-1.

Results and Discussion

The fluorescence and absorption maxima and the fluorescence lifetimes of monoprotonated and diprotonated 3-aminoacridine are presented in Table 6-1. Values of H_+ in H_2SO_4 may be found in reference (87). A recent

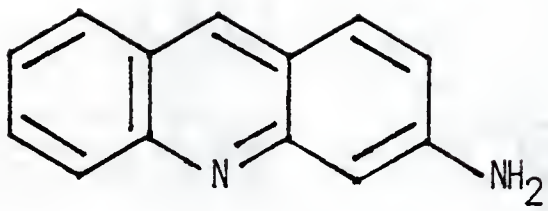

Figure 6-1

Structure of 3-aminoacridine.

Table 6-1

Fluorescence ($\bar{\nu}_f$) and longest wavelength absorption ($\bar{\nu}_a$) maxima and fluorescence lifetimes of monoprotonated and diprotonated 3-aminoacridine.

3-aminoacridine species	$\bar{\nu}_a$, cm^{-1}	$\bar{\nu}_f$, cm^{-1}	fluorescence lifetime, ns
monocation	2.20×10^4	1.91×10^4[a]	4.12±0.08[b]
dication	2.32×10^4[a]	2.13×10^4	26.0 ± 0.3[c]

[a] These energies were estimated from strongly pronounced (but not well resolved) vibrational features in the spectra.

[b] τ_o', measured in 3.1 $\underline{M}$ H_2SO_4, $H_+ = -1.6$.

[c] τ_o, measured in 16.3 $\underline{M}$ H_2SO_4, $H_+ = -8.7$.

study (89) showed that the values of H_+ in reference (87) for $H_2SO_4 \geq 7$ M are inaccurate due to poor choices of indicators. Correct values of H_+ for this concentration range may be found in reference (89). It was also shown that $H_+ = H_o$ for $H_2SO_4 \geq 7$ M, and values of H_o in references (63,64) could be used as H_+ for $H_2SO_4 \geq 7$ M.

Spectrophotometric titration curves for 3-aminoacridine are shown in Figures 6-2 and 6-3. These titration data were best fitted according to equation (60) using h_+ in place of h_o, which resulted in a value of $pK_a = -1.76 \pm 0.02$ with $(n - r_g) = 0$.

The fluorimetric titration curve of 3-aminoacridine is shown in Figure 6-4. The fluorescence spectrum of the dication overlaps and eclipses that of the monocation, and hence ϕ'/ϕ_o' was calculated according to the relationship $\phi'/\phi_o' = 1 - \phi/\phi_o$. Figure 6-5 shows the 3-aminoacridine titration data plotted according to equation (84) with n = 1 and r = 1 (other values of n and r did not fit the data). Values of $k_a(0)$, $k_b(0)$, and $pK_a^*(0)$ determined from this plot, as well as the values of pK_a and pK_a^*(F.C.), are presented in Table 6-2.

The linearity of the plot shown in Figure 6-5 suggests that the model under consideration is valid for H_+ type molecules. The criteria for the establishment of prototropic equilibrium within the lifetime of the excited state are the same for H_+ type molecules as they are for

Figure 6-2

Plot of absorbance versus H_+ for 1.9×10^{-5} M 3-aminoacridine in H_2SO_4. Analytical wavelength = 275 nm.

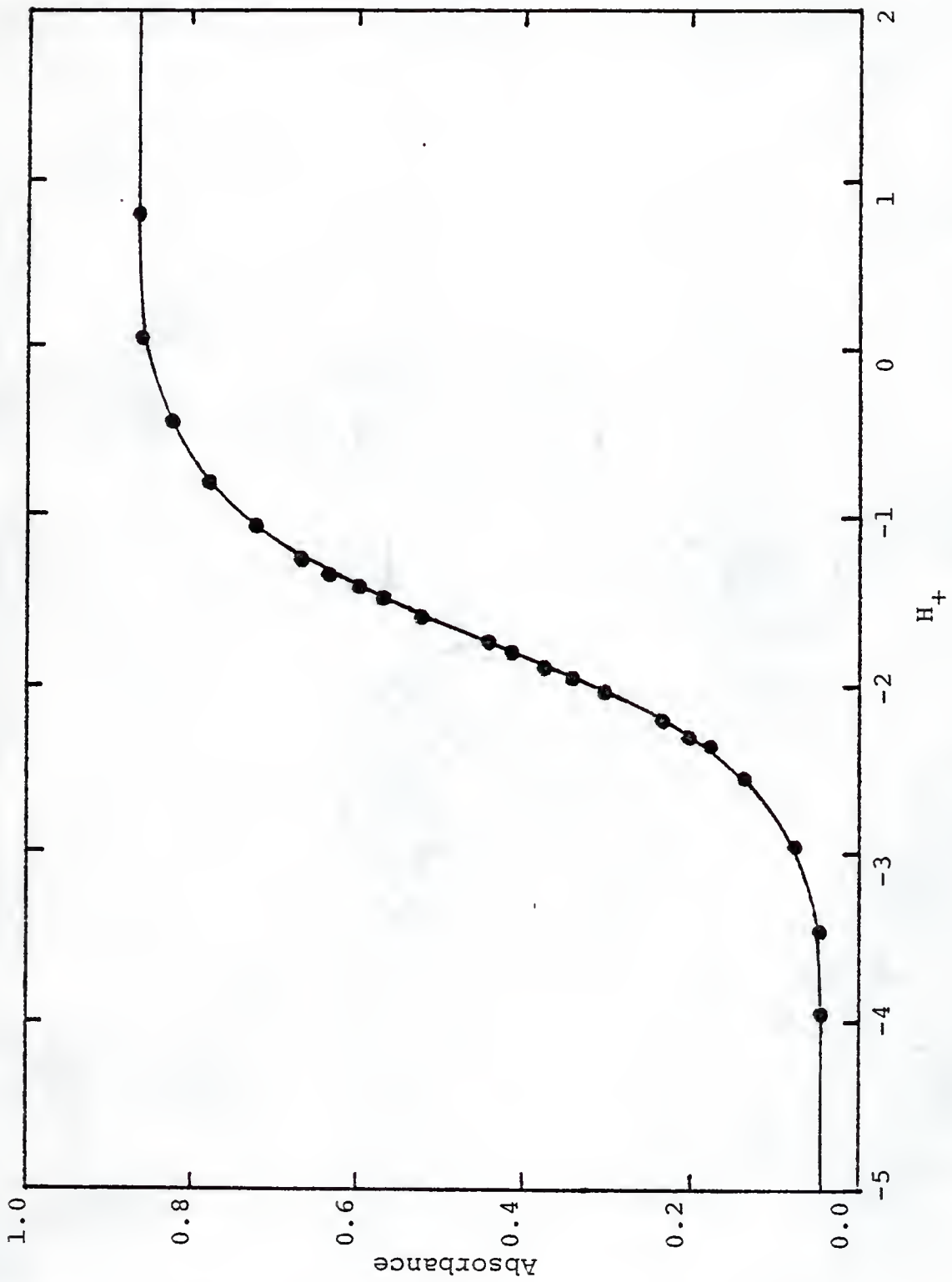
Absorbance
1.0
0.8
0.6
0.4
0.2
0.0
2
1
0
-1
-2
-3
-4
-5
H_+

Figure 6-3

Plot of absorbance versus H_+ for 1.9×10^{-5} M 3-aminoacridine in H_2SO_4. Analytical wavelength = 454 nm.

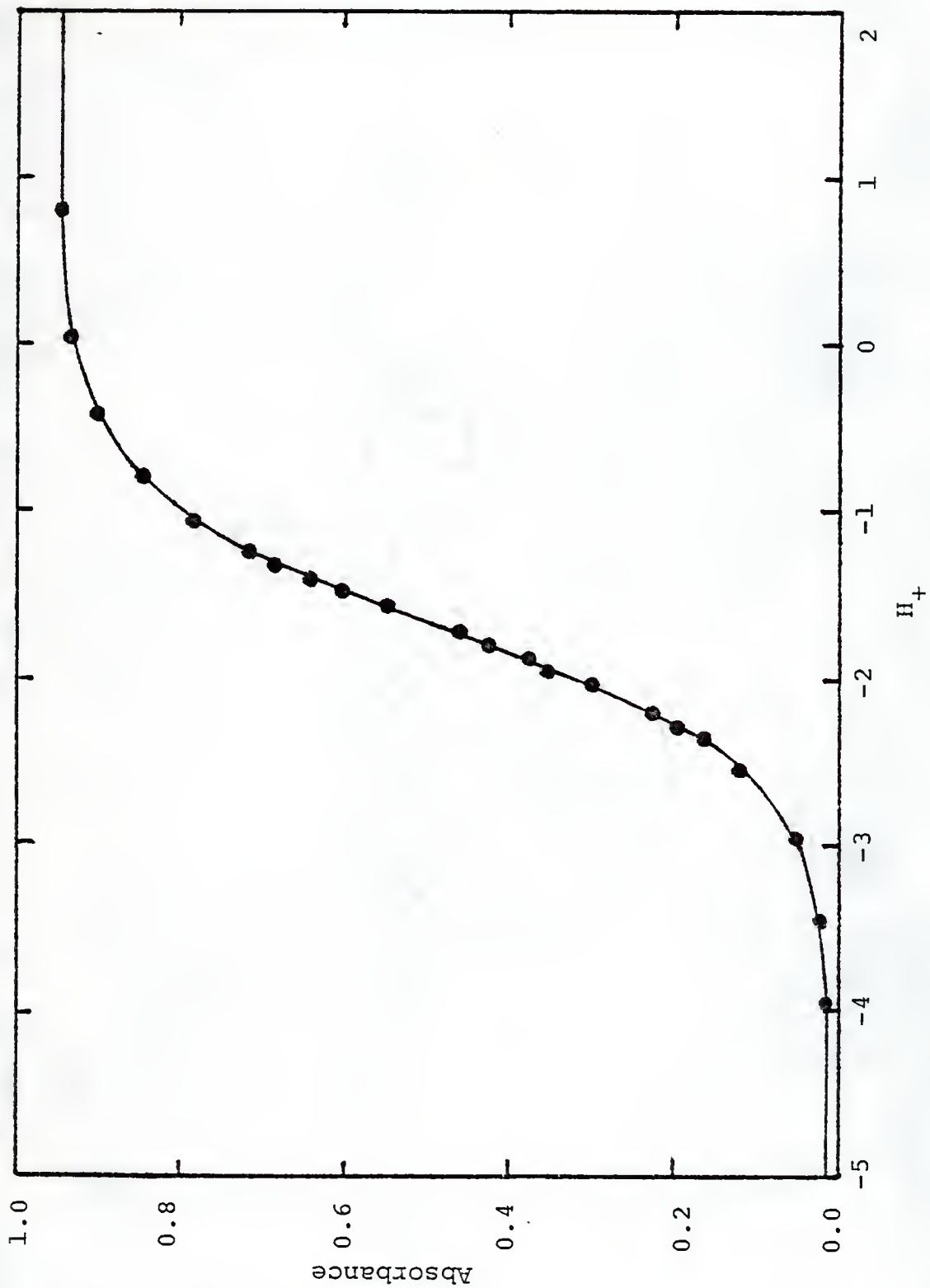
Absorbance
1.0
0.8
0.6
0.4
0.2
0.0
2
1
0
-1
-2
-3
-4
-5
H_+

Figure 6-4

Plot of the relative quantum yield of fluorescence (ϕ/ϕ_o) of 1.9×10^{-6} M doubly protonated 3-aminoacridine in H_2SO_4 versus H_+^-. Analytical wavelength = 470 nm. Excitation wavelength = 358 nm (isosbestic point.

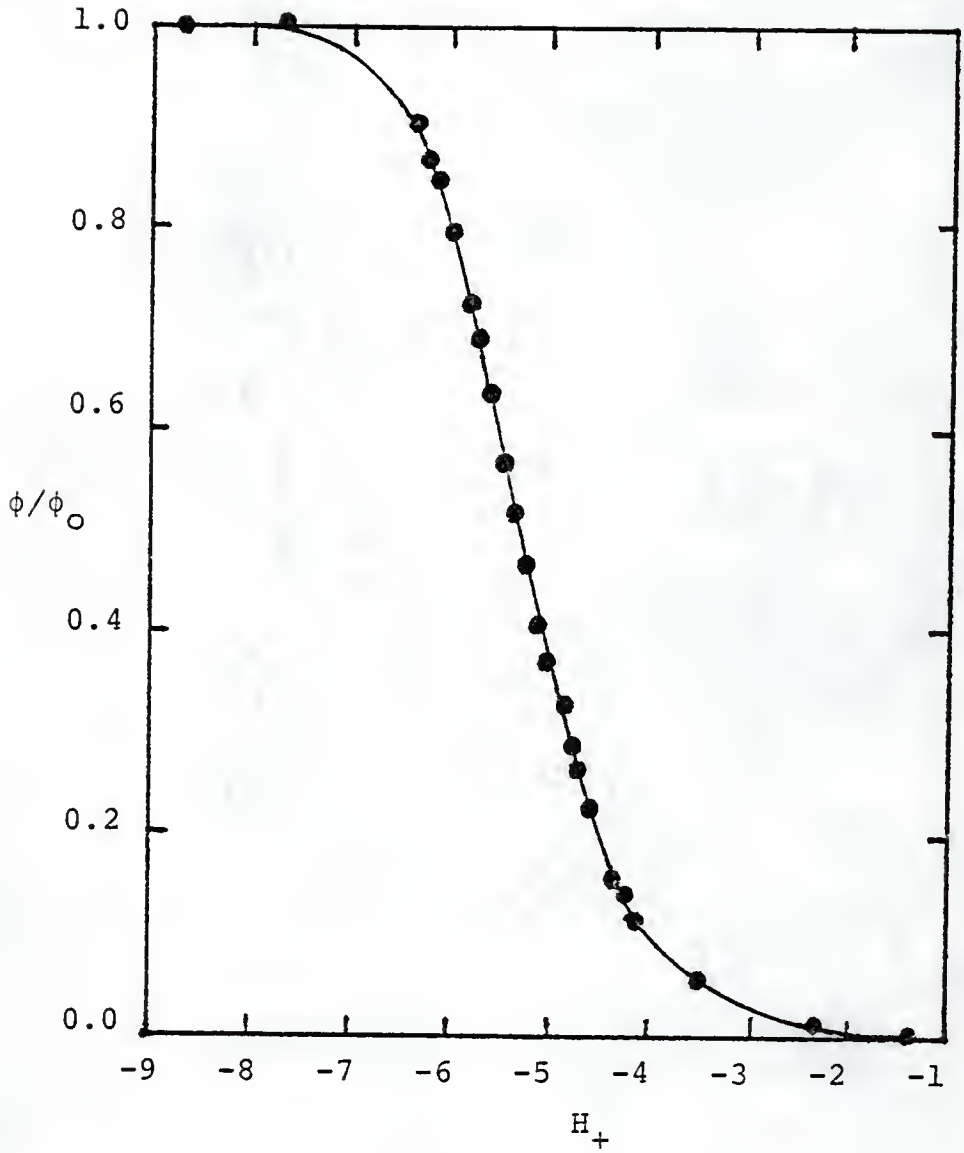
1.0
0.8
0.6
ϕ/ϕ_o
0.4
0.2
0.0
-9
-8
-7
-6
-5
-4
-3
-2
-1
H_+

Figure 6-5

Plot of $((\phi/\phi_o)/(\phi'/\phi_o'-\alpha_B))a_w^r$ versus $h_+a_w^n(\phi'/\phi_o')/(\phi'/\phi_o'-\alpha_B)$ for 3-aminoacridine with n = 1 and r = 1.

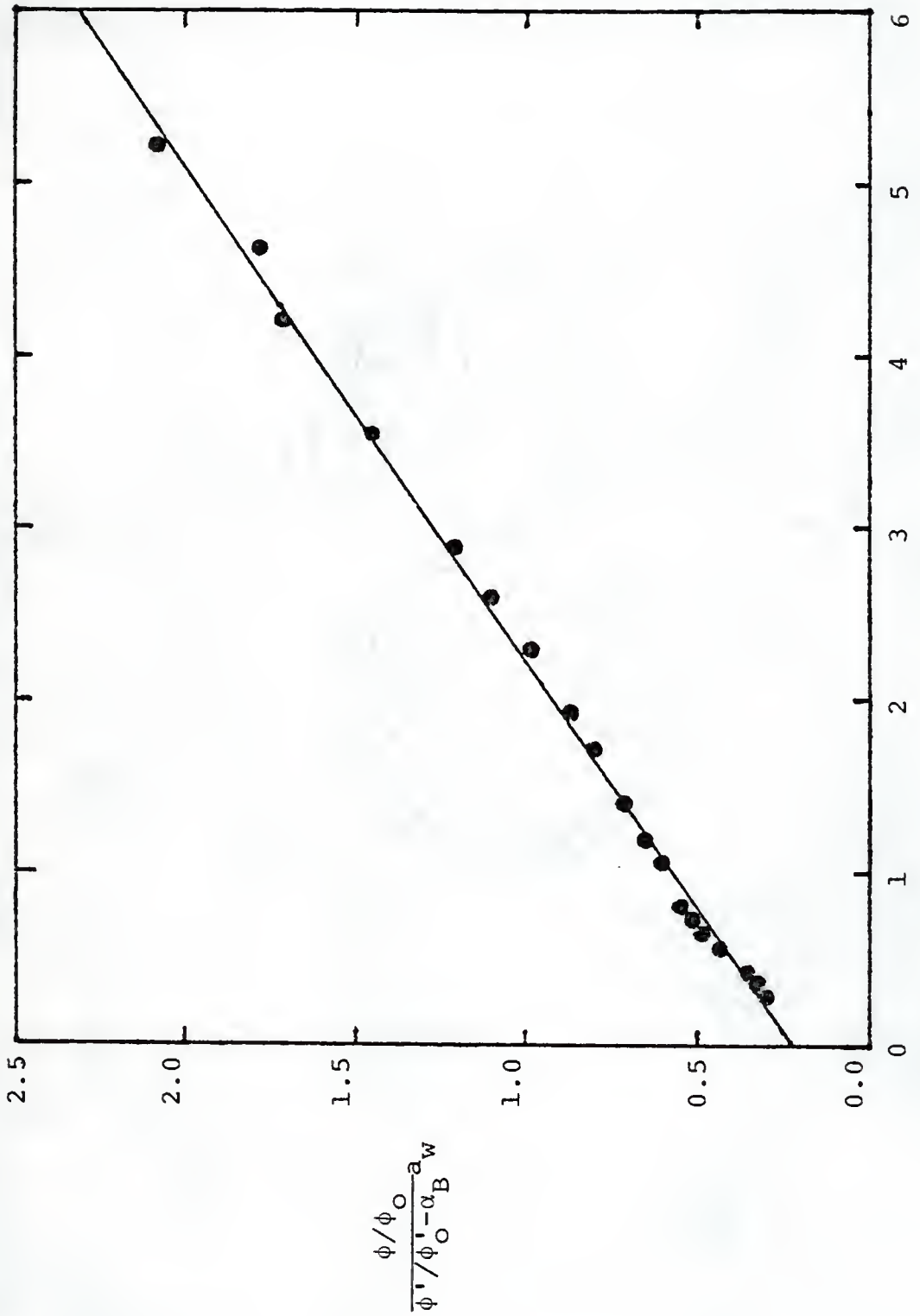
2.5
2.0
1.5
1.0
0.5
0.0
0
1
2
3
4
5
6
$\frac{\phi/\phi_o}{\phi'/\phi_o'-\alpha_B}a_w$
$\frac{\phi'/\phi_o'}{h_+ a_w \phi'/\phi_o'-\alpha_B}$

Table 6-2

Ground-state acid-dissociation constant of diprotonated 3-aminoacridine and rate constants and pK_a^* for the excited-state proton transfer between monoprotonated and diprotonated 3-aminoacridine.

pK_a	$k_a(0)$, s^{-1}	$k_b(0)$, $M^{-1}s^{-1}$	pK_a^*
-1.76 ± 0.02[a]	$1.73\pm0.08 \times 10^{9}$[b]	$3.8\pm0.2 \times 10^{4}$[b]	-4.66 ± 0.01[c] -5.1 ± 0.3[d]

[a] Determined spectrophotometrically in this work with $(n - r_g) = 0$.

[b] Determined graphically from Figure 6-5.

[c] $pK_a^*(0)$, determined graphically from Figure 6-5.

[d] pK_a^*(F.C.), estimated with the Förster cycle.

H_o type molecules. Since the intercept of the line in Figure 6-5 is not zero, we may conclude that the excited-state proton transfer between monoprotonated and diprotonated 3-aminoacridine does not attain equilibrium within the lifetime of the excited state. When nonequilibrium conditions prevail for an excited-state proton transfer in dilute, aqueous solution, there is some pH range over which there will be a plateau region in the titration curve. This pH independence is the result of the rate of the excited-state protonation of the conjugate base becoming immeasurably small. Equations (77) and (84), however, predict that both ϕ/ϕ_o and ϕ'/ϕ_o' will vary continuously with acid concentration even when nonequilibrium conditions prevail. Both the acidity of the medium and a_w vary with acid concentration, and thus even if ϕ/ϕ_o and ϕ'/ϕ_o' become acidity independent, they will still vary because they are dependent on a_w. This behavior is observed for both 3-aminoacridine (Figure 6-4) and 2-quinolone (Figure 4-4). The ability of equations (77) and (84) to predict titration behavior further confirms the validity of the model.

The value of the pK_a^* of 3-aminoacridine estimated with the Förster cycle is expected to be somewhat inaccurate because of the difficulty encountered in estimating the 0-0 energy of the dication. This energy was estimated from strongly pronounced (but not well

resolved) vibrational features in the absorption and fluorescence spectra of the doubly protonated molecule. Since these features are not well resolved, the estimation of the 0-0 energy of the dication is difficult and subject to inaccuracy. In spite of this, there is reasonable agreement between $pK_a^*(0)$ and $pK_a^*(F.C.)$ (see Table 6-2). The small difference between $pK_a^*(0)$ and $pK_a^*(F.C.)$ is attributed to error in the estimated values of $\bar{\nu}_{dication}$. The agreement between $pK_a^*(0)$ and $pK_a^*(F.C.)$ further confirms the validity of the model under consideration and also suggests that equation (60) (modified to include h_+ instead of h_o) correctly describes the ground-state ionization of 3-aminoacridine. Since the ground- and excited-state ionizations occur in media of radically different acid composition, we also see that the Förster cycle may be used with some confidence to relate the acid-base behavior of 3-aminoacridine in one medium to its behavior in another medium.

Since both reactions occur in moderately concentrated acid, it is of interest to compare the values of $k_a(0)$ and $k_b(0)$ (Table 6-2) for the excited-state ionization of 3-aminoacridine to their values for the excited-state ionization of 2-quinolone (Table 4-2). Since neither of these reactions attains prototropic equilibrium, it is not surprising that the value of $k_a(0)$ for the 3-aminoacridine excited-state ionization ($k_a(0) = 1.73 \times 10^9\ s^{-1}$) is

similar to that for the 2-quinolone excited-state ionization ($k_a(0) = 4 \times 10^9\ s^{-1}$). The value of $k_b(0)$ for the 3-aminoacridine reaction ($k_b(0) = 3.8 \times 10^4\ M^{-1}s^{-1}$) is, however, substantially lower than it is for the 2-quinolone reaction ($k_b(0) = 1.0 \times 10^8\ M^{-1}s^{-1}$). This observation is not surprising if one considers the charge types of the reactants. The conjugate base of 2-quinolone is a neutral molecule, whereas the conjugate base of 3-aminoacridine is a cation. Because of the electrostatic repulsion between species of like charge, it is expected that the rate constant for the combination of two cations (the proton and monoprotonated 3-aminoacridine) will be lower than that for the combination of a cation (the proton) with a neutral species (the conjugate base of 2-quinolone). Whether or not this comparison is legitimate, of course, depends upon whether or not the conjugate bases in the two reactions are in the same standard state. As has already been discussed in Chapters III and IV, differences in standard state could result from changes in hydration, and these changes would not necessarily be detectable with the Förster cycle. It is not possible, therefore, to state at this time whether or not the above comparison of rate constants is legitimate. The comparison does seem qualitatively justified because of the electrostatic considerations already given and because of the similarity between the reactions (both occur in

moderately concentrated acid but neither attains prototropic equilibrium within the lifetime of the excited state).

CHAPTER VII
SUMMARY

Many questions were raised before and during the research carried out for this dissertation. While this work has not definitively answered all of these questions, it has certainly contributed to the understanding of the fundamental process of proton transfer in concentrated electrolytes. It was found that the model supported by the data of Lovell and Schulman (10-12) for ground-state ionizations occurring in concentrated acid was applicable to the compounds examined in this dissertation. This model has now been successfully applied to unsubstituted and substituted carboxamides, tertiary anilines, aromatic lactams, and several other heterocylic bases (including those with oxygen or nitrogen as the heteroatom). This broad application to molecules of dissimilar structure suggests that equation (12) will find wide application to ground-state ionizations occurring in concentrated acid.

The model proposed to quantitate the kinetics of excited-state proton transfer in concentrated acid appears to be valid. This conclusion is supported by several observations. In the first place, equations (77) and (84) correctly predicted the shapes of the fluoimetric titration curves both in the cases where excited-state

nonequilibrium conditions prevailed and in the case where excited-state prototropic equilibrium was observed. Secondly, the model predicted that the fluorimetric titration data of the molecules exhibiting excited-state ionizations in concentrated acid should result in linear plots when plotted according to equation (77) or (84) (depending upon the charge types of the species involved). Linearity was observed in these plots when the appropriate combinations of n and r were used. Thirdly, the Förster cycle, which is independent of the titration curves themselves and of kinetic considerations, was, in most cases, successful in relating pK_a and pK_a^* to each other. This not only confirms the validity of the model for excited-state ionizations which occur in concentrated acid, but also further confirms the applicability of the ground-state model as well.

That both the models for ground- and excited-state ionizations were successful in predicting the acid-base titration behavior of both H_o and H_+ type molecules suggests that these models may be applicable to species of other charge types as well. Further research should show whether or not this is true. It would also be interesting to see if these models apply to ionizations which occur in concentrated base (NaOH or KOH).

Further research also needs to be done in order to clarify the question of whether or not the standard states

of the reactants change when the composition of the medium is changed. The success of the Förster cycle in the research presented in this dissertation suggests that either the standard states do not change with a change in acid composition or that they do change but in such a way that the standard free energies of all the species involved in a given reaction change by the same amount. It was not possible, however, to discern which one of these circumstances was responsible for the success of the Förster cycle. Furthermore, it appears that acid-base chemistry in concentrated acid may be simply and fundamentally related to acid-base chemistry in dilute, aqueous solution by the inclusion of water as a reactant in the equilibrium expressions of interest.

Finally, a look at the possible utility of the methods developed in this dissertation is in order. The application of these methods to the investigation of acid-base chemistry in a mixed solvent system such as methanol:sulfuric acid could be of great benefit. The addition of methanol would greatly increase the number of aromatic acids and bases that could be studied because more of these compounds are soluble in methanolic sulfuric acid than are soluble in nonmethanolic sulfuric acid. If the acid-base properties of molecules in dilute, aqueous solution could be related to those same properties in methanolic sulfuric acid, then it may be possible to devise

a general method for predicting the thermodynamics of proton transfer in dilute, aqueous solution based on measurements made in nonaqueous or mixed-aqueous solvents. This would greatly simplify the determination of the pK_a's of many water-insoluble pharmaceuticals, for then the thermodynamic pK_a's of relatively water-insoluble species could be calculated from measurements made in nonaqueous or mixed-aqueous solvents in which the species are soluble. A study of acid-base thermodynamics in methanolic sulfuric acid could not be performed, however, until an acidity scale for the medium is determined. Values of a_w in the solvent, and perhaps of the activity of methanol in the solvent, would also have to be measured.

APPENDIX A
SIMPLE LINEAR LEAST-SQUARES REGRESSION ANALYSIS

The statistics of the straight line are well understood and may be found in many basic and advanced statistics books (90-93). The derivation of these equations is not relevant here. Their importance to this dissertation lies in how the slope and intercept of a given line may be statistically estimated.

The equation of a straight line is given by

$$Y = a_o + a_1 X \qquad (85),$$

where Y is the dependent variable, X is the independent variable, a_o is the ordinate intercept, and a_1 is the slope. The values of the intercept and slope may be calculated (90) as

$$a_o = \frac{(\Sigma Y)(\Sigma X^2) - (\Sigma X)(\Sigma XY)}{N\Sigma X^2 - (\Sigma X)^2} \qquad (86)$$

and

$$a_1 = \frac{N\Sigma XY - (\Sigma X)(\Sigma Y)}{N\Sigma X^2 - (\Sigma X)^2} \qquad (87),$$

where N is the number of (X,Y) data points. The various sums in equations (86) and (87) are short-form notation for the following:

$$\Sigma Y = \sum_{i=1}^{N} Y_i \qquad (88),$$

$$\Sigma X = \sum_{i=1}^{N} X_i \qquad (89),$$

$$\Sigma XY = \sum_{i=1}^{N} X_i Y_i \qquad (90),$$

and

$$\Sigma X^2 = \sum_{i=1}^{N} X_i^2 \qquad (91).$$

The standard deviation of the slope (91), S_{a_1}, is given by

$$S_{a_1} = (S^2/(\Sigma X^2 - N\bar{X}^2))^{1/2} \qquad (92),$$

where $\bar{X} = \Sigma X/N$. The term S in equation (92) is calculated as

$$S=((\Sigma Y^2-(\Sigma Y)^2/N-(\Sigma XY-\Sigma X\Sigma Y/N)^2/(\Sigma X^2-(\Sigma X)^2/N))/(N-2))^{1/2} \qquad (93).$$

The standard deviation of the intercept (91), S_{a_o}, is calculated as

$$S_{a_o}=(S(\Sigma X^2/(N\Sigma X^2-(\Sigma X)^2)))^{1/2} \qquad (94).$$

The cofficient of correlation (90), r, is given by

$$r=(N\Sigma XY-(\Sigma X)(\Sigma Y))/((N\Sigma X^2-(\Sigma X)^2)(N\Sigma Y^2-(\Sigma Y)^2))^{1/2} \qquad (95).$$

The value of r will fall into the range $-1 \leq r \leq 1$, and the data are best fitted to a straight line when $|r| = 1$.

The sign of r simply indicates whether the slope is positive ($r > 0$) or negative ($r < 0$). When $r \simeq 0$, then Y is not linearly dependent on X.

The equations in this appendix are short-form computational formulae which are particularly useful when computation is limited to devices with small amounts of RAM (random access memory). Because of this, equations (86-95) are well suited for the estimation of r, a_o, S_{a_o}, a_1, and S_{a_1} with handheld programmable calculators. Simple linear regression analysis may also be performed with matrix operations (92), but this method is beyond the capabilities of most of the currently available handheld computing devices.

APPENDIX B
MULTIPLE LINEAR LEAST-SQUARES REGRESSION ANALYSIS

In some cases it is postulated that experimental data will fit an equation of the form

$$Z = a_o + a_1 X + a_2 Y \qquad (96),$$

where Z is the dependent variable, X and Y are the independent variables, and a_o, a_1, and a_2 are the regression coefficients (unknowns). The regression coefficients may be estimated by the simultaneous solution of the three normal equations (90)

$$\Sigma Z = a_o N + a_1 \Sigma X + a_2 \Sigma Y \qquad (97),$$

$$\Sigma XZ = a_o \Sigma X + a_1 \Sigma X^2 + a_2 \Sigma XY \qquad (98),$$

and

$$\Sigma YZ = a_0 \Sigma Y + a_1 \Sigma XY + a_2 \Sigma Y^2 \qquad (99),$$

where all of the symbols are the same as defined in equations (88-91) and ΣZ, ΣXZ, and ΣYZ are given by

$$\Sigma Z = \sum_{i=1}^{N} Z_i \qquad (100),$$

$$\Sigma XZ = \sum_{i=1}^{N} X_i Z_i \qquad (101),$$

and

$$\Sigma YZ = \sum_{i=1}^{N} Y_i Z_i \qquad (102),$$

respectively. Equations (97-99) can be put into matrix form:

$$D = CA \qquad (103),$$

where

$$D = \begin{bmatrix} \Sigma Z \\ \Sigma XZ \\ \Sigma YZ \end{bmatrix} \qquad (104),$$

$$C = \begin{bmatrix} N & \Sigma X & \Sigma Y \\ \Sigma X & \Sigma X^2 & \Sigma XY \\ \Sigma Y & \Sigma XY & \Sigma Y^2 \end{bmatrix} \qquad (105),$$

and

$$A = \begin{bmatrix} a_o \\ a_1 \\ a_2 \end{bmatrix} \qquad (106).$$

Simple matrix arithmetic shows that

$$A = C^{-1}D \qquad (107),$$

where C^{-1} is the inverse matrix of matrix of C. Therefore, the regression coefficients may be estimated from N (X,Y,Z) points by calculating matrix elements and subsequently performing matrix inversion and matrix multiplication. The elements of matrix C may be calculated by multiplication:

$$C = I^t I \qquad (108),$$

where

$$I = \begin{bmatrix} 1 & X_1 & Y_1 \\ 1 & X_2 & Y_2 \\ 1 & X_3 & Y_3 \\ \cdot & \cdot & \cdot \\ \cdot & \cdot & \cdot \\ \cdot & \cdot & \cdot \\ 1 & X_N & Y_N \end{bmatrix} \tag{109}$$

and I^t is the transpose of matrix I. Matrix D is then given by the product

$$D = I^t P \tag{110},$$

where

$$P = \begin{bmatrix} Z_1 \\ Z_2 \\ Z_3 \\ \cdot \\ \cdot \\ \cdot \\ Z_N \end{bmatrix} \tag{111}.$$

The matrix of fitted values of the dependent variable is given by

$$F = IA \tag{112}$$

and the matrix of residuals is given by

$$R = P - F \tag{113},$$

where the residual of the i^{th} point is

$$R_i = Z_i - F_i \tag{114}.$$

The sum of the squares of the residuals is

$$S_r = \sum_{i=1}^{N} R_i^2 \qquad (115).$$

The estimated standard deviations of a_o, a_1, and a_2 are given by (92)

$$S_{a_o} = ((S_r/(N-3))C^{-1}_{1,1})^{1/2} \qquad (116),$$

$$S_{a_1} = ((S_r/(N-3))C^{-1}_{2,2})^{1/2} \qquad (117),$$

and

$$S_{a_2} = ((S_r/(N-3))C^{-1}_{3,3})^{1/2} \qquad (118),$$

respectively, and $C^{-1}_{i,i}$ is the $(i,i)^{th}$ element of matrix C^{-1}. The coefficient of multiple determination (90), R^2, is given by

$$R^2 = 1 - \frac{S_r}{\sum_{i=1}^{N} (Z_i - \bar{Z})^2} \qquad (119),$$

where

$$\bar{Z} = \frac{\sum_{i=1}^{N} Z_i}{N} \qquad (120).$$

The value of R^2 may range from zero to one, and when $R^2 \simeq 1$ the data are well described by equation (96).

The rapid calculation of the regression coefficients and their estimated standard deviations for a data set of

even modest size (ten points) requires many calculations and the storage of many numbers. The computation and storage requirements of this statistical analysis are not found in any currently available handheld computing devices, and hence digital computers are used for this type of curve fitting.

REFERENCES

1. Tortora, G.J., and Anagnostakos, N.P., Principles of Anatomy and Physiology, San Francisco, Canfield Press, 1975, chapter 16.

2. Beall, P.T., The Sciences, January (1981), 6.

3. Hallenga, K., Grigera, J.R., and Berendsen, H.J.C., J. Phys. Chem., 84 (1980), 2381.

4. Paul, M.A., J. Am. Chem. Soc., 76 (1954), 3236.

5. Brønsted, J.N., Recl. Trav. Chim. Pays-Bas, 42 (1953), 718.

6. Lowry, T.M., Chem. Ind. (London), 42 (1923), 43.

7. Henderson, L.J., J. Am. Chem. Soc., 30 (1908), 954.

8. Hasselbach, K.A., Biochem. Bull., 2 (1913), 367.

9. Hammett, L.P., and Deyrup, A.J., J. Am. Chem. Soc., 54 (1932), 2721.

10. Lovell, M.W., and Schulman, S.G., Anal. Chim. Acta, 127 (1981), 203.

11. Lovell, M.W., and Schulman, S.G., Int. J. Pharm., 11 (1982), 345.

12. Lovell, M.W., The Influence of Hydration on Prototropic Equilibria in Acidic Aqueous Media, Doctoral dissertation, University of Florida, 1982.

13. Förster, T., Naturwiss., 36 (1949), 186.

14. Weber, K., Z. Phys. Chem. B, 15 (1931), 18.

15. Klöpffer, W., Adv. Photochem., 10 (1977), 311.

16. Schulman, S.G., and Winefordner, J.D., Talanta, 17 (1970), 607.

17. Vander Donckt, E., Prog. React. Kinetics, 5 (1970), 273.

18. Jackson, G., and Porter, G., Proc. Roy. Soc. London A, 260 (1961), 13.

19. Grabowska, A., and Pakula, B., Chem. Phys. Letts., 1 (1967), 369.

20. Bulska, H., Chodkowska, A., Grabowska, A., and Pakula, B., J. Lumin., 10 (1975), 39.

21. Herbich, J., and Grabowska, A., Chem. Phys. Letts., 46 (1977), 372.

22. Bulska, H., and Kotlicka, J., Pol. J. Chem., 53 (1979), 2103.

23. Paul, W.L., Kovi, P.J., and Schulman, S.G., Spec. Letts., 6 (1973), 1.

24. Capellos, G., and Porter, G., J. Chem. Soc. Faraday Trans. II, 70 (1974), 1159.

25. Peterson, S.H., and Demas, J.N., J. Am. Chem. Soc., 101 (1979), 6571.

26. Ireland, J.F., and Wyatt, P.A.H., Adv. Phys. Org. Chem., 12 (1976), 131.

27. Förster, T., Z. Phys. Chem. Frankfurt am Main, 54 (1950), 42.

28. Lippert, E., Accts. Chem. Res., 3 (1970), 74.

29. Levschin, W.L., Z. Phys., 43 (1927), 230.

30. Schulman, S.G., and Capomacchia, A.C., Spetrochim. Acta, 28A (1972), 1.

31. Schulman, S.G., and Underberg, W.J.M., Anal. Chim. Acta, 107 (1979), 411.

32. Schulman, S.G., in Modern Fluorescence Spectroscopy, v. 2, ed. E.L. Wehry, New York, Plenum, 1976, chapter 6.

33. Grabowski, Z.R., and Grabowska, A., Z. Phys. Chem. N. F., 101 (1976), 197.

34. Rosenberg, J.L., and Brinn, I., J. Phys. Chem., 76 (1972), 3558.

35. Schulman, S.G., Capomacchia, A.C., and Rietta, M.S., Anal. Chim. Acta, 56 (1971), 91.

36. Schulman, S.G., Tidwell, P.T., Cetorelli, J.J., and Winefordner, J.D., J. Am. Chem. Soc., 93 (1971), 3179.

37. Schulman, S.G., Capomacchia, A.C., and Tussey, B., Photochem. Photobiol., 14 (1971), 733.

38. Wehry, E.L., and Rogers, L.B., Spectrochim. Acta, 21 (1965), 1976.

39. Jaffe, H.H., and Jones, H.L., J. Org. Chem., 30 (1965), 964.

40. Weller, A., Prog. React. Kinetics, 1 (1961), 187.

41. Schulman, S.G., Rev. Anal. Chem., 1 (1971), 85.

42. Parker, C.A., Photoluminescence of Solutions, Amsterdam, Elsevier, 1968, pp. 333-343.

43. Martynov, I., Demyashkevitch, A., Uzhinov, B., and Kuzmin, M., Usp. Chem. (Akad. Nauk USSR), 47 (1977), 3.

44. Shim, S.C., Hwahak Kwa Kongop Ui Chinbo, 20 (1980), 81.

45. Harris, C.M., and Selinger, B.K., J. Phys. Chem., 84 (1980), 891.

46. Hafner, F., Wörner, J., Steiner, U., and Hauser, M., Chem. Phys. Letts., 73 (1980), 139.

47. Campillo, A.J., Clark, J.H., Shapiro, S.L., Winn, K.R., and Woodbridge, P.K., Chem. Phys. Letts., 67 (1979), 218.

48. Kobayashi, T., and Rentzepis, P.M., J. Chem. Phys., 70 (1979), 886.

49. Shizuka, H., Tsutsumi, K., Takeuchi, H., and Tanaka, I., Chem. Phys. Letts., 62 (1979), 408.

50. Smith, K.K., Kaufmann, K.J., Huppert, D., and Gutman, M., Chem. Phys. Letts., 64 (1979), 522.

51. Gafni, A., and Brand, L., Chem. Phys. Letts., 58 (1978), 346.

52. Demjaschkewitch, A.B., Zaitsev, N.K., and Kuzmin, M. G., Chem. Phys. Letts., 55 (1978), 80.

53. Escabi-Perez, J.R., and Fendler, J.H., J. Am. Chem. Soc., 100 (1978), 2234.

54. Gafni, A., Modlin, R.L., and Brand, L., J. Phys. Chem., 80 (1976), 898.

55. Ofran, M., and Feitelson, J., Chem. Phys. Letts., 19 (1973), 427.

56. Weller, A., Z. Elektrochem., 56 (1952), 662.

57. Weller, A., Z. Phys. Chem. N. F., 15 (1958), 438.

58. Weller, A., Z. Elektrochem., 61 (1957), 956.

59. Rosenberg, L.S., A Thermodynamic Evaluation of DNA-Ligand Interactions, Doctoral dissertation, University of Florida, 1980.

60. Martin, R.F., and Tong, J.H.Y., Aust. J. Chem., 22 (1969), 487.

61. Weast, R.C., ed., CRC Handbook of Chemistry and Physics, 54th ed., Cleveland, CRC Press, 1973, section C.

62. Dominique, P., and Carpentier, J.M., J. Chem. Res., S (1979), 58.

63. Paul, M.A., and Long, F.A., Chem. Rev., 57 (1957), 1.

64. Jorgensen, M.J., and Hartter, D.R., J. Am. Chem. Soc., 85 (1963), 878.

65. Giaque, W.F., Hornung, E.M., Kunzler, J.E., and Rubin, T.R., J. Am. Chem. Soc., 82 (1960), 62.

66. Robinson, R.A., and Stokes, R.H., Electrolyte Solutions, London, Butterworths, 1955.

67. Long, F.A., and Purchase, M., J. Am. Chem. Soc., 72 (1950), 3267.

68. Rosenthal, D., and Dwyer, J.S., Can. J. Chem., 41 (1963), 80.

69. O'Conner, C.J., J. Chem. Ed., 46 (1969), 686.

70. Kokobun, H., Z. Elektrochem., 62 (1958), 559.

71. Watkins, A.R., Z. Phys. Chem. N. F., 75 (1971), 327.

72. Watkins, A.R., Z. Phys. Chem. N. F., 78 (1972), 103.

73. Watkins, A.R., J. Chem. Soc. Faraday Trans. I., 68 (1972), 28.

74. Schulman, S.G., Vogt, B.S., and Lovell, M.W., Chem. Phys. Letts., 75 (1980), 224.

75. Albert, A., and Phillips, J.N., J. Chem. Soc., Pt. 2 (1956), 1294.

76. Ireland, J.F., and Wyatt, P.A.H., J. Chem. Soc. Faraday Trans. I, 68 (1972), 1053.

77. Vogt, B.S., and Schulman, S.G., Chem. Phys. Letts., in press (1983).

78. Schulman, S.G., and Vogt, B.S., J. Phys. Chem., 85 (1981), 2074.

79. Teng, T.T., and Lenzi, F., Can. J. Chem., 50 (1972), 3283.

80. Bascombe, K.N., and Bell, R.P., Discuss. Faraday Soc., 24 (1957), 158.

81. Strickler, S.J., and Berg, R.A., J. Chem. Phys., 37 (1962), 814.

82. El-Bayoumi, M.A., Dalle, J.P, and O'Dwyer, M.F., J. Am. Chem. Soc., 92 (1970), 3494.

83. Ross, R.T., Photochem. Photobiol., 21 (1975), 401.

84. Werner, T.C., in Modern Fluorescence Spectroscopy, v. 2, ed. E.L. Wehry, New York, Plenum, 1976, p. 277.

85. Schulman, S.G., Rosenberg, L.S., and Vincent, W.R., J. Am. Chem. Soc., 101 (1979), 139.

86. Vogt, B.S., and Schulman, S.G., Chem. Phys. Letts., 95 (1983), 159.

87. Vetesnik, P., Bielavsky, J., and Vecera, M., Coll. Czech. Chem. Comm., 33 (1968), 1687.

88. Vogt, B.S., and Schulman, S.G., submitted to Chem. Phys. Letts. (1983).

89. Lovell, M.W., and Schulman, S.G., Anal. Chem., in press (1983).

90. Spiegel, M.R., Theory and Problems of Statistics, New York, McGraw-Hill, 1961, chapters 13-14.

91. Youden, N.J., Statistical Methods for Chemists, New York, John Wiley & Sons, 1951, chapter 5.

92. Wolberg, J., Prediction Analysis, Princeton, D. Van Nostrand, 1967, chapters 3-4.

93. Afifi, A.A., and Azen, S.P., Statistical Analysis: A Computer Oriented Approach, New York, Academic, 1973, chapter 3.

BIOGRAPHICAL SKETCH

Brian Stanley Vogt was born on April 29, 1956, in the Clover Hill Hospital in Lawrence, Massachusetts, to Stanley and Blanche Vogt. He is their second son and has one brother and one sister.

He attended kindergarten, elementary school, junior high school, and high school in the Andover, Massachusetts, public system between the years of 1961 and 1974. He became a member of the National Honor Society in the 1973-1974 school year.

Subsequent to graduation from high school in 1974, he attended Bob Jones University in Greenville, South Carolina. He had a double major (biology/chemistry), and graduated cum laude with a Bachelor of Science in 1979. The science faculty at Bob Jones University selected him as the outstanding biology graduate in the 1979 graduating class.

He participated in the sports of fencing, soccer, and table tennis while in undergraduate school. He also enjoys fishing, bicycling, photography, birdwatching, classical music, and woodworking.

When he was young, he made a personal committment to the Lord Jesus Christ. He has read and studied the Bible, and has used the principles found therein to guide his

decisions and establish his priorities. He has been actively involved in church choir and Sunday school programs.

He went to the College of Pharmacy at the University of Florida in the fall of 1979. At UF he coauthored eight publications for scientific journals and coauthored chapters for two books. He also presented papers at four meetings on the state and regional levels. At one of these meetings (American Chemical Society meeting, Florida section, 1981) he was given first prize for the best student research presentation in the physical chemistry division.

I certify that I have read this study and that in my opinion it conforms to acceptable standards of scholarly presentation and is fully adequate, in scope and quality, as a dissertation for the degree of Doctor of Philosophy.

Stephen G. Schulman, Chairman
Professor of Pharmacy

I certify that I have read this study and that in my opinion it conforms to acceptable standards of scholarly presentation and is fully adequate, in scope and quality, as a dissertation for the degree of Doctor of Philosophy.

Frederico A. Vilallonga
Professor of Pharmacy

I certify that I have read this study and that in my opinion it conforms to acceptable standards of scholarly presentation and is fully adequate, in scope and quality, as a dissertation for the degree of Doctor of Philosophy.

Kenneth B. Sloan
Assistant Professor of Medicinal Chemistry

I certify that I have read this study and that in my opinion it conforms to acceptable standards of scholarly presentation and is fully adequate, in scope and quality, as a dissertation for the degree of Doctor of Philosophy.

John H. Perrin
Professor of Pharmacy

I certify that I have read this study and that in my opinion it conforms to acceptable standards of scholarly presentation and is fully adequate, in scope and quality, as a dissertation for the degree of Doctor of Philosophy.

James D. Winefordner
Graduate Research Professor of Chemistry

This dissertation was submitted to the Graduate Faculty of the College of Pharmacy and to the Graduate Council, and was accepted as partial fulfillment of the requirements for the degree of Doctor of Philosophy.

August, 1983

_____
Dean, College of Pharmacy

_____
Dean for Graduate Studies and Research